STUDY OF SOLITARY WAVE SOLUTIONS FOR GENERALIZED NONLINEAR SCHRÖDINGER EQUATION

A THESIS

Submitted to the

FACULTY OF SCIENCE

PANJAB UNIVERSITY, CHANDIGARH

for the degree of

DOCTOR OF PHILOSOPHY

2014

VIVEK KUMAR SHARMA

DEPARTMENT OF PHYSICS

CENTRE OF ADVANCED STUDY IN PHYSICS

PANJAB UNIVERSITY

CHANDIGARH, INDIA

This thesis is dedicated to my parents,

wife & daughter

for their love, endless support

and encouragement.

Acknowledgements

At this moment of accomplishment, I owe my gratitude to all those people who have made this thesis possible and because of whom my research experience has been one that I will cherish forever. Above all, I am humbly grateful to Almighty for granting me the strength to undertake this research work and helping me in overcome all obstacles. First of all I pay my homage to my superiors Prof. C. Nagaraja Kumar, Department of Physics, Panjab University, Chandigarh and Dr. J. K. Goswamy, University Institute of Engineering and Technology, Panjab University, Chandigarh for their sincere encouragement and inspiration throughout my research work. I am highly indebted to Prof. C. Nagaraja Kumar for his motivation, encouragement, support, expert guidance and constant supervision as well as for providing necessary information from time to time without which this research work could not be possible. My sincere gratitude to our collaborator Prof. P. K. Panigrahi and Dr. T. Soloman Raju for their advices and suggestions from time to time.

I extend my sincere thanks to the Chairman, Department of Physics, Panjab University for providing me the required facilities in the department. I express my gratitude to Prof. Manjit Kaur, Prof. D. Mehta, Prof. R. K. Puri, Prof. M. M. Gupta, Prof. K. Tankeshwar, Prof. V. Bhatnagar, Prof. N. Goyal and all other staff members of Physics department, Panjab University for their cooperation and help during this work. I am fortunate to have the company and help of my lab members Alka, Jasvinder, Rama, Amit, Shally, Harleen, Kanchan and Ritu for completion of various research projects. I am thankful to Dr. Amit Goyal and Dr. Rama Gupta for enlightening discussions and valuable suggestions. I am grateful to Dr. Amit Goyal for his valuable advice in my work, spending his precious times which helped me a lot for completion of various research projects. I have been blessed with a friendly people which includes Anup chaurahi, Jasbinder kumar and Dr. Mukesh. I greatly value their friendship and I deeply appreciate their belief in me.

My heartiest regard to my father Sh. Santosh Sharma and my mother Smt. Lalita Sharma for all the achievements in my life. I express my deepest gratitude towards my parents for their kind co-operation and encouragement and blessings which help me in completion of this research work. My heart-felt gratitude to sisters, Minakshi, Nigam brother in laws Sh. Umesh Sharma, Sh. Anil Sharma and Gaurav who have been a constant source of love, concern, support and strength all these years. I express my thanks to my younger brother Ashish whose presence always motivated me to work hard so that I could be a source of inspiration for him. I am highly thankful *to my father in law Sh. Rakesh Sharma and mother in law Smt. Meera Sharma for their love and blessings. I would like to express appreciation to my beloved wife Neha, without whose love and understanding I would not have completed this work. Words cannot express how grateful I am to my wife for her endless encouragement and support during my difficult moments. Last but not the least; I would like to express my affectionate thanks to my lovable sweet daughter Sejal whose sweet smile always relieved me in my stressful moments and motivated me to work hard to achieve the goal. I would like to acknowledge all the people whoever helped me directly or indirectly in successful completion of my Ph.D. thesis work.*

Date: **(Vivek Kumar Sharma)**

Abstract

This thesis deals with the investigation of solitary wave solutions of generalized nonlinear Schrödinger equations. In the second chapter, after a brief introduction to solitary waves and negative index materials (NIMs), we discuss the probability of pulse propagation in terms of solitary waves for NIMs. We present a detailed analysis for the existence of dark and bright solitary waves and also fractional-transform solutions in a nonlinear Schrödinger equation model for competing cubicquintic and higher-order nonlinearities with dispersive permittivity and permeability. We delineate parameter domains in which these ultrashort optical pulses exist in NIMs. For example, dark solitons exist for the case of normal second-order dispersion, anomalous third-order dispersion, self-focusing Kerr nonlinearity, and non-Kerr nonlinearities, while the bright solitons exist for the case of anomalous second-order dispersion, normal third-order dispersion, self-focusing Kerr nonlinearity, and non-Kerr nonlinearities. This is contrary to the situation in ordinary materials. In the second part of this chapter, we obtain travelling wave solutions for pulse propagation in NIMs in presence of external source, however the higher order effects like quintic nonlinearity and self-steepening are not considered in this case. The solutions are necessarily of fractional type containing trigonometric and hyperbolic functions. The last part of this chapter contains the investigations carried out for the existence of bright, dark solitons and periodic solutions for the coupled generalized nonlinear Schrödinger equation governing the pulse propagation in NIMs. We observe that, depending upon nature of dispersion, all travelling waves propagate with specific value of velocity and initial chirp. For the normal dispersion, the propagating solitons restrict to a unique velocity. On the other hand for the anomalous dispersion, velocity belong to a specific domain. In the anomalous dispersion, NIMs also allows the propagation of nonlinear periodic waves through them. We obtain expressions for nonlinear chirp associated with each of these waves.

In the third chapter, we investigate modulational instability (MI) in twin-core optical fibers (TCF), with a Kerr and non-Kerr polarizations based on a (3+1)-dimensional coupled nonlinear Schrödinger equations in the presence of coupling coefficient dispersion (CCD) and other higher order effects such as third order dispersion (TOD), fourth order dispersion (FOD), and self-steepening (SS). By employing a standard linear stability analysis, we obtain analytically, the explicit expression for the MI growth rate as a function of spatial and temporal frequencies of the perturbation and the material response time. We explicate three different types of

modulational instabilities— spatial, temporal, and spatio-temporal MI, and emphasize that the earlier studies on MI in TCF do not account for this physics. Despite the fact that the MI growth rate in these three different types of MI is impervious to TOD, the presence of quintic nonlinearity, CCD, FOD, and SS enhances the formation of MI sidebands, both in anomalous as well as normal dispersion regimes. For example, the spatial MI gain is directly proportional to the strength of quintic nonlinearity, while the temporal MI gain crucially depends on strength of quintic nonlinearity, FOD, CCD, and SS terms. We observe that for the case of focusing medium with anomalous dispersion, as the strength of quintic nonlinearity decreases, MI growth rate increases, and the MI gain reaches its optimum value and the pulse breaks-up into a train of ultrashort pulses. Thirdly, the spatio-temporal MI can occur for focusing medium in the normal dispersion regime with an enhanced formation of sidebands, while for the defocusing nonlinearity and anomalous dispersion, there is a suppression of generation of MI sidebands. To sum up, we affirm that all these additional terms provide extra freedom to control the amplitude of the MI gain profile.

In the last chapter, we study the existence of solitary wave solution and modulational instability for a class of nonlinear Schrödinger equations. In first section of this chapter, we present bright and dark optical solitons induced by the non-Kerr terms in generalized nonlinear Schrödinger equation. The reported solutions consist of various soliton-like solutions including double-kink and algebraic solitons. These solitons are of sub 10 femtosecond width and are helpful to increase the information carrying capacity in order to make ultra-fast communication. In second section, we study the Modulation instability for nonlinear Schrödinger equation phase locked with an external source. We analyze the possibility of existence of MI for self-focussing and self-defocussing nonlinearities for positive and negative value of source term coefficient. We further investigate the impact of variation of nonlinear coefficient and variation of source term coefficient on MI.

Contents

List of Figures

Chapter 1

Introduction

A system is said to be nonlinear if its output is not linearly proportional to input; on the basis of this definition, one can say that most of the systems in this universe qualify to be nonlinear. The science which deals with nonlinear systems is known as nonlinear science. In the past few decades, nonlinear science has emerged as a tool to study all those complex natural phenomenon which cannot be studied completely by linear science. It is not a new subject or branch of science, although it delivers a whole set of fundamentally new ideas and surprising results. Nonlinear science qualifies to be a revolution due to its wide scope and coverage because it find applications in almost all branches of science such as plasma physics, hydrodynamics, mechanics, biology, chemistry etc. Hence, due to feasibility of nonlinear science on system of every scale, it is possible to study same nonlinear phenomena in very distinct way, with the corresponding experimental tools.

The study of nonlinear system means to study the nonlinearity present in it. Nonlinearity plays an important role in dynamics of various physical phenomena [1, 2], such as in electronic circuits, laser physics, nonlinear mechanical vibrations, population dynamics, astrophysics, plasma physics, chemical reactions, nonlinear wave motions, heart beat, nonlinear diffusion, time-delay processes etc. Nonlinearity in any system make the system more complex and it become very difficult to study. A small disturbance induced in nonlinear system even by little variation in initial conditions can results into big difference in behavior in time evolution of the system. Hence a nonlinear system exhibits a sensitive dependence on initial conditions. However, linear systems are generally gradual, smooth and regular, common example of linear system are slowly flowing streams, engines working at low power, slowly reacting chemicals, etc. Any system with large input generally show nonlinear behavior. For example, the behavior of a spring is linear for small displacement, but if the initial displacement is large the spring shows nonlinear behavior. In similar way, for small initial displacement simple pendulum behaves as linear system however as the initial displacement become large enough, its motion become nonlinear.

The nonlinear system which is to be studied is described by a nonlinear evolution equation (NLEE). These NLEE's are having complex structures due to linear and nonlinear effects. By solving NLEE for different parameter regime one can analyze the behavior of system. To find the exact or approximate solution of the NLEE is a challenging aspect of nonlinear dynamics. The mathematical tools like Fourier and Laplace transform, Green's function, superposition principle are applicable for linear systems only. However analytical solutions of NLEE may be obtained by applications of several approximate methods such as inverse scattering transform (IST), Painleve analysis, Darboux transformation, ansatz method, factorization method. In recent times, the research in the field of finding exact solution of NLEE have reached an advanced stage due to development of several mathematical software and due to advancement in high speed computing. There are a large number of NLEEs such as reaction diffusion equation, KdV equation, sine Gordon equation, nonlinear Schrödinger equation (NLSE) etc., studied widely in different physical contexts. KdV equation is used to study the weakly dispersive system such as blood pressure waves and internal waves in oceans. Sine Gordon equation is used to study the properties of Josephson junctions, charge density waves, etc. Similarly, NLSE plays a vital role in the study of nonlinear fiber optics, condensed matter physics, plasma physics, etc. The study of exact solutions of NLEE's such as solitary waves and periodic solution plays a vital role in illustration of several natural phenomenon. This thesis involves the study of NLSE and its variants in contexts of nonlinear optics.

1.1 Nonlinear Schrödinger equation and its derivation

A nonlinear Schrödinger equation is an example of a nonlinear model which describes wide class of nonlinear systems. It has been widely used to address the physical, biological and engineering systems and found applications in fluid dynamics [3], nonlinear optics [4], plasma physics [5, 6] etc. The general form of NLSE is given by [7]

$$i\psi_t = -\frac{1}{2}\psi_{zz} + \gamma|\psi|^2\psi. \tag{1.1}$$

First term on the right hand side (RHS) is group velocity dispersion (GVD) term and γ is the coefficient of cubic nonlinearity. The term on the left hand side (LHS) represent the time evolution, t is time and z is space coordinate. The NLSE is one of the most important NLEE. It plays an important role in theory of propagation of the envelope of wave train in many dispersive physical phenomena in which no dissipation occurs.

In dielectric media and in the absence of free charges or currents, Maxwell's equations are given as [8]

$$\nabla \times \mathbf{E} = -\frac{\partial \mathbf{B}}{\partial t}, \tag{1.2}$$

$$\nabla \times \mathbf{H} = \frac{\partial\ \mathbf{D}}{\partial t}, \tag{1.3}$$

$$\nabla.\mathbf{D} = 0, \tag{1.4}$$

$$\nabla.\mathbf{B} = 0, \tag{1.5}$$

where **E** and **H** are the electric and magnetic field vectors, respectively, and **D** and **B** are electric and magnetic flux densities which arise in response to **E** and **H** propagating inside the medium and are related to them through the constitutive relations given as

$$\mathbf{D} = \epsilon_0 \mathbf{E} + \mathbf{P} \tag{1.6}$$

$$\mathbf{B} = \mu_0 \mathbf{H} + \mathbf{M} \tag{1.7}$$

where **P** and **M** are the induced electric and magnetic polarization. μ_0, ϵ_0 are permeability and permittivity of free space respectively. For nonmagnetic material $\mathbf{M} = 0$, Eqs. (1.2)- (1.5) can be used to obtain the wave equation for light propagation in optical waveguides. Taking curl of Eq. (1.2) and using Eq. (1.3), Eq. (1.6) and Eq. (1.7), one can eliminate **B** and **D** in favor of **E** and **P** and obtain

$$\nabla \times \nabla \times \mathbf{E} = -\frac{1}{c^2}\frac{\partial^2 \mathbf{E}}{\partial t^2} - \mu_0 \frac{\partial^2 \mathbf{P}}{\partial t^2}, \tag{1.8}$$

where c is the speed of light in vacuum and the relation $\mu_0 \epsilon_0 = 1/c^2$ was used.

Far away from the resonance, polarization **P** is given by

$$\mathbf{P}(\mathbf{r}, t) = \epsilon_0(\chi^{(1)}\mathbf{E} + \chi^{(2)} : \mathbf{EE} + \chi^{(3)} : \mathbf{EEE} + ...), \tag{1.9}$$

with ϵ_0 as the vacuum permittivity and χ^j is the j order susceptibility. Considering only 3rd order nonlinear effect, polarization is therefore conveniently expressed as sum of linear and nonlinear terms

$$\mathbf{P}(\mathbf{r}, t) = \mathbf{P}_L(\mathbf{r}, t) + \mathbf{P}_{NL}(\mathbf{r}, t). \tag{1.10}$$

Using Eq. (1.10) and $\nabla.\mathbf{E} = 0$, and introducing the linear refractive index $n^2(\omega) = 1 + \chi^{(1)}$, Eq. (1.8) can be written as

$$-\nabla^2 \mathbf{E}(\mathbf{r}, t) + \frac{n^2(\omega)}{c^2}\frac{\partial^2 \mathbf{E}(\mathbf{r}, t)}{\partial t^2} = -\mu_0 \frac{\partial^2 \mathbf{P}_{NL}(\mathbf{r}, t)}{\partial t^2}, \tag{1.11}$$

This expression shows that the nonlinear polarization acts as a source term for the driven wave equation. In absence of $\mathbf{P}_{NL}$, the radiation simply propagates as a free wave with speed $v = c/n$.

Most nonlinear effects are well described by this equation and can be related to given $\chi^{(j)}$ tensor. For instance, real part of $\chi^{(2)}$ is responsible for second harmonic generation (SHG) and real part of $\chi^{(3)}$ is responsible for third harmonic generation, self phase modulation (SPM), self focussing and four wave mixing. The imaginary part of $\chi^{(3)}$ is responsible for two photon absorption, Raman gain etc. Still higher order effects are usually weak and can be neglected. In optics, all even orders of $\chi^{(j)}$ vanishes due to the inversion symmetry in the amorphous silica and hence significant nonlinear contribution is from $\chi^{(3)}$.

Linear P_L and nonlinear polarization P_{NL} are related to electric field as [9, 10, 11]

$$P_L = \epsilon_0 \int_{-\infty}^{t} \chi^{(1)} \mathbf{E}(\mathbf{r}, t') dt', \tag{1.12}$$

$$P_{NL}(r,t) = \epsilon_0 \int \int \int_{-\infty}^{t} dt_1 \int_{-\infty}^{t} dt_2 \int_{-\infty}^{t} dt_3 \chi^{(3)}(t-t_1, t-t_2, t-t_3).\mathbf{E}(\mathbf{r}, t_1)\mathbf{E}(\mathbf{r}, t_2)\mathbf{E}(\mathbf{r}, t_3), \tag{1.13}$$

where $\chi^{(3)}(t, t_1, t_2, t_3)$ is approximated by

$$\chi^{(3)}(t, t_1, t_2, t_3) = \chi^{(3)} R(t - t_1)\delta(t - t_2)\delta(t - t_3). \tag{1.14}$$

Neglecting the nonlinear terms, Eq. (1.11) can be conveniently written in Fourier space as

$$\nabla^2 E(r, \omega) = \frac{\omega^2}{c^2} n^2(\omega) \mathbf{E}(\mathbf{r}, \omega). \tag{1.15}$$

A superposition of plane wave is solution to this equation and since light is also confined in the transverse dimensions of fiber, a linearly polarized solution must be of the form

$$\mathbf{E}(\mathbf{r}, \omega - \omega_0) = \hat{x} F(x, y) A(z, \omega - \omega_0) e^{-i(\beta_0 z - \omega_0 t)}, \tag{1.16}$$

where $F(x, y)$ is the transverse field distribution, A is slowly varying envelop, ω_0 is a fast carrier frequency and β_0 is the wave number corresponding to the central frequency. A is normalized such that $|A|^2$ represents the optical power. The product of the independent transverse and longitudinal parts leads to two conditional equations:

$$\left(\frac{\partial^2}{\partial x^2}+\frac{\partial^2}{\partial y^2}\right)F(x,y)+n^2(\omega)\frac{\omega^2}{c^2}F(x,y)=\beta^2F(x,y), \tag{1.17}$$

$$2i\beta_0\frac{\partial A}{\partial z}+2\beta_0(\beta-\beta_0)A(z,\omega)=0, \tag{1.18}$$

where the second derivative of slowly varying envelop has been neglected and the approximation $\beta^2-\beta_0^2=2\beta_0(\beta-\beta_0)$ has been used. Both the conditions are justified as long as $\triangle\omega << \omega$. Eq. (1.17) is an eigen value equation, known as scalar Helmholtz equation, and leads to condition of guided mode and their field distribution $F(x,y)$ in the fibers. β is the eigen value of transverse field distribution. In the absence of nonlinear polarization, solution of Eq. (1.17) is superposition of Bessel and Neumann functions and it can be shown that these can have confined modes only for $kn_1^2>\beta^2>kn_2^2$. There may be several β fulfilling the conditions corresponding to multimode, which implies that more than one spatial distribution of field is possible in the fiber. When Kerr nonlinearity is included in Eq. (1.11), the effective refractive index $n(\omega)$ is modified by the weak nonlinear effect, $\tilde{n^2}=\epsilon=1+\chi^{(1)}+3/4\chi^{(3)}|E|^2$. The change in $\tilde{n}$ is small, so

$$\tilde{n}^2=(n+\triangle n)^2=n^2+2n\triangle n, \tag{1.19}$$

which enables us to solve Eq. (1.17) by first order perturbation method. First n^2, is used to find the field distribution $F(x,y)$ and propagation parameter β. Then eigen function $F(x,y)$ are used to calculate the first order correction to the term β due to the term $2n\triangle n$,

$$\tilde{\beta}(\omega)=\beta(\omega)+\triangle\beta(\omega). \tag{1.20}$$

Unperturbed linear propagation constant is approximated by Taylor expansion around central frequency ω_0

$$\beta(\omega)=\beta_0+\beta_1(\omega-\omega_0)+\frac{1}{2}\beta_2(\omega-\omega_0)^2+...... \tag{1.21}$$

This expression is inserted in Eq. (1.18) and a Fourier transformation back to time domain gives the following equation for time dependent slowly varying envelope.

$$\frac{\partial A}{\partial z} + \sum_{n=1} \beta_n \frac{i^{n-1}}{n!} \frac{\partial^n A}{\partial t^n} = i\triangle\beta A. \tag{1.22}$$

$\Delta\beta$ include the effect of fiber loss and nonlinearity and can be written as

$$\Delta\beta = \frac{\alpha}{2} + i\gamma(\omega_0)|\psi|^2, \tag{1.23}$$

where α represent the loss or gain coefficient. If we consider lossless materials then on substituting Eq. (1.23) in Eq. (1.22), we obtain the resulting equation

$$i\frac{\partial A}{\partial z} = -\beta_2 \frac{\partial^2 A}{\partial t^2} + \gamma|A|^2 A. \tag{1.24}$$

Interchanging z and t, we get resulting equation as Eq.(1.1), which is known as nonlinear Schrödinger equation (NLSE). There are various variants of NLSE, the structure of which depend upon the properties of the system under study.

1.1.1 Higher order nonlinear Schrödinger equation (HNLSE)

In most of the applications, the Eq. (1.1) is well satisfied, but with technological advances of creating shorter and shorter pulses with duration in the femto-second range this equation is no longer valid. Indeed if a pulse contain a few oscillations of the carrier wave, the hypothesis of a slowly varying amplitude has to be replaced with a new approach which is required to describe the propagation of ultrashort pulses in nonlinear media. One possibility is to consider the NLS equation with additional higher-order dispersive and nonlinear terms [12, 13, 14]. Recently a new approach, based on the fact that the pulse is broad in the Fourier space, was developed by several authors [15, 16, 17, 18]. It lead to the higer-order NLSE (HNLSE) for ultrashort pulses which can be written as

$$i\psi_t + \frac{1}{2}\psi_{xx} + |\psi|^2\psi + i\epsilon\ [\ A\ \psi_{xxx} + B\ |\psi|^2\psi_x + C\ \psi|\psi|^2_x\ ] = 0, \tag{1.25}$$

apart from the terms occurring in NLSE, it contain additional terms like third order dispersion term (TOD) ψ_{xxx}, $\psi|\psi|_x^2$ is responsible for Raman induced frequency shift, $|\psi|^2\psi_x$ is self steepening (SS) term. A large number of research groups have studied HNLSE in different parameter regime to obtain solitary wave like solutions [19, 20, 21].

1.1.2 Nonlinear Schrödinger equation with source term

The general form of NLSE with source term is given by

$$i\psi_t + \frac{1}{2}\psi_{xx} + g|\psi|^2\psi + \mu\psi = Ke^{i(kx-\omega t)}, \tag{1.26}$$

where ψ_t is time evolution term, ψ_{xx} is GVD term, g is the coefficient of cubic nonlinearity, μ is gain or loss term coefficient and K is source term coefficient. Externally driven, NLSE with a source has been investigated in the context of a variety of physical processes. It arises in the problem of Josephson junction [22], twin-core fibers [23, 24, 25, 26], density waves [27] and a number of other problems.

1.1.3 Coupled Nonlinear Schrödinger equation

While deriving Eq. (1.24), we assumed that the polarization of the incident beam is preserved during propagation. If the system is relaxed from this condition and the coupling between the orthogonal polarization components is considered then the governing equation becomes the coupled NLSE. The propagation of coupled modes of light through nonlinear waveguide is modelled by coupled NLSE. In the simplest form coupled NLSE is expressed as

$$i\psi_{1t} + c_1\psi_{1xx} + (2\alpha|\psi_1|^2 + 2\beta|\psi_2|^2)\psi_1 = 0 \tag{1.27}$$

$$i\psi_{2t} + c_2\psi_{2xx} + (2\gamma|\psi_2|^2 + 2\beta|\psi_1|^2)\psi_2 = 0. \tag{1.28}$$

here ψ_1 and ψ_2 are two components of polarization, r_{11} and r_{22} are coefficients of self phase modulation (SPM) and r_{12} and r_{21} are coefficients of cross phase modulation (XPM). This is the XPM coefficients that take care of the coupling between the polarization modes. XPM always accompanies SPM and can also arise between two optical fields of different wavelengths. This equation appears in the nonlinear optics in several different contexts. For example this equation is used in the theoretical analysis of various nonlinear effects in the model of metamaterials [28, 29], which features a combination of negative dielectric permittivity and magnetic permeability and gives rise to negative refractive index. It promises a number of applications that are impossible in ordinary optical media. For example- super–lensing, describe left handed wave guide, negative refraction at optical frequency.

1.1.4 Nonlinear Schrödinger equation with distributive coefficients

NLSE and HNLSE with constant coefficients describes an idealized system. But most of systems are inhomogeneous in nature e.g. optical fiber with nonuniform diameter [30, 31, 32], Bose-Einstein condensates (BECs) [33, 34] and plasma physics [35, 36, 37] etc. Therefore, Eq. (1.24) and Eq. (1.25) with variable coefficients can be a more realistic approach for study of such systems. In the context of nonlinear optics, the coefficients of NLSE are space dependent and we call the system as inhomogeneous system and the governing equation is the inhomogeneous NLSE or generalized NLSE (GNLSE). In the context of BECs, the coefficients of NLSE are time dependent and we call the system as nonautomous system, where time appears explicitly and the governing equation is the nonautonomous NLSE. A general form of NLSE with distributive coefficients is given by

$$i\psi_t + \frac{1}{2}\psi_{zz} + g(z)|\psi|^2\psi + \mu(z)\psi = 0. \tag{1.29}$$

In above equation nonlinearity and gain are space dependent. Such an approach has vital applications in various fields of engineering and sciences. Recently a number of researchers have studied this equation and have obtained solitary wave solutions [31, 38, 39]

Hence we have seen that NLSE and its variants are used to describe various systems such as BECs, dynamics of rotating fluid, pulse propagation in optical fiber, pulse propagation in negative refractive index materials etc. Our focus is on the study of pulse propagation in ordinary materials and negative index materials, which is modelled by NLSE and its various variants.

GNLSE have large number of solutions however we are here interested in localized solutions.

1.2 Solitary waves and solitons

1.2.1 Solitary wave

In some media, such as layer of water or an optical fiber, under suitable conditions the widening of wavepacket due to dispersion could be balanced exactly by narrowing effect of nonlinearity of medium. In these cases, it is possible to have localized waves, propagating with constant velocity and undistorted shape, often known as solitary waves.

1.2.2 Solitons

Solitons are those solitary waves which retain their individuality under collisions and eventually travel with their original shapes and speeds.

This property looks like interaction between free particles. Due to this particle nature of solitary waves, they are named as 'Solitons'. This property is illustrated in Fig. 1.1. The solitons are mainly of two types i.e. bright and dark solitons. The solitons pulse, intensity of which is larger than the background is known as bright solitons, as shown in Fig. (1.2). The soliton with lower intensity than background is known as dark solitons. The evolution of dark soliton is shown in Fig. (1.3).

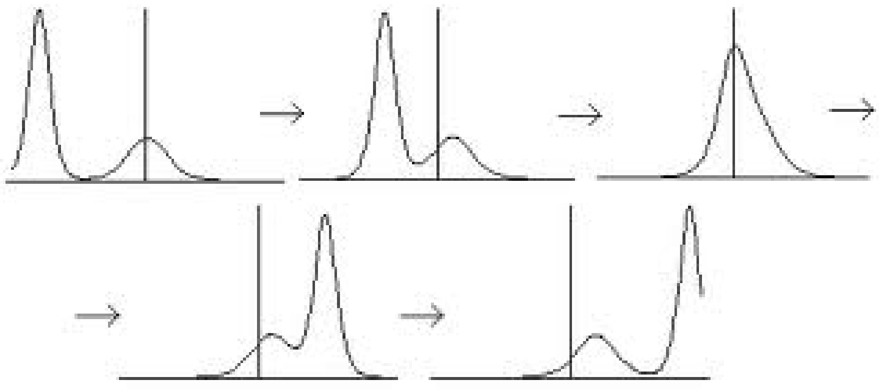

Figure 1.1: Collision of solitary waves

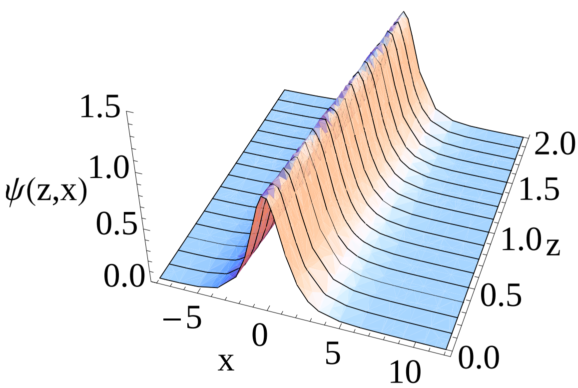

Figure 1.2: Evolution of bright soliton.

1.2.3 Historical background

The solitary wave were first observed in 1834 by J. Scott Russel during his experiment on efficient design of canal boat [40]. During experiment he saw a long water wave propagating without change in shape. He named this wave as "Great Wave" of translation or "Solitary Wave" and performed further investigations to study the nature of this wave. The speed of such wave is given by

$$c = \sqrt{g(h+a)}, \tag{1.30}$$

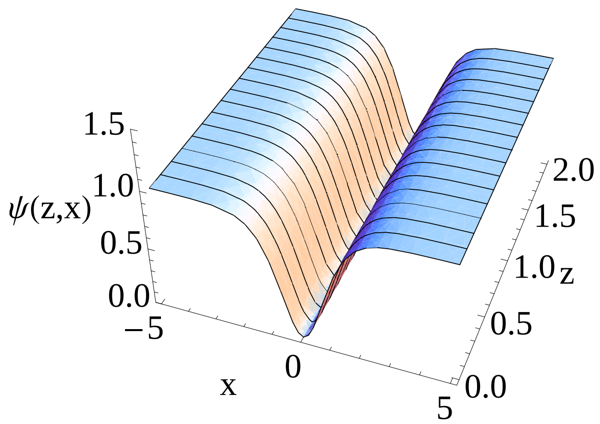

Figure 1.3: Evolution of dark soliton.

where g is acceleration due to gravity, h is depth of water channel, a is maximum amplitude of solitary wave. He published this work in the British Association in 1844 with the name Report on Waves. His description of solitary waves contradicted the theories of water waves according to G. B. Airy and G. G. Stokes; they raised questions on the existence of Russells solitary waves and conjectured that such waves cannot propagate in a liquid medium without a change of form. Despite the mathematical theory, the experimental evidence in favor of solitary waves was convincing. It was not until the 1870s that Russells prediction was finally and independently confirmed by both J. Boussinesq in 1871 and Lord Rayleigh in 1876.

In 1895, D. J. Korteweg and G. de Veries formulated a mathematical model for solitary wave known as KdV equation, which can be express as

$$\psi_t + \psi\psi_x + \delta\psi_{xxx} = 0, \tag{1.31}$$

where ψ is amplitude of wave having functional dependence on space x and time t coordinate, second term is nonlinear term and δ is the coefficient of nonlinear term

Dispersive term is responsible for the broadning of pulse while nonlinear term leads to the steepening effect. In 1965, Zabusky and Kruskal [41] solved the KdV equation numerically as a model for nonlinear lattice and found that solitary wave solutions interacted elastically with each other. Due to this particle-like property, they termed these solitary wave solutions as solitons. When nonlinearity is balanced by dispersion then waveform take the shape of permanent form known as soliton. This research work attracted the attention of large number of research groups all over the world and hence soliton concept was widely accepted. With the acceptance of concept of solitons, a lot of research work was undergone to obtain the soliton solutions which leads to development of several mathematical methods. Gardener et al. reported the existence of multi-soliton solutions of KdV equation by using inverse scattering transform (IST) [42]. Lax generalized these results and proposed the concept of Lax pair [43]. In 1971 Zakharov and Shabat [44] showed that the method worked for another physically significant NLEE, the NLSE, which is the underlying mechanism for the BenjaminFeir instability in water waves. Hirota [45] introduced a new method, known as Hirota direct method, to solve the KdV equation for exact solutions for multiple collision of solitons. Then in 1974 Ablowitz et al. [46] showed how those techniques could be used to solve a wide class of NLEE. Since then the theory of solitons has blossomed into a rich and diverse field.

1.2.4 Properties of solitary waves

- The waves are stable, and can travel over very large distances without change in shape and size.
- The speed of the wave depends on the size of the wave, and its width depends on the depth of channel.
- Solitary waves do not survive collisions.

1.2.5 Applications of solitary wave and solitons

Fiber optics

An optical soliton can propagate without distortion over long distances. This feature of optical soliton helpful in high speed communication through an optical fiber [47]. Apart from the field of communications, solitons also find application soliton photonic switches [48], logic gates [49], fiber laser [50], timing jitter [51], pulse compression [52] and pulse amplification [53].

Bose-Einstein condensates (BECs)

At very low temperatures, particles in a dilute Bose gas can occupy the same quantum (ground) state, forming a BEC. This phenomenon was first predicted by Bose and Einstein in 1924. It is a coherent cloud of atoms which appears as a sharp peak in both position and momentum space. In 1995, BECs were realized experimentally when atoms of dilute alkali vapors were confined in a magnetic trap and cooled down to extremely low temperature, of the scale of fractions of microkelvins [54, 55]. The macroscopic dynamics of BECs near zero temperature is modeled by an NLSE type equation, known as the Gross-Pitaevskii (GP) equation. This equation contain nonlinear term which arises due to the interatomic interactions which describes the existence of nonlinear waves, such as solitons and vortices. Hence, these matter-wave solitons can be viewed as nonlinear excitations of BECs [56].

Fluid dynamics

Solitary wave was first noticed and studied by Russell, which was shallow water-wave soliton. The shallow water wave soliton is modelled by KdV equation. Solitary waves also arise in deep water, as shown by the pioneering work of Vladimir Zakharov [57] in 1968. Hence solitons find application in the study of various problems of fluid dynamics. For instance, recently large number of research groups have attempted to explain the large and seemingly spontaneous freak waves [3] or rogue waves as solitary waves. Additionally, tidal bores have been explained in terms of dispersive shock waves, which consist of a front followed by a train of solitary waves.

Biophysics

There have been some attempts to use solitary-wave descriptions to describe various biophysical phenomena. One example is the Davydov soliton, which satisfies an equation that was designed to model energy transfer in hydrogen-bonded spines that stabilize protein α-helices [58]. The Davydov soliton represents a state composed of an excitation of amide-I and its associated hydrogen-bond distortion. It has been used to describe a local conformational change of the DNA α-helix. Solitary waves also find application the various studies related to DNA molecule [59].

Josephson junctions

A Josephson junction is a nonlinear oscillator consisting of two weakly coupled superconductors that are connected by a non-conducting barrier. Such junctions might prove to be important for producing quantum-mechanical circuits such as super conducting quantum interference devices (SQUIDs). Solitons also find application in the study of Josephson junctions because various intrinsic localized mode emerge in the study of such devices [60, 61].

Plasma Physics

Plasma consists of large number of charged ions. In perturbation of charge density, the local ion density can be studied by using KdV equation and Kadomtsev-Petviashvili (KP) equation. These equations admits soliton solutions. Soliton concept penetrated into plasma physics in the late 50s. Later on number of researchers showed interest in study of soliton solutions for plasmas [62, 63]

Field Theory

Solitons are also important in the study of both classical and quantum field theory [64]. Topological solitons such as monopoles, kinks, vortices, and skyrmions are key to the modern understanding of field theory. In (1+1)-dimensional quantum field theory, topological soliton solutions of the sine-Gordon equation can be mapped to elementary excitations of an exactly solvable quantum field theory. This provides a toy model for more physically relevant examples in which, the role of solitons is played by magnetic monopoles which can be mapped to electrically charged elementary particles via an equivalence that is given the name strong-weak duality or, more commonly, S-duality. S-duality is also an essential feature of string theory.

1.3 Other localized solutions

Since the discovery of solitary wave and solitons, a number of localized pulses have been discovered in one dimensions as well as in multiple spatial dimensions. These pulses are considered as similar to solitary wave although they don't have interaction properties similar to solitons. Some of the prominent examples of these pulses are discussed below:

1.3.1 Gap solitons

Solitary waves that occur in finite gaps in the spectrum of continuous systems are known as gap solitons. Optical gap solitons are refers to nonlinear waves propagating in optical fibers whose linear refractive index has a periodic variation. The gap solitons have been studied for NLSE equations with spatially periodic potentials and have been observed experimentally in the context of both nonlinear optics [65] and Bose-Einstein condensation [66].

1.3.2 Breathers

A breather is a nonlinear wave in which energy concentrates in a localized and oscillatory fashion as shown in Fig. (1.4). The term breather originates from the

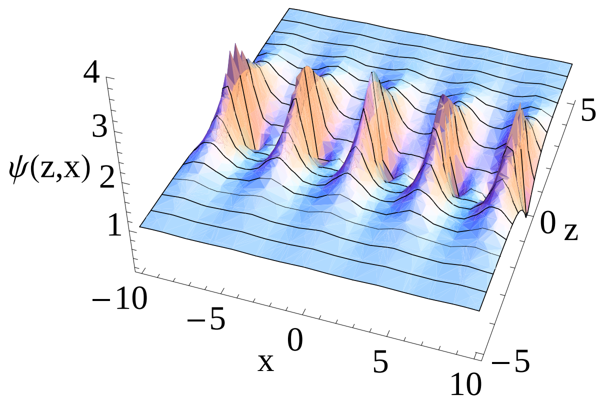

Figure 1.4: Breather soliton.

characteristic that most breathers are localized in space and oscillate (breathe) in time. Breathers are extremely spatially-localized, time-periodic, stable or very long-lived excitations in spatially extended, discrete, periodic or quasi-periodic systems [67, 68]. These solutions increase their amplitude either exponentially or according to power law in time t. Breathers achieve their maximum amplitude and finally decay symmetrically to disappear forever. For NLSE there are two types of breathers.
(1) Ma soliton/ Breather [69] *(2) Akhmediev Breather* [70]

1.3.3 Kink solitons

Kink-solitons is one-dimensional topological solitary wave [71]. These represents a twist in the value of a solution and causes a transition from one value to another. The plot of kink-soliton is as shown in Fig. (1.5).

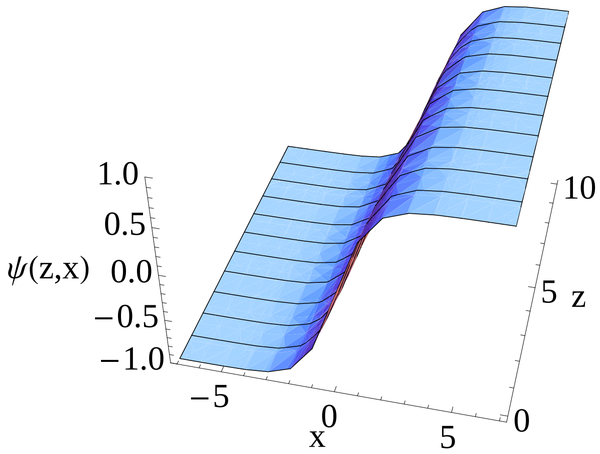

Figure 1.5: Kink soliton

1.3.4 Rogue waves

Rogue waves are relatively large and spontaneous ocean surface waves that occur far out at sea, and are a threat even to large ships [72]. Therefore these waves are also known as freak waves, monster waves, killer waves, extreme waves, and abnormal waves. The defining characteristic of these waves is that they appear from nowhere and disappear without trace. An image of plot of rouge wave is as shown in Fig. (1.6). Rogue waves are unusually steep waves, with the amplitude approximately three times that of background (average wave crest). These were first recorded in 1994, in the north sea. Rogue waves seem not to have a single distinct cause, but occur where physical factors such as high winds and strong currents cause waves to merge to create a single exceptionally large wave.

1.4 Negative refractive index materials (NIMs)

In optics, the refractive index of a material is conventionally taken to be a measure of the optical density and is defined as $n = \frac{c}{v}$, where c is the speed of light in vacuum and v is the speed of an electromagnetic plane wave in the medium. From Maxwell's equations the refractive index is given by the Maxwell relation, $n = \pm\sqrt{\mu\epsilon}$ where ϵ

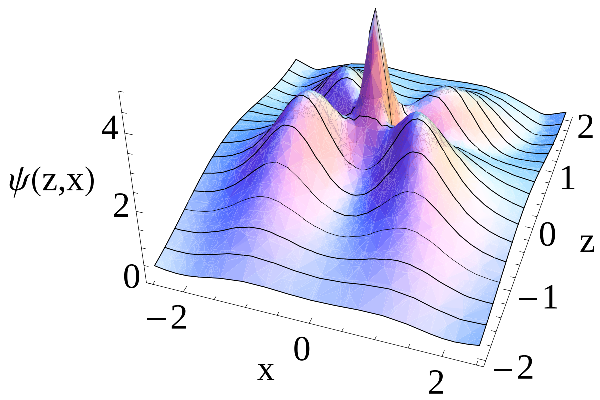

Figure 1.6: Rogue wave

is the relative dielectric permittivity and μ is the relative magnetic permeability of the medium. Usual optical materials have a positive ϵ, μ and n could easily be taken as $\sqrt{\epsilon\mu}$ without any problems. Although it was realized that the refractive index would have to be a complex quantity to account for absorption and even a tensor to describe anisotropic materials, the question of the sign of the refractive index never assumed significance. In 1967, Veselago [73] first considered the case of a medium that had both negative dielectric permittivity and negative magnetic permeability at a given frequency and concluded that the medium should then be considered to have a negative refractive index. However this result remained an academic curiosity for a long time due to unavailability of naturally occurring materials with simultaneously negative ϵ and μ. However, in the last few years, theoretical proposals [74, 75] for structured photonic media, whose ϵ and μ could become negative in certain frequency ranges were developed experimentally [76, 77] and this has brought Veselago's result into the limelight. The striking demonstration by Pendry [78] that NIMs can be used to make perfect lenses with resolution capabilities not limited by the conventional diffraction limit has provided an enormous boost to the interest in NIMs. This field has become a hot topic of scientific research and debate over the past few years.

1.4.1 Properties of NIMs

Electromagnetic properties of NIMs

(a) Left handed system:-

Electrodynamics of NIMs can be explained by considering Maxwell's equations.

$$\vec{\nabla} \times \vec{E} = -\frac{1}{c}\frac{\partial \vec{B}}{\partial t}, \tag{1.32}$$

and

$$\vec{\nabla} \times \vec{H} = -\frac{1}{c}\frac{\partial \vec{D}}{\partial t}, \tag{1.33}$$

for uniform plane wave $\vec{E} = \vec{E}_0 e^{(\omega t - Kx)}$ and $\vec{B} = \vec{B}_0 e^{(\omega t - Kx)}$, where $\vec{E}_0$ and $\vec{B}_0$ are initial amplitude of electric field and magnetic field respectively. ω is angular frequency and K is propagation vector. On substituting E and B in Eq. (1.32) and in Eq. (1.33), we obtain

$$\vec{K} \times \vec{E} = \omega\mu\vec{H}, \tag{1.34}$$

and

$$\vec{K} \times \vec{H} = \omega\epsilon\vec{E}. \tag{1.35}$$

It is clear from Eq. (1.34) and Eq. (1.35) that propagation of wave through a material depends upon the sign of ϵ and μ. The behavior of electromagnetic wave for various possibilities of sign of ϵ and μ is as shown in Fig. (1.7). For positive ϵ and μ the $\vec{K}$, $\vec{E}$, $\vec{H}$ form a right handed system (RHS) as shown in Fig. 1.8(a). However if μ and ϵ are simultaneously negative then $\vec{K}$, $\vec{E}$, $\vec{H}$ form the left handed system (LHS) as shown in Fig. 1.8(b). Hence due to this property these materials are also known as left handed materials (LHM).

(b) Negative phase velocity:-

We know phase velocity of a wave is the velocity of wave fronts having constant

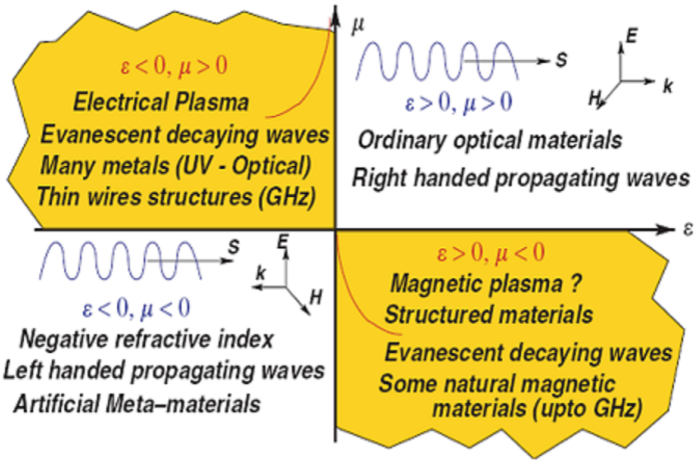

Figure 1.7: Classification of materials based upon propagation of wave

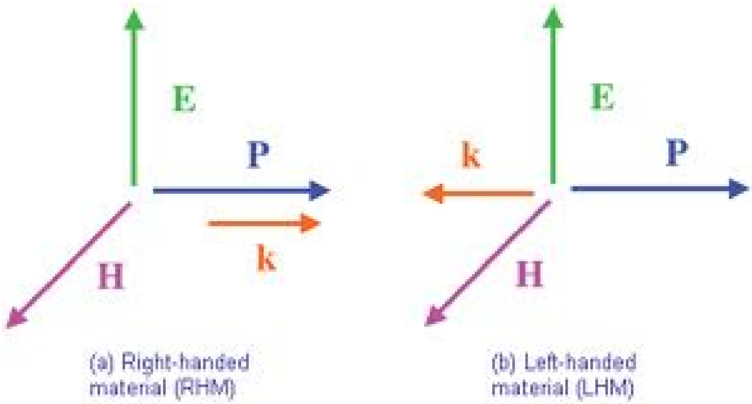

Figure 1.8: (a) Right handed system and (b) Left handed system.

phase. The phase velocity for a wave is given by

$$v = \frac{\omega}{k}, \tag{1.36}$$

for LHM k is negative this will lead to negative value of v, which shows that in NIMs phase velocity of the propagating wave is negative.

(c) Backward wave propagation:-

We also know for any wave the time averaged flux of energy is determined by Poynting vector.

$$\vec{P} = \frac{1}{2}(\vec{E} \times \vec{H}). \tag{1.37}$$

$\vec{P}$ always points in the direction of group velocity of wave which is the velocity of propagation of the envelope of the wave packet. Hence in NIMs group velocity of wave is always positive. $\vec{P}$ is positive in both LHM and RHM. Therefore in LHM the Group velocity and Phase velocity always points in opposite directions which is shown in Fig. 1.9, hence it shows that there is backward wave propagation in NIMs.

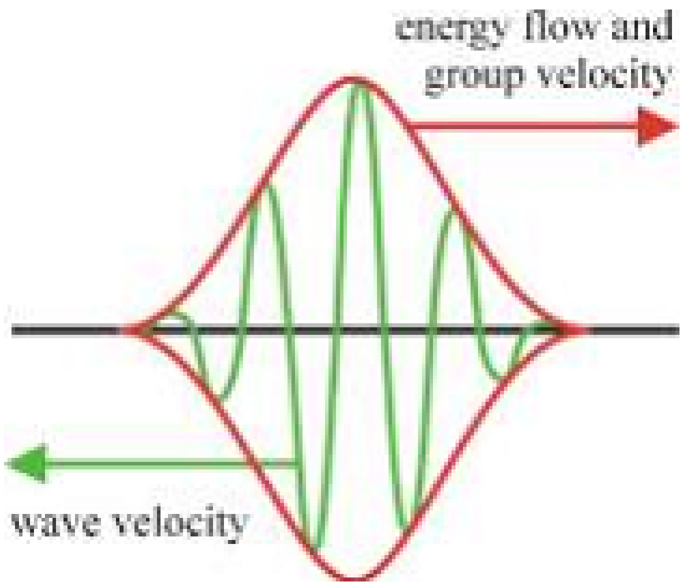

Figure 1.9: Wave velocity and group velocity in NIMs

Optical properties of NIMs

(a) Negative refraction:-

We know that snell's law describes bending of light when it moves from one medium to other. It states that the ray of light bends towards the normal when it enters from rearer to the denser medium, however it bends away from the normal when it enters from denser to the rearer medium. To describe negative refraction or inverse snell's law, let us consider the refraction of a ray at the interface of two media one of which is RHM and second is LHM. Let n_1 is refractive index of RHM and n_2 is refractive index of LHM, then according to Snell's Law

$$\frac{sin\theta_1}{sin\theta_2} = \frac{-n_2}{n_1}, \tag{1.38}$$

$$n_1 sin\theta_1 = -n_2 sin\theta_2, \tag{1.39}$$

$$n_1 sin\theta_1 = n_2 sin(-\theta_2). \tag{1.40}$$

The relation shows that after refraction there is bending of ray on negative side of normal. This explains the negative refraction in NIMs. Fig. 1.10 shows both positive and negative refraction

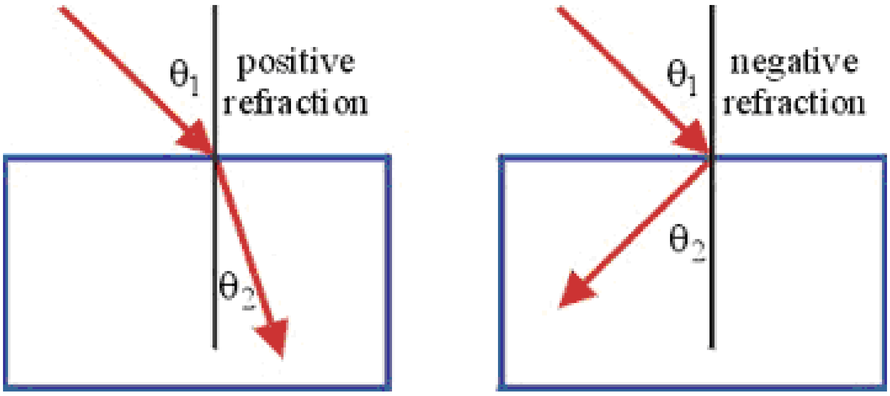

Figure 1.10: Positive refraction in ordinary materials and negative refraction in NIMs

(b) Convex and concave lens:-

In NIMs the roles of convex and concave lens are interchanged. The convex lens become diverging in nature and concave lens become converging in nature. This feature of NIMs is as shown in Fig. 1.11.

(c) Inverse doppler effect:-

We know in conventional doppler effect, the frequency of waves that are emitted by a moving source increases when the source is moving towards the observer and decreases when the source is moving away from the observer. The conventional

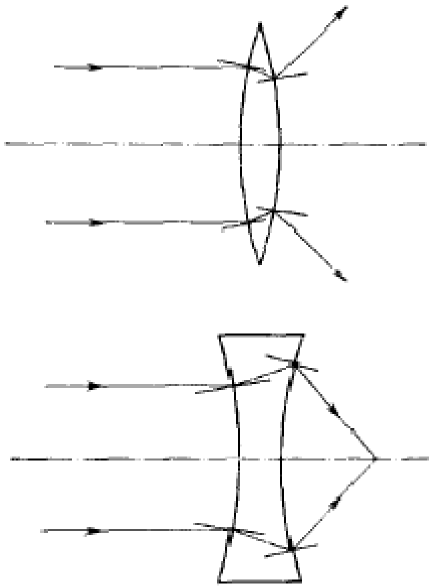

Figure 1.11: Convex and concave lense in NIM's

doppler effect is shown in Fig. 1.12(a). However in 1968 soviet physicist Victor Veselago [73] predicted that electromagnetic waves travelling through materials with a negative permittivity and a negative permeability would do the opposite. The frequency should drop for a source moving towards an observer and increase for a source moving away from the observer. The reverse doppler effect is as shown in Fig. 1.12(b). Reverse doppler effect occurs because the magnitude of the doppler effect is proportional to the refractive index of the medium through which the wave propagate. The refractive index of all the materials is positive however for NIMs refractive index is negative.

$$f = f_0 \left(\sqrt{\frac{1+\beta}{1-\beta}} \right), \tag{1.41}$$

where $\beta = \frac{v}{c}$, v is relative velocity of the source and observer and c is velocity of light.

(d) High resolution:-

The diffraction limit is an inherent limit in conventional optical devices or lenses beyond which resolution is not possible. NIMs are having resolution beyong

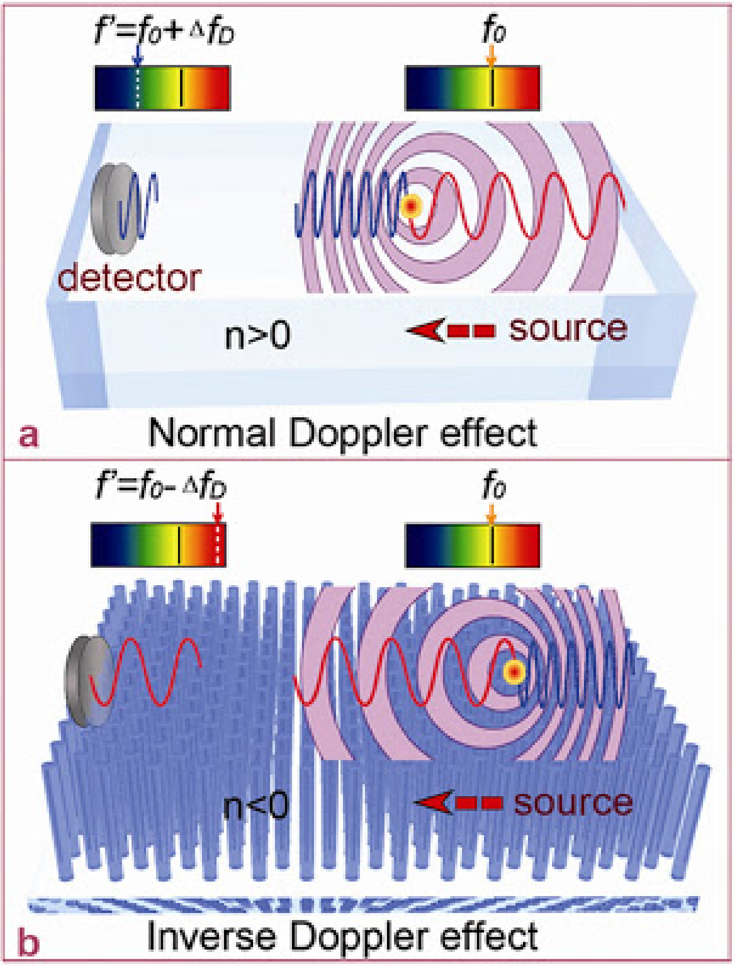

Figure 1.12: (a) Doppler effect in a right-handed substance ($n > 0$) (b) Doppler effect in a left handed substance ($n < 0$).

the diffraction limit. This property of NIMs can be useful in making superlenses.

1.4.2 Applications of NIMs

NIMs are under consideration for many applications. Some of the potential future applications are as discussed below

Antennas

NIMs can be used to design highly domesticated and efficient antennas. Due to negative magnetic permeability NIMs can be used to make antennas small in size, having high directivity and tunable operational frequency. NIMs are also helpful in enhancing radiated power of antenna.

Absorber

An absorber is a type of device which can efficiently absorb electromagnetic radiation such as light. NIMs utilizes the effective medium design and loss components of electric permittivity and magnetic permeability to create a material that has a high ratio of electromagnetic radiation absorption. The metamaterial absorber find applications in solar phovoltaic, photonic metamaterials, antenna systems etc.

Superlens

Most interesting property of NIMs is that, these materials could lead to the creation of a superlens [78]. Such a lens would image objects with details smaller than that wavelength of light used. Ordinary lenses with positive refractive indices, are only able to capture details of the object at the size of the wavelength of the light used or larger. The superlens on the other hand is capable of capturing the finest detail (smaller than the wavelength of light used) of the object.

Cloaking devices

NIMs can direct and control the propagation and transmission of specified parts of the light spectrum and demonstrate the potential to render an object seemingly invisible. This property of NIMs can be used to design invisible cloaking device. This device is based on transformation optics, which describes the process of shielding something from view by controlling electromagnetic radiation.

Seismic metamaterials

NIMs can be used to design the materials which can counteract the adverse effects of seismic waves on artificial structure which exist on the surface of earth. We know that velocity of the seismic waves depends on density of the materials. The NIMs has the ability to reduce the velocity of seismic wave and hence shorten its wavelength. This property of NIMs would pass the wave around the building which is standing on earth, so as to arrive in phase as earthquake wave.

Light and sound filtering

NIMs textured with nonoscale wrinkles could control the sound and light signal. This property is useful in techniques like nondestructive material testing, medical diagnostics and sound suppression.

1.4.3 Pulse propagation through NIMs

In electromagnetic properties of NIMs, it has been discussed that there is reverse wave propagation through NIMs. This property has given the insight that wave propagation is possible in NIMs. This has created a significant theocratical as well as experimental interest, in the use of NIMs in optical communication systems. In this context, study of nonlinear pulse propagation, particularly optical solitons is new and exciting field of research [79, 80], because NIMs are artificially designed materials, so we have flexibility of controlling the behavior of pulse propagation through these materials. NIMs are composed of regular array of unit cells whose size is usually much smaller than the wavelengths of propagating E. M. waves. Therefore, NIMs may be considered as continuous and homogeneous according to effective medium theory and may be described by dispersive permittivity $\epsilon(\omega)$ and dispersive permeability $\mu(\omega)$. Due to difference in properties of NIMs and ordinary materials, it was not an easy task to develop pulse propagation equation for NIMs. In 2005 Scalora et. al. considered dispersive nature of electrical permittivity $\epsilon(\omega)$ and magnetic permeability $\mu(\omega)$, and modelled pulse propagation equation for NIMs. This was a significant breakthrough in the field of pulse propagation through NIMs.

The pulse propagation for NIMs is given by

$$\frac{\partial E}{\partial Z} = i\frac{k_2}{2}\frac{\partial^2 E}{\partial t^2} + k_3\frac{\partial^3 E}{\partial t^3} + iP_3|E|^2E - iP_5|E|^4E + S_1\frac{\partial(|E|^2E)}{\partial t} - iS_2\frac{\partial^2(|E|^2E)}{\partial t^2} \quad (1.42)$$

where k_2 is group velocity dispersion (GVD) coefficient, k_3 is third order dispersion (TOD) term, P_3 and P_5 are nonlinear term and S_1 is self steepening (SS) coefficient and S_2 is second order nonlinear dispersion coefficient. This equation basically describe the propagation of ultra short pulses in NIMs. This equation is known as generalized nonlinear Schrödinger wave equation (GNLSE).

1.5 Outline of Thesis

The layout of the thesis is as follows.

Chapter 2 include the discussion about possibility of solitary waves and other localized solutions in NIMs. This chapter is divided into three parts. We have discussed about the wave propagation in NIMs. In first section, we present periodic and solitary waves propagating through NIMs. The NLSE containing higher order effects like quintic nonlinearity, self-steepening and nonlinear dispersive terms governs the pulse propagation through NIMs and we have explored dark and bright solitary wave solutions for some constraints. We further studied fractional-transform solutions, containing periodic, hyperbolic and cnoidal solitary wave solutions for GNLSE, in absence of quintic and nonlinear dispersion terms. In second section, we have studied solitary wave solutions for NLSE containing an external source. In this case, we have obtained the periodic and solitary wave solution again, by using ansatz method. Third section deals with study of chirped pulses in NIMs. We have considered the coupled pulse propagation equation in NIMs in the presence of electric and magnetic self-steepening effects. In order to make the work self contained, we have sketched the essential steps of derivation of coupled NLSE. We have obtained exact chirped soliton and periodic solutions for normal as well as anomalous dispersion. For the normal dispersion, we obtained the bright and dark soliton solutions having unique velocity but different initial chirp for same normalized frequency; on the other hand for the anomalous dispersion, it possesses the fractional solutions having different velocity for a particular normalized frequency. Moreover, there is also a possibility of obtaining the periodic nonlinear waves in NIMs in anomalous dispersion regime. We have plotted these solutions for different normalized frequencies. It is shown that nonlinear chirp associated with each of these solutions is directly proportional to the intensity of the pulse and saturates at some finite value as the retarded time approaches its asymptotic value.

In Chapter 3, discussion begin with the introduction of modulation instability (MI) and description about twin-core fiber (TCF). Later on pulse propagation equation for TCF is introduced, which is a (3+1)-dimensional coupled NISE with coupling coefficient dispersion (CCD) and other higher order effects such as third order dispersion (TOD), fourth order dispersion (FOD), and self-steepening (SS). By employing a standard linear stability analysis, we obtain analytically the explicit expression for the MI growth rate as a function of spatial and temporal frequencies of the perturbation and the material response time. We investigate three different types of modulational instabilities— spatial, temporal, and spatio-temporal MI in TCF in presence of higher order effects. Despite the fact that the effect of TOD on MI growth rate in these three different types of MI is minimal, the presence of quintic nonlinearity, CCD, FOD, and SS enhances the formation of MI sidebands, both in anomalous as well as normal dispersion regimes. For the spatial case, we studied the variation of MI gain with strength of quintic nonlinearity, while the temporal MI gain crucially depends on strength of quintic nonlinearity, FOD, CCD, and SS terms. So for temporal case we illustrated the impact of all the higher order terms for focussing and defocussing case separately. Thirdly, the spatio-temporal MI has been studied for focussing and defocussing regime.

Chapter 4 is divided into two parts. In first part, we studied the GNLSE with non-Kerr terms, which is short wave equation. We demonstrated that the non-Kerr terms induces different types of bright and dark solitons, which are subjected to constraint relations among the parameters. The higher order terms are responsible for compensation of the nonlinear absorption when pulse propagate through highly nonlinear media and play an important role for the post-soliton compression to get stable compressed optical pulse. These femtosecond pulses are useful to increase the capacity of carrying information in order to make ultra fast communication which is useful for trans-continental and trans-ocean. In second part, we have investigated the modulational instability for NLSE with source term by using linear stability analysis. We have explored various regions where MI is possible. We have also illustrated the variation of MI gain with source term coefficient for focussing as well as for de-focussing nonlinearity.

In conclusion, Chapter 5 discusses the results obtained in the preceding chapters and provides a summary of key findings.

Bibliography

[1] S Strogatz. *Nonlinear dynamics and chaos: With applications to physics, biology, chemistry and engineering.* Westview Press, 2001.

[2] M Lakshmanan and S Rajasekar. *Nonlinear dynamics: Integrability, chaos and patterns.* Springer, 2003.

[3] DH Peregrine. Water waves, nonlinear Schrödinger equations and their solutions. *The Journal of the Australian Mathematical Society*, 25(01):16–43, 1983.

[4] RW Boyd. Nonlinear optics 3rd edn (New York: Academic). 2008.

[5] W Mro, T Ogino, K Minami, and S Takeda. Modified nonlinear Schrödinger equation for alfven waves propagating along the magnetic field in cold plasmas. *Journal of Physical Society of Japan*, 41:265–271, 1976.

[6] MV Goldman. Strong turbulence of plasma waves. *Reviews of Modern Physics*, 56(4):709–735, 1984.

[7] VE Zakharov and SV Manakov. On the complete integrability of a nonlinear Schrödinger equation. *Teoreticheskaya i Matematicheskaya Fizika*, 19(3):332–343, 1974.

[8] JD Jackson and F Ronald. Classical electrodynamics. *American Journal of Physics*, 67:841, 1999.

[9] YR Shen. The principles of nonlinear optics. *New York, Wiley-Interscience*, 1:575, 1984.

[10] M Schubert and B Wilhelmi. Nonlinear optics and quantum electronics. 1986.

[11] PN Butcher and D Cotter. *The elements of nonlinear optics*, volume 9. Cambridge University Press, 1991.

[12] KJ Blow and D Wood. Theoretical description of transient stimulated raman scattering in optical fibers. *IEEE Journal of Quantum Electronics*, 25(12):2665–2673, 1989.

[13] PV Mamyshev and SV Chernikov. Ultrashort-pulse propagation in optical fibers. *Optics Letters*, 15(19):1076–1078, 1990.

[14] SV Chernikov and PV Mamyshev. Femtosecond soliton propagation in fibers with slowly decreasing dispersion. *Journal of Optical Society of America B*, 8(8):1633–1641, 1991.

[15] D Alterman and J Rauch. Diffractive short pulse asymptotics for nonlinear wave equations. *Physics Letters A*, 264(5):390–395, 2000.

[16] D Alterman and J Rauch. Diffractive nonlinear geometric optics for short pulses. *SIAM journal on mathematical analysis*, 34(6):1477–1502, 2003.

[17] T Schäfer and CE Wayne. Propagation of ultra-short optical pulses in cubic nonlinear media. *Physica D: Nonlinear Phenomena*, 196(1):90–105, 2004.

[18] Y Chung, CKRT Jones, T Schäfer, and CE Wayne. Ultra-short pulses in linear and nonlinear media. *Nonlinearity*, 18(3):1351–1371, 2005.

[19] M Gedalin, TC Scott, and YB Band. Optical solitary waves in the higher order nonlinear Schrödinger equation. *Physical Review Letters*, 78(3):448–451, 1997.

[20] CN Kumar and P Durganandini. New phase modulated solutions for a higher-order nonlinear Schrödinger equation. *Pramana–J. Phys*, 53(2):271–277, 1999.

[21] B Li. Exact soliton solutions for the higher-order nonlinear Schrödinger equation. *International Journal of Modern Physics*, 16(8):1225–1237, 2005.

[22] PS Lomdahl, OH Soerensen, and PL Christiansen. Soliton excitations in josephson tunnel junctions. *Physical Review B*, 25(9):5737–5748, 1982.

[23] TS Raju, PK Panigrahi, and K Porsezian. Self-similar propagation and compression of chirped self-similar waves in asymmetric twin-core fibers with nonlinear gain. *Physical Review E*, 72(4):046612, 2005.

[24] AW Snyder and J Love. *Optical waveguide theory*, volume 190. Springer, 1983.

[25] BA Malomed. Bound solitons in a nonlinear optical coupler. *Physical Review E*, 51(2):R864–R866, 1995.

[26] G Cohen. Soliton interaction with an external traveling wave. *Physical Review E*, 61(1):874–879, 2000.

[27] DJ Kaup and AC Newell. Theory of nonlinear oscillating dipolar excitations in one-dimensional condensates. *Physical Review B*, 18(10):5162–5167, 1978.

[28] AK Sarma and M Saha. Modulational instability of coupled nonlinear field equations for pulse propagation in a negative index material embedded into a kerr medium. *Journal of Optical Society of America B*, 28(4):944–948, 2011.

[29] R Gupta, TS Raju, CN Kumar, and PK Panigrahi. Modulational instability of copropagating light beams induced by cubic–quintic nonlinearity in nonlinear negative-index material. *Journal of Optical Society of America B*, 29(12):3360–3366, 2012.

[30] A Hasegawa. *Optical solitons in fibers.* Springer, 1989.

[31] VI Kruglov, AC Peacock, and JD Harvey. Exact self-similar solutions of the generalized nonlinear Schrödinger equation with distributed coefficients. *Physical Review Letters*, 90(11):113902, 2003.

[32] GP Agrawal. *Nonlinear fiber optics.* Academic Press, 2007.

[33] F Dalfovo, S Giorgini, LP Pitaevskii, and S Stringari. Theory of Bose-Einstein condensation in trapped gases. *Reviews of Modern Physics*, 71(3):463–512, 1999.

[34] L Pitaevskii, S Stringari, and A Leggett. Bose-Einstein condensation. *Physics Today*, 57(10):74–76, 2004.

[35] HH Chen and CS Liu. Solitons in nonuniform media. *Physical Review Letters*, 37(11):693–697, 1976.

[36] HH Chen and CS Liu. Nonlinear wave and soliton propagation in media with arbitrary inhomogeneities. *Physics of Fluids*, 21(3):377–380, 1978.

[37] AC Newell. Nonlinear tunnelling. *Journal of Mathematical Physics*, 19(5):1126–1133, 1978.

[38] H Ruiyu, L Lu, L Zhonghao, X Wenrui, and Z Guosheng. A new approach to exact soliton solutions and soliton interaction for the nonlinear Schrödinger equation with variable coefficients. *Optics Communications*, 236(1):79–86, 2004.

[39] CQ Dai, YY Wang, Q Tian, and JF Zhang. The management and containment of self-similar rogue waves in the inhomogeneous nonlinear Schrödinger equation. *Annals of Physics*, 327(2):512–521, 2012.

[40] Russell JS. Reports on waves. *Communications on Pure and Applied Mathematics*, 311:390, 1844.

[41] NJ Zabusky and MD Kruskal. Interaction of "solitons" in a collisionless plasma and the recurrence of initial states. *Physical Review Letters*, 15(6):240–243, 1965.

[42] CS Gardner, JM Greene, MD Kruskal, and RM Miura. Method for solving the Korteweg-de Vries equation. *Physical Review Letters*, 19:1095–1097, 1967.

[43] PD Lax. Integrals of nonlinear equations of evolution and solitary waves. *Communications on Pure and Applied Mathematics*, 21(5):467–490, 1968.

[44] AB Shabat and VE Zakharov. Exact theory of two-dimensional self-focusing and one-dimensional self-modulation of waves in nonlinear media. *Soviet Physics JETP*, 34:62–69, 1972.

[45] R Hirota. Exact solution of the Kortewegde Vries equation for multiple collisions of solitons. *Physical Review Letters*, 27(18):1192–1194, 1971.

[46] MJ Ablowitz, DJ Kaup, AC Newell, and H Segur. The inverse scattering transform-fourier analysis for nonlinear problems. *Studies in Applied Mathematics*, 53:249–315, 1974.

[47] A Hasegawa. An historical review of application of optical solitons for high speed communications. *Chaos: An Interdisciplinary Journal of Nonlinear Science*, 10(3):475–485, 2000.

[48] TT Shi and S Chi. Nonlinear photonic switching by using the spatial soliton collision. *Optics Letters*, 15(20):1123–1125, 1990.

[49] MN Islam. Ultrafast all-optical logic gates based on soliton trapping in fibers. *Optics Letters*, 14(22):1257–1259, 1989.

[50] B Oktem, C Ülgüdür, and F Ilday. Soliton–similariton fibre laser. *Nature Photonics*, 4(5):307–311, 2010.

[51] M Suzuki, I Morita, N Edagawa, S Yamamoto, H Taga, and S Akiba. Reduction of gordon-haus timing jitter by periodic dispersion compensation in soliton transmission. *Electronics Letters*, 31(23):2027–2029, 1995.

[52] SV Chernikov, DJ Richardson, DN Payne, and EM Dianov. Soliton pulse compression in dispersion-decreasing fiber. *Optics Letters*, 18(7):476–478, 1993.

[53] GP Agrawal. Amplification of ultrashort solitons in erbium-doped fiber amplifiers. *IEEE Photonics technology letters*, 2(12):875–877, 1990.

[54] MH Anderson, JR Ensher, MR Matthews, CE Wieman, and EA Cornell. Observation of Bose–Einstein condensation in a dilute atomic vapor. *Science*, 269(5221):198–201, 1995.

[55] KB Davis, MO Mewes, MR Van Andrews, NJ Van Druten, DS Durfee, DM Kurn, and W Ketterle. Bose-Einstein condensation in a gas of sodium atoms. *Physical Review Letters*, 75(22):3969–3973, 1995.

[56] R Carretero-González, DJ Frantzeskakis, and PG Kevrekidis. Nonlinear waves in Bose–Einstein condensates: Physical relevance and mathematical techniques. *Nonlinearity*, 21(7):R139, 2008.

[57] VE Zakharov. Stability of periodic waves of finite amplitude on the surface of a deep fluid. *Journal of Applied Mechanics and Technical Physics*, 9(2):190–194, 1968.

[58] A Scott. Davydov's soliton. *Physics Reports*, 217(1):1–67, 1992.

[59] W Alka, A Goyal, and CN Kumar. Nonlinear dynamics of DNA–Riccati generalized solitary wave solutions. *Physics Letters A*, 375(3):480–483, 2011.

[60] A Barone, F Esposito, CJ Magee, and AC Scott. Theory and applications of the sine-Gordon equation. *La Rivista del Nuovo Cimento*, 1(2):227–267, 1971.

[61] DK Campbell, S Flach, and YS Kivshar. Localizing energy through nonlinearity and discreteness. *Physics Today*, 57(1):43–49, 2004.

[62] CS Gardner and GK Morikawa. The effect of temperature on the width of a small-amplitude, solitary wave in a collision-free plasma. *Communications on Pure and Applied Mathematics*, 18(1-2):35–49, 1965.

[63] RZ Sagdeev. Cooperative phenomena and shock waves in collision-less plasmas. *Reviews of Plasma Physics*, 4:23, 1966.

[64] R Rajaraman. *Solitons and instantons: an introduction to solitons and instantons in quantum field theory.* North-Holland Amsterdam, 1982.

[65] W Chen and DL Mills. Gap solitons and the nonlinear optical response of superlattices. *Physical Review Letters*, 58(2):160–163, 1987.

[66] O Zobay, S Pötting, P Meystre, and EM Wright. Creation of gap solitons in bose-einstein condensates. *Physical Review A*, 59(1):643–648, 1999.

[67] S Flach and C R Willis. Discrete breathers. *Physics Reports*, 295(5):181–264, 1998.

[68] S Aubry. Breathers in nonlinear lattices: existence, linear stability and quantization. *Physica D: Nonlinear Phenomena*, 103(1):201–250, 1997.

[69] B Kibler, J Fatome, C Finot, G Millot, G Genty, B Wetzel, N Akhmediev, F Dias, and JM Dudley. Observation of kuznetsov-ma soliton dynamics in optical fibre. *Scientific Reports*, 2(463), 2012.

[70] JM Dudley, G Genty, F Dias, B Kibler, and N Akhmediev. Modulation instability, Akhmediev breathers and continuous wave supercontinuum generation. *Optics Express*, 17(24):21497–21508, 2009.

[71] GP Agrawal and C Headley. Kink solitons and optical shocks in dispersive nonlinear media. *Physical Review A*, 46(3):1573–1577, 1992.

[72] DR Solli, C Ropers, P Koonath, and B Jalali. Optical rogue waves. *Nature*, 450(7172):1054–1057, 2007.

[73] VG Veselago. The electrodynamics of substances with simultaneously negative values of electrical permittivity ϵ and mgnetic permeability μ. *Physics-Uspekhi*, 10(4):509–514, 1968.

[74] JB Pendry, AJ Holden, WJ Stewart, and I Youngs. Extremely low frequency plasmons in metallic mesostructures. *Physical Review Letters*, 76(25):4773–4776, 1996.

[75] JB Pendry, AJ Holden, DJ Robbins, and WJ Stewart. Magnetism from conductors and enhanced nonlinear phenomena. *Microwave Theory and Techniques, IEEE Transactions*, 47(11):2075–2084, 1999.

[76] DR Smith, WJ Padilla, DC Vier, SC Nemat-Nasser, and S Schultz. Composite medium with simultaneously negative permeability and permittivity. *Physical Review Letters*, 84(18):4184–4187, 2000.

[77] RA Shelby, DR Smith, and S Schultz. Experimental verification of a negative index of refraction. *Science*, 292(5514):77–79, 2001.

[78] JB Pendry. Negative refraction makes a perfect lens. *Physical Review Letters*, 85(18):3966–3969, 2000.

[79] Y Liu, G Bartal, DA Genov, and X Zhang. Subwavelength discrete solitons in nonlinear metamaterials. *Physical Review Letters*, 99(15):153901, 2007.

[80] G D'Aguanno, N Mattiucci, M Scalora, and MJ Bloemer. Bright and dark gap solitons in a negative index fabry-perot etalon. *Physical Review Letters*, 93(21):213902, 2004.

Chapter 2

Solitary wave solutions in negative index materials

2.1 Introduction

In this chapter, we discuss about NIMs, and also investigate the possibility of soliton-like solutions in NIMs. This chapter is divided into three sections. In first section, we present a detailed analysis for the existence of dark, bright solitary waves and fractional-transform solutions in a NLSE model for competing cubic-quintic and higher-order nonlinearities with dispersive permittivity and permeability. Parameter domains are delineated in which these ultrashort optical pulses exist in NIMs.

The second section is special case of section one. In this section, we consider the same model equation in the presence of external source but the effects like quintic nonlinearity and self-steepening are absent. For this model, we obtained travelling wave solutions for pulse propagation in NIMs in the presence of external source. The reported solutions are necessarily of the fractional-type containing trigonometric and hyperbolic functions.

In third section, we investigate the existence of bright, dark solitons, and periodic solutions for the coupled generalized nonlinear Schrödinger equation governing the pulse propagation in NIMs. It is observed that depending upon nature of dispersion different form of travelling wave propagate through NIMs for specific value of velocity and initial chirp. We also obtained expressions for nonlinear chirp associated with each of these solutions.

2.2 Background

As discussed in first chapter, the materials with simultaneously negative real parts of the dielectric permittivity ϵ and magnetic permeability μ has negative refractive index n [1]. We have know that NIMs are artificially designed and demonstrate many peculiar properties due which these materials have attracted the attention of large number of research groups. Recently various research groups have proposed and studied different potential applications of NIMs [2, 3]. In this context, study of nonlinear pulse propagation, particularly optical solitons is new and exciting field of research [4, 5]. This is mainly due to the fact that apart from the richness of physics, as NIMs are artificially structured materials, we might have flexibility of controlling these pulses as per our requirement. Since there are many differences between ordinary materials and NIMs, it was a complex task to derive pulse propagation equation for NIMs. The first significant step in this direction was taken by Scalora et al. [6]. They considered dispersive nature of electric permittivity ϵ, magnetic permeability μ and developed GNLSE for NIMs without taking nonlinear magnetization into account. After development of GNLSE for NIMs a lot of progress has been made in study of pulse propagation, which also paved a way for the effective fabrication of such materials. GNLSE was studied by various authors in the context of pulse propagation [7, 8, 9]. Later on Lazarides and Tsironis derived a system of coupled NLSE (CNLSE) for the propagating envelopes of electric and magnetic fields in an homogeneous, isotropic, quasi-one-dimensional NIMs [10]. This model have been studied to explore the nonlinear properties of NIMs such as modulation instability (MI) [11]. Since then a lot of development has taken place in the study of NIMs. More recently, nonlinear effects in NIMs have been extensively studied, including second-harmonic generation [12], parametric amplification [13], modulation instability [5], and soliton propagation [14, 15]. It is well known that nonlinear NIMs not only possess dispersive magnetic permeability but also dispersive electric permittivity which leads to the difference between the dynamic models for the envelopes of the electromagnetic wave in NIMs and in ordinary materials, and support rich localized modes [14, 15]. These localized modes in nonlinear NIMs can take the forms of gap solitons [14], spatial solitons [15], spatiotemporal solitons [16, 10], and temporal solitons [17, 18]. In particular, small-amplitude dark and bright solitons on the background of a continuous wave in NIMs have been obtained by employing small-amplitude soliton approximation method [17]. Dark solitons and their interactions in metamaterials have been studied by using a Korteweg-de Vries description [18].

Motivated by these works and keeping into account various interesting features of NIMs and their future applications, we investigate the soliton solutions for pulse propagation through NIMs. We study the influence of quintic nonlinearity, self-steepening coefficient, source term on soliton-like solutions. We further study the solitary wave solutions and the corresponding chirping for each solution of coupled NLSE's.

2.3 Ultrashort pulse propagation in NIMs

2.3.1 Governing equation

NIMs have a regular periodic structure with unit cells having size much smaller than the wavelengths of propagating electromagnetic (E. M.) waves. Therefore, NIMs may be considered as continuous and homogeneous according to effective medium theory, and may be described by dispersive permittivity $\epsilon(\omega)$ and dispersive permeability $\mu(\omega)$. We consider the propagation of E. M. waves in an isotropic and homogeneous NIMs whose $\epsilon(\omega)$ and $\mu(\omega)$ can be expanded in Taylor's series [6] as

$$\omega\epsilon(\omega) = \sum_{n=0}^{\infty}[\frac{\partial^n[\omega\epsilon(\omega)]}{\partial\omega^n} \mid_{\omega-\omega_0} \frac{(\omega-\omega_0)^n}{n!}], \tag{2.1}$$

and

$$\omega\mu(\omega) = \sum_{n=0}^{\infty}[\frac{\partial^n[\omega\mu(\omega)]}{\partial\omega^n}\mid_{\omega-\omega_0}\frac{(\omega-\omega_0)^n}{n!}], \tag{2.2}$$

where ω_0 is carrier frequency of incident E. M. wave. Using above two expressions in Maxwell's equations, we get

$$\frac{\partial E_x(z,t)}{\partial z} = \frac{i}{c}\exp i(kz-\omega_0 t)\sum_{n=0}^{\infty}\left(i^n\frac{\partial^n[\omega\mu(\omega)]}{\partial\omega^n}\mid_{\omega-\omega_0}\frac{1}{n!}\frac{\partial^n H(z,t)}{\partial t^n}\right), \tag{2.3}$$

and

$$\frac{\partial H_y(z,t)}{\partial z} = \frac{i}{c}\exp i(kz-\omega_0 t)\sum_{n=0}^{\infty}\left(i^n\frac{\partial^n[\omega\epsilon(\omega)]}{\partial\omega^n}\mid_{\omega-\omega_0}\frac{1}{n!}\frac{\partial^n E(z,t)}{\partial t^n}-\frac{1}{c}\frac{\partial P_{nl}(z,t)}{\partial t}\right), \tag{2.4}$$

where $E_x(z,t) = E(z,t)e^{i(kz-\omega t)}$ and $H_y(z,t) = H(z,t)e^{i(kz-\omega t)}$. $E(z,t)$ and $H(z,t)$ are envelope of the electric and magnetic fields respectively. We know that in nonlinear medium the polarization can be written as $P_{nl}(z,t) = \chi^{(3)}\ |E|^2E + \chi^{(5)}\ |E|^5E +$ ...., where $\chi^{(n)}$ is n_{th} order nonlinear susceptibility. Eq. (2.3) and Eq. (2.4) are general equations because these include dispersion effect to any desired level, but for ultra short pulse we need dispersion effect up to third order so we can write above two equations as

$$\alpha\frac{\partial E}{\partial\tau} + i\frac{\alpha'}{4\pi}\frac{\partial^2 E}{\partial\tau^2} - \frac{1}{6}\frac{\alpha''}{4\pi^2}\frac{\partial^3 E}{\partial\tau^3} = i\beta\epsilon E - i\beta nH - \frac{\partial H}{\partial\xi} + i\beta\chi^{(3)}|E|^2E - \chi^{(3)}\frac{\partial(|E|^2E)}{\partial\tau}, \tag{2.5}$$

$$\gamma\frac{\partial H}{\partial\tau} + i\frac{\gamma'}{4\pi}\frac{\partial^2 H}{\partial\tau^2} - \frac{1}{6}\frac{\gamma''}{4\pi^2}\frac{\partial^3 H}{\partial\tau^3} = i\beta\mu H - i\beta nE - \frac{\partial E}{\partial\xi}, \tag{2.6}$$

where

$\alpha = \frac{\partial[\omega_1\epsilon(\omega_1)]}{\partial\omega_1}$, $\alpha' = \frac{\partial^2[\omega_1\epsilon(\omega_1)]}{\partial^2\omega_1}$, $\alpha'' = \frac{\partial^3[\omega_1\epsilon(\omega_1)]}{\partial^3\omega_1}$, $\gamma = \frac{\partial[\omega_1\mu(\omega_1)]}{\partial\omega_1}$

$\gamma' = \frac{\partial^2[\omega_1\mu(\omega_1)]}{\partial^2\omega_1}$, $\gamma'' = \frac{\partial^3[\omega_1\mu(\omega_1)]}{\partial^3\omega_1}$, $z = \frac{\xi}{\lambda_p}$, $t = \frac{c\tau}{\lambda_p}$,

$\beta = 2\pi\omega_1$, $\omega_1 = \omega/\omega_p$, $V_g = \frac{2n}{(\epsilon\gamma+\mu\alpha)}$,

$\chi^{(3)}$ and $\chi^{(5)}$ are the third-order and fifth-order susceptibility respectively, which comes due to nonlinear response of material medium during interaction of bound electrons when intense electric field is applied. λ_p is the corresponding wavelength. Combining Eq. (2.5) and Eq. (2.6) and eliminating magnetic field, we obtain

$$\begin{aligned}\frac{\partial E}{\partial \xi}+\frac{\epsilon\gamma+\mu\alpha}{2n}\frac{\partial E}{\partial \tau}=&\frac{i}{2\beta n}\left(\frac{\partial^2 E}{\partial \xi^2}-\alpha\gamma\frac{\partial^2 E}{\partial \tau}\right)+\frac{i}{8\pi\beta n}\left(\alpha\gamma'+\gamma\alpha'+\beta\frac{\epsilon\gamma''+\mu\alpha''}{6\pi}\right)\frac{\partial^3 E}{\partial \tau^3}\\&+\frac{i\beta\mu\chi^(3)}{2n}|E|^2E-\frac{(\gamma+\mu)\chi^{(3)}}{2n}\frac{\partial(|E|^2E)}{\partial\tau}-i\frac{\epsilon\gamma'+\mu\alpha'}{8\pi n}\frac{\partial^2 E}{\partial \tau^2}\\&-\frac{i\chi^{(3)}}{2\beta n}\left(\gamma+\frac{\beta\gamma'}{4\pi}\right)\frac{\partial^2(|E|^2E)}{\partial\tau^2}.\end{aligned}\tag{2.7}$$

From Eq. (2.7), it is clear that the wave propagate at group velocity $V_g = 2n/(\epsilon\gamma+\mu\alpha)$ in the unit of c. For transparent NIMs [6, 19], $\alpha > 0$, $\gamma > 0$, and $n < 0$, therefore, V_g is always positive. Introducing a retarded coordinate $\partial/\partial Z = \partial/\partial\xi + (1/V_g)(\partial/\partial\tau)$, Eq. (2.7) can be written as

$$\begin{aligned}\frac{\partial E}{\partial Z}=&\frac{i}{2\beta n}\left(\frac{1}{V_g^2}-\alpha\gamma-\beta\frac{\epsilon\gamma'+\mu\alpha'}{4\pi}\right)\frac{\partial^2 E}{\partial \tau^2}+\frac{i}{8\pi\beta n}\left(\alpha\gamma'+\gamma\alpha'+\beta\frac{\epsilon\gamma''+\mu\alpha''}{6\pi}\right)\frac{\partial^3 E}{\partial \tau^3}\\&+\frac{i\beta\mu\chi^(3)}{2n}|E|^2E+\frac{i}{2\beta n}\left(\frac{\partial^2 E}{\partial Z^2}-\frac{2}{V_g}\frac{\partial^2 E}{\partial Z\partial\tau}\right)-\frac{(\gamma+\mu)\chi^{(3)}}{2n}\frac{\partial(|E|^2E)}{\partial\tau}\\&-\frac{i\chi^{(3)}}{2\beta n}\left(\gamma+\frac{\beta\gamma'}{4\pi}\right)\frac{\partial^2(|E|^2E)}{\partial\tau^2}.\end{aligned}\tag{2.8}$$

Differentiating Eq. (2.8) with respect to Z and τ, respectively, and neglecting the fourth-order linear derivative and third-order nonlinear temporal derivative [20], we obtain $\partial^2E/\partial Z^2$ and $\partial^2E/\partial Z\partial\tau$. Substituting $\partial^2E/\partial Z^2$ and $\partial^2E/\partial Z\partial\tau$ in Eq. (2.8) and taking $\tau = t$ we obtain a generalized higher-order NLS equation.

$$\frac{\partial E}{\partial Z}-iP\frac{\partial^2 E}{\partial t^2}-Q\frac{\partial^3 E}{\partial t^3}-i\gamma|E|^2E+iR|E|^4E-\Lambda\frac{\partial(|E|^2E)}{\partial t}+iS\frac{\partial^2(|E|^2E)}{\partial t^2}=0,\tag{2.9}$$

where P is group velocity dispersion (GVD) coefficient, Q is third-order dispersion (TOD) coefficient, γ and R represent cubic and quintic nonlinear coefficients respectively, Λ represents self-steepening (SS) coefficient and S represents second-order nonlinear dispersive coefficient. All parameters discussed above are defined as

$$P=\frac{1}{2\beta n}\left[\frac{1}{V_g^2}-\alpha\gamma-\beta(\alpha\gamma'+\mu\alpha')/4\pi\right],$$

$$Q = \frac{1}{2\beta n}\left[\frac{P}{V_g} + \beta(\alpha\gamma'' + \mu\alpha'')/24\pi^2 + (\alpha\gamma' + \mu\alpha')/4\pi\right],$$

$$\gamma = \frac{\beta\mu\chi^{(3)}}{2n},$$

$$R = \frac{\beta\mu^2(\chi^{(3)})^2}{8n^3},$$

$$\Lambda = \frac{\chi^{(3)}}{2n}\left[\frac{\mu}{V_g n} - (\gamma + \mu)\right],$$

$$S = \frac{\mu\chi^{(3)}}{2n}\left[\frac{P}{4n} + \frac{\gamma}{\mu\beta} + \frac{\gamma'}{4\pi\mu}\right].$$

The variation of all above parameters with normalized frequency is depicted in Fig. 2.1. Eq. (2.9) with linear and nonlinear higher-order effects describes the

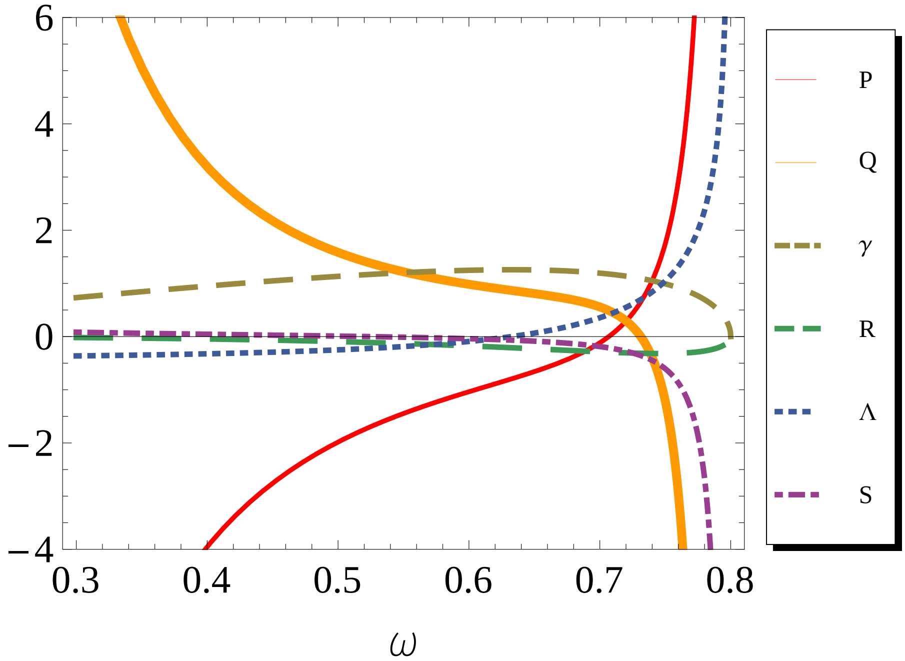

Figure 2.1: Curves of GVD, TOD, cubic nonlinearity, quintic nonlinearity, self-steepening and second order nonlinear dispersive term versus normalized frequency in focusing NIMs for $\frac{\omega_m}{\omega_p} = 0.8$. Here, P is plotted in units of $\frac{1}{c\ \omega_p}$, Q in units of $\frac{1}{c\ \omega_p^2}$, and γ, Λ, S are plotted in units of $\chi^{(3)}$ and R in units of $(\chi^{(3)})^2$. Here $\chi^{(3)} = 10^{-10}$ (esu).

propagation of few cycle ultrashort pulses in NIMs. For inhomogeneous NIMs we can take the distributive coefficients which could be a more realistic approach for study of NIMs. Recently Li et al. [8] have reported gray solitary wave solutions for this equation. Also, Boardman et al. [21] have reported temporal solitons in magneto-optic and metamaterial waveguides. Further neglecting the higher order effects such as quintic nonlinearity and nonlinear dispersion then Eq. (2.9) will reduce to equation discussed in ref. [22], which admits the bright and dark solitons. The Eq. (2.9) is a model that is used to describe few cycle pulses. The model parameters are related to ϵ and μ so one can easily analyze the effect of these parameters on propagation of ultrashort pulses. As per Drude model [19], $\epsilon(\omega_1) = 1 - \frac{1}{\omega_1(\omega_1+i\gamma_e)}$ and $\mu(\omega_1) = 1 - \frac{\omega_m^2/\omega_p^2}{\omega_1(\omega_1+i\gamma_m)}$, where $\omega_1 = \omega/\omega_p$, ω_p and ω_m are electric and magnetic plasma frequencies. Also, $\gamma_e = \gamma_m = 4.5 \times 10^{-4}$ are electric and magnetic loss terms, which result in low absorption [23, 24].

2.3.2 Solitary wave solutions

In order to find exact solitary wave solutions of Eq. (2.9), we have chosen the following form for the complex envelope travelling wave solution

$$E(\xi, z) = \alpha(\xi) e^{i(\psi(\xi)-kz)}, \tag{2.10}$$

where $\xi = \eta t - uz$ is the travelling coordinate and α and ψ are real functions of ξ. Substituting Eq. (2.10) into Eq. (2.9) and separating real and imaginary parts we obtain

$$\begin{aligned} -u\alpha' + \eta^2 \frac{P}{2}\alpha\psi'' + \eta^2 P\alpha'\psi' - Q\eta^3\alpha''' + 3\eta^3 Q\alpha\psi'\psi'' + 3\eta^3 Q\alpha'(\psi')^2 - 3\eta\Lambda\alpha^2\alpha' \\ - 6\eta^2 S\alpha^2\alpha'\psi' - \eta^2 S\alpha^3\psi'' = 0, \end{aligned} \tag{2.11}$$

$$\begin{aligned} -u\alpha\psi' - k\alpha - \frac{P}{2}\eta^2\alpha'' + \frac{P}{2}\eta^2\alpha(\psi')^2 - 3Q\eta^3\alpha'\psi'' - 3Q\eta^3\alpha''\psi' - Q\eta^3\alpha\psi''' \\ + Q\eta^3\alpha(\psi')^3 - \gamma\alpha^3 + R\alpha^5 - \Lambda\eta\alpha^3\psi' + 6S\eta^2\alpha(\alpha')^2 + 3S\eta^2\alpha^2\alpha'' \\ - S\eta^2\alpha^3(\psi')^2 = 0. \end{aligned} \tag{2.12}$$

Assuming $\psi' = m$ (a constant) and substituting in Eq. (2.11) and Eq. (2.12), we arrive at the coupled equations in α and ψ,

$$-u\alpha' + m\eta^2 P\alpha' + 3m^2\eta^3 Q\alpha' - Q\eta^3\alpha''' - 3\eta\Lambda\alpha^2\alpha' - 6m\eta^2 S\alpha^2\alpha' = 0, \tag{2.13}$$

$$\begin{aligned}&-mu\alpha - k\alpha - \frac{P}{2}\eta^2\alpha'' + \frac{m^2P}{2}\eta^2\alpha - 3mQ\eta^3\alpha'' + m^3Q\eta^3\alpha - \gamma\alpha^3 + R\alpha^5\\ &-m\Lambda\eta\alpha^3 + 6S\eta^2\alpha(\alpha')^2 + 3S\eta^2\alpha^2\alpha'' - m^2S\eta^2\alpha^3 = 0.\end{aligned} \tag{2.14}$$

Integrating Eq. (2.13), we obtain

$$\alpha'' = a\alpha + b\alpha^3 + c_1, \tag{2.15}$$

where $a = \frac{3Q\eta^3m^2+P\eta^2m-u}{Q\eta^3}$, $b = -\frac{\eta\Lambda+2\eta^2Sm}{Q\eta^3}$ and c_1 is a integration constant. Substituting Eq. (2.15) into the Eq. (2.14), and equating the coefficients of α^i's ($i = 1, 3, 5$) to zero, we get a set of equations given as

$$\begin{aligned}&-um - k + \frac{P}{2}\eta^2(m^2 - a) - 3Q\eta^3ma + Q\eta^3m^3 + 6S\eta^2c_2 = 0,\\ &-\frac{P}{2}\eta^2 b - 3Q\eta^3mb - \gamma - \Lambda\eta m + 9S\eta^2a - S\eta^2m^2 = 0,\\ &R + 6\eta^2Sb = 0.\end{aligned} \tag{2.16}$$

Here we have assumed $c_1 = 0$ to avoid complex calculations. Solving these equations consistently, we obtain the following relations

$$\begin{aligned}&u = \eta\left(\frac{26Q\nu^2}{9} + \left(\frac{Q^2R}{18S^2} + P - \frac{Q\Lambda}{9S}\right)\nu - \frac{Q\gamma}{9S} + \frac{PQR}{108S^2}\right),\\ &k = Q\nu^3 + \frac{P}{2}\nu^2 - um + \left(6Sc_2 - 3Qa\nu - \frac{P}{2}a\right)\eta^2,\\ &\text{and} \qquad m = \frac{\nu}{\eta},\end{aligned} \tag{2.17}$$

for $\nu = \frac{QR}{12S^2} - \frac{\Lambda}{2S}$. Here c_2 is a integration constant which arises upon integrating the Eq. (2.15) as

$$(\alpha')^2 = a\alpha^2 + \frac{b}{2}\alpha^4 + c_2. \tag{2.18}$$

Eq. (2.18) is a well known first-order ordinary differential equation which can be solved for dark and bright solitary wave solutions for different parametric conditions [25].

Dark solitary wave

For $a < 0$, $b > 0$ and $c_2 = \frac{a^2}{2b}$, Eq. (2.18) can be solved for dark solitary wave solutions of the form

$$\alpha(\xi) = \sqrt{\frac{-a}{b}} \tanh\left(\sqrt{\frac{-a}{2}}\xi\right). \tag{2.19}$$

The complete solution for Eq. (2.9) reads

$$E(t,z) = \sqrt{\frac{-a}{b}} \tanh\left(\sqrt{\frac{-a}{2}}\xi\right) e^{i(m\xi - kz)}. \tag{2.20}$$

The typical profile for normalized intensity of dark solitary wave solutions is depicted in Fig. 2.3.

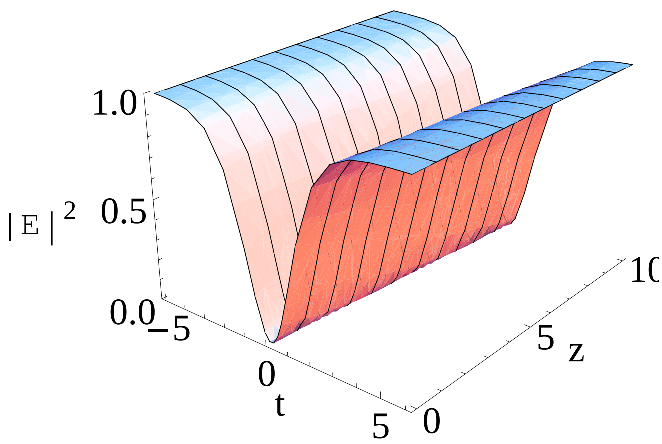

Figure 2.2: Evolution of dark solitary waves for $\frac{\omega_m}{\omega_p} = 0.8$. Here, intensity of dark solitary wave is plotted in normalized form. The physical units of intensity is $(\text{statvolts/cm})^2$, z in units of nm and t in units of fs.

Bright solitary wave

For $a > 0$, $b < 0$ and $c_2 = 0$, Eq. (2.18) can be solved for bright solitary wave solutions given by

$$\alpha(\xi) = \sqrt{\frac{-2a}{b}} \operatorname{sech}\left(\sqrt{a}\xi\right), \tag{2.21}$$

For this case, the complete solution for Eq. (2.9) reads

$$E(t,z) = \sqrt{\frac{-2a}{b}} \operatorname{sech}\left(\sqrt{a}\xi\right) e^{i(m\xi - kz)}. \tag{2.22}$$

The typical profile for normalized intensity of bright solitary wave solutions is depicted in Fig. 2.3.

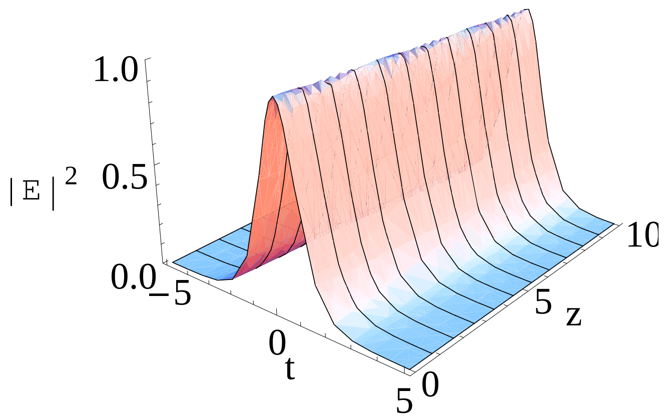

Figure 2.3: Evolution of bright solitary waves for $\frac{\omega_m}{\omega_p} = 0.8$. Here, intensity of bright solitary wave is plotted in normalized form. The physical units of intensity is $(\text{statvolts/cm})^2$, z in units of nm and t in units of fs.

Hence the existence of dark or bright solitary wave solutions for Eq. (2.9) depends on the sign of variables a and b which in turn depends on normalized frequency through various equation parameters. In the focusing NIMs for $\frac{\omega_m}{\omega_p} = 0.8$, the condition for dark solitary wave solutions i.e. $a < 0$ and $b > 0$, should be fulfilled in the frequency range of $0.36 \leq \omega \leq 0.53$. On the other hand, condition for bright solutions i.e. $a > 0$ and $b < 0$, do not exist for any range of ω. However a change in the size of element of NIMs may influence the plasma frequencies of electric and magnetic fields, which results in the change of model parameters of equation Eq.

(2.9). This property may provide possibilities for the formation of bright solitons in NIMs. In Fig. 2.4, we have depicted the evolution of dark solitary wave for $\omega = 0.4$ and $\frac{\omega_m}{\omega_p} = 0.8$. In Fig. 2.1, the values of various model parameters used for $\omega = 0.4$ are $P = -3.95304,\ Q = 3.19295,\ \gamma = 9.49928 \times 10^{-11},\ R = -4.52347 \times 10^{-22},\ \Lambda = -3.2397 \times 10^{-11}$ and $S = 4.39908 \times 10^{-12}$. The corresponding wave parameters are found to be $\eta = 1,\ u = 91.446,\ m = -2.53729$ and $k = 34.0524$.

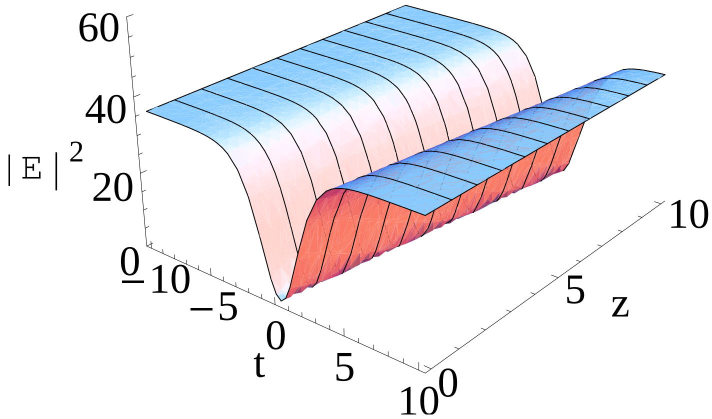

Figure 2.4: Evolution of dark solitary wave in focusing NIMs for $\omega = 0.4$, $\lambda_p = 1\ \mu$m and $\frac{\omega_m}{\omega_p} = 0.8$. The intensity is plotted in units of $10^{10} \times (\text{statvolts/cm})^2$, z in units of nm and t in units of fs.

2.3.3 Fractional-transform solutions in absence of quintic nonlinearity and second-order nonlinear dispersive term

In the absence of quintic nonlinearity and second-order nonlinear dispersion term, we obtain very interesting fractional-transform solutions. For $R = 0$ and $S = 0$, both of the Eqs. (2.13) and (2.14) can be solved consistently to obtain

$$\alpha'' = a\alpha + b\alpha^3 + c_1, \tag{2.23}$$

for $a = \frac{1}{Q\eta^3}(Pm\eta^2 + 3Qm^2\eta - u)$, $b = \frac{-6\gamma}{P\eta^2}$, $m = \frac{-\gamma}{\Lambda\eta}$ and $K = Qm^3\eta^3 + \frac{P}{2}m^2\eta^2 - um$, along with a constraint condition on self-steeping parameter as $\Lambda = \frac{6Q\gamma}{P}$.

Eq. (2.23) can be solved for travelling wave solutions by using a fractional transformation [26, 27]

$$\alpha(\xi) = \frac{A + By^2(\xi)}{1 + Dy^2(\xi)}, \tag{2.24}$$

which maps the solutions of Eq.(2.23) to the elliptic equation $y'' \pm py \pm qy^3 = 0$, where p and q are real, provided the determinant $AD \neq B$. For explicitness, we consider the case where $y = \mathrm{cn}(\xi, m_0)$ with m_0 as modulus parameter. Then upon substitution of Eq. (2.24) into Eq. (2.23) and equating the coefficients of equal powers of $\mathrm{cn}(\xi, m_0)$ will yield the following consistency conditions:

$$-aA - 2(AD - B)(1 - m_0) - bA^3 - c_1 = 0, \tag{2.25}$$

$$-2aAD - aB + 6(AD - B)D(1 - m_0) - 4(AD - B)(2m_0 - 1) - 3bA^2B - 3c_1D = 0, \tag{2.26}$$

$$-aAD^2 - 2aBD + 4(AD - B)D(2m_0 - 1) + 6(AD - B)m_0 - 3bAB^2 - 3c_1D^2 = 0, \tag{2.27}$$

$$-aBD^2 - 2(AD - B)Dm_0 - bB^3 - c_1D^3 = 0. \tag{2.28}$$

For different values of m_0, we obtain different types of travelling wave solutions.

Periodic solution

For $m_0 = 0$ and $A = 0$, Eq. (2.23) admits the non-singular periodic solution of the following type

$$\alpha(\xi) = \frac{2c_1}{a}\left(\frac{\cos^2\xi}{1 - \frac{2}{3}\cos^2\xi}\right), \tag{2.29}$$

where $a = 4$ and ${c_1}^2 = (-128/27b)$. It is possible if $b = \frac{-6\gamma}{P\eta^2}$ is negative. Using this, the complete solution for GNLSE can be written as

$$E(t, z) = \frac{c_1}{2}\left(\frac{\cos^2\xi}{1 - \frac{2}{3}\cos^2\xi}\right)e^{i(m\xi - kz)}, \tag{2.30}$$

for ${c_1}^2 = (64P\eta^2/81\gamma)$. Here one can find that the solution is consistent only for

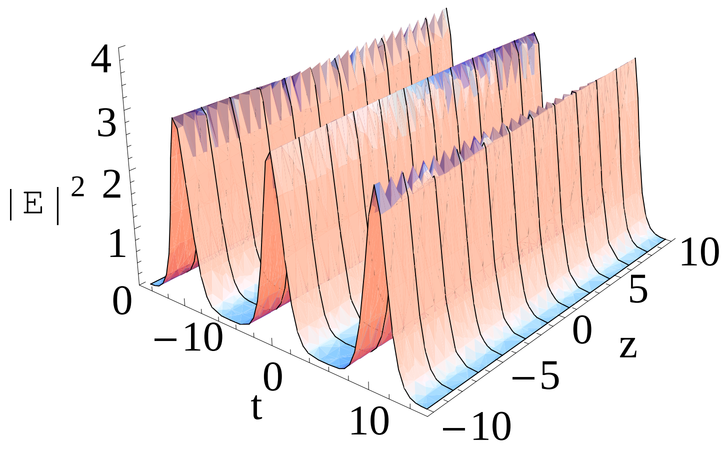

Figure 2.5: Evolution of periodic pulse in focusing NIMs for $\omega = 0.75$, $\lambda_p = 1$ μm and $\frac{\omega_m}{\omega_p} = 0.8$. The intensity is plotted in units of $10^{10} \times (\text{statvolts/cm})^2$, z in units of nm and t in units of fs.

same signs of P and γ, which is possible in specific range of normalized frequency ω. Hence, a physically interesting periodic solution will emerge for normalized frequency in the range of $\omega \geq 0.71$. For example, evolution of periodic solution for $\omega = 0.75$ and $\frac{\omega_m}{\omega_p} = 0.8$, corresponding to $P = 1.74536$, $Q = -1.2109$ and $\gamma = 9.91683 \times 10^{-11}$, is shown in Fig. 2.5. The corresponding wave parameters are found to be $\eta = 1$, $u = 5.05324$, $m = 0.240229$ and $k = -1.18036$. The value of self-steeping parameter, as given by constraint condition, used here is $\Lambda = -4.12807 \times 10^{-10}$.

Dark/bright solitary wave solution

We found general localized solution for the case when the Jacobian elliptic modulus $m_0 = 1$. The set of Eqs. (2.25) to (2.29) can be solved consistently for the unknown parameters A, B, D and for a particular value of c_1. The generic profile of the solution reads

$$\alpha(\xi) = \frac{A + B\ \text{sech}^2\xi}{1 + D\ \text{sech}^2\xi}. \tag{2.31}$$

Since the analytical form of solution is known, a simple maxima-minima analysis can be done to distinguish parameter regimes supporting dark and bright soliton solutions [26]. In this case, when $AD < B$ one gets a bright soliton, whereas if $AD > B$ then a dark soliton exists. The complete solution of GNLSE reads

$$E(t,z) = \left(\frac{A + B\ \mathrm{sech}^2\xi}{1 + D\ \mathrm{sech}^2\xi}\right) e^{i(m\xi - kz)}. \tag{2.32}$$

We have worked out a physically interesting case for $\omega = 0.5$, corresponding to $P = 1.74536$, $Q = -1.2109$ and $\gamma = 9.91683 \times 10^{-11}$, and shown the evolution of bright solitary wave in Fig. 2.6. The various unknown parameters are $A = 9676.83$, $B = -8504.92$, $D = -0.8789$, and corresponding wave parameters are found to be $\eta = 1$, $u = 0.1$, $m = 0.20887$ and $k = -1.08431$. The value of self-steeping parameter is comes out to be $\Lambda = -5.42307 \times 10^{-10}$.

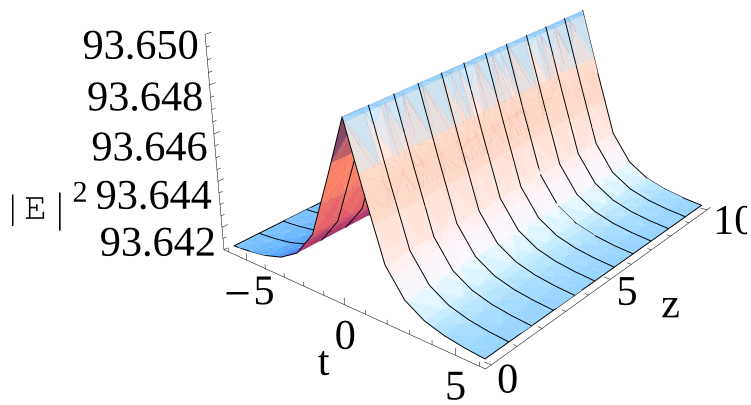

Figure 2.6: Evolution of bright solitary wave in focusing NIMs for $\omega = 0.5$ and $\lambda_p = 1\ \mu$m. The intensity is plotted in units of $10^{10} \times (\text{statvolts/cm})^2$, z in units of nm and t in units of fs.

Pure cnoidal solution

For $0 < m_0 < 1$, we can found different types of cnoidal solutions. We list here one particular case, for $m = 5/8$, $A = 0$ and $D = 1$, we obtain the solution

$$\alpha(\xi) = \frac{-14c_1}{3a}\left(\frac{\mathrm{cn}^2(\xi, m_0)}{1 + \mathrm{cn}^2(\xi, m_0)}\right), \tag{2.33}$$

where $a = -7/2$ and ${c_1}^2 = (9/4b)$. Using this, we found the solution for Eq. (2.9) as

$$E(t,z) = \frac{4c_1}{3}\left(\frac{\mathrm{cn}^2(\xi, m_0)}{1+\mathrm{cn}^2(\xi, m_0)}\right) e^{i(m\xi - kz)}, \tag{2.34}$$

for ${c_1}^2 = (-3P\eta^2/8\gamma)$. Here one can find that the solution is consistent only for opposite signs of P and γ, which is possible in specific range of normalized frequency $\omega < 0.71$.

2.3.4 Conclusions

We have obtained dark and bright solitary wave solutions in NIMs with higher order effects for some constraints. The evolution of dark solitary waves is shown for specific range of normalized frequency while the existence of bright solitary waves are possible under some conditions on model parameters which can be achieved through the structural changes in negative index materials. We further studied fractional-transform solutions, containing periodic, hyperbolic and cnoidal solitary wave solutions for GNLSE, in absence of quintic and nonlinear dispersion terms.

The work presented in this sub-section appeared in [9].

2.4 Pulse Propagation in NIMs in the presence of external source

2.4.1 Governing equation

To control the dynamics of a nonlinear system, it is essential to investigate the effects of dissipation, noise and external force on the system. Dissipation leads to loss of energy and hence affects the dynamics of system under consideration, whereas the external tunable driving acts as a source of energy and helps in stabilizing the dynamical system. Barashenkov *et al.* [28] considered the parametrically driven damped NLSE and showed the existence of stable solitons only if the strength of the driving force would be more than the damping constant. The studies of ac-driven NLSE date back to the works of Malomed *et al.* [29, 30]. Since then it has been studied in many fields [31, 32, 26, 33, 34, 35, 36, 37]. For NIMs soliton-like solutions are studied for different structures of NLSE, however the wave propagation in NIMs in the presence of external source has not been discussed so far. The pulse propagation for NIMs in presence of exteranal source can be modeled by following equation (GNLSE)

$$i\frac{\partial \phi}{\partial z} - \frac{P}{2}\frac{\partial^2 \phi}{\partial t^2} - iQ\frac{\partial^3 \phi}{\partial t^3} + \gamma|\phi|^2\phi + i\Lambda\frac{\partial(|\phi|^2\phi)}{\partial t} = \beta\ e^{i(\psi(\xi)-kz)}, \tag{2.35}$$

where ϕ is complex envelop of the field and $P, Q, \gamma, \Lambda, \beta$ represent GVD, TOD, cubic nonlinearity, SS and external source coefficients respectively. In absence of external source, Eq. (2.35) is similar to Eq. (2.9) if quintic nonlinearity and nonlinear dispersion terms are absent This equation without source has already been studied for solitary wave [7] and for fractional solutions [9].

2.4.2 Fractional transform solutions

In order to find exact travelling wave solutions, we have chosen the following ansatz

$$\phi(z,t) = \alpha(\xi)\ e^{i[\psi(\xi)-kz]}, \tag{2.36}$$

where $\xi = (t - uz)$ is the travelling coordinate. Substituting Eq. (2.36) in Eq. (2.35), and separating real and imaginary part we obtain two equations.

$$\begin{aligned} &u\alpha\psi' + k\alpha - \frac{P}{2}\alpha'' + \frac{P}{2}\alpha(\psi')^2 + 3Q\alpha''\psi' + 3Q\alpha'\psi'' + Q\alpha\psi''' - Q\alpha(\psi')^3 \\ &\quad + \gamma\alpha^3 - \Lambda\alpha^3\psi' - \beta = 0, \end{aligned} \tag{2.37}$$

$$-u\alpha' - P\alpha'\psi' - \frac{P}{2}\alpha\psi'' - Q\alpha''' + 3Q\alpha'(\psi')^2 + 3Q\alpha'\psi'\psi'' + 3\Lambda\alpha^2\alpha' = 0. \tag{2.38}$$

Choosing

$$\psi'(\xi) = m, \tag{2.39}$$

on substituting Eq. (2.39) in Eq. (2.37) and integrating we obtain

$$\alpha'' = a\alpha + b\alpha^3 + c_1, \tag{2.40}$$

for $a = -\frac{P+u-3Qm^2}{Q}$, $b = \frac{\Lambda}{Q}$. On substituting Eq. (2.39) and Eq. (2.40) in Eq. (2.38), we obtain

$$m = \frac{1}{4\Lambda}\left(\gamma + \frac{P\Lambda}{2Q}\right), \tag{2.41}$$

$$\beta = 3Qmc - \frac{Pc}{2}, \tag{2.42}$$

and

$$k = \frac{Pa}{2} + Qm^3 - um - 3Qma + \frac{Pm^2}{2}. \tag{2.43}$$

Eq. (2.40) can be solved for travelling wave solutions by using a fractional transformation

$$\alpha(\xi) = \frac{A + By^2(\xi)}{1 + Dy^2(\xi)}, \tag{2.44}$$

which maps the solutions of Eq.(2.40) to the elliptic equation $y'' \pm py \pm qy^3 = 0$, provided $AD \neq B$. For explicitness, we consider the case where $y = \mathrm{cn}(\xi, m_0)$ with m_0 as modulus parameter. Then upon substitution of Eq. (2.44) into Eq. (2.40) and equating the coefficients of equal powers of $\mathrm{cn}(\xi, m_0)$ will yield the following consistency conditions:

$$-aA - 2(AD - B)(1 - m_0) - bA^3 - c_1 = 0, \tag{2.45}$$

$$\begin{aligned}-2aAD - aB + 6(AD - B)D(1 - m_0) - 4(AD - B)(2m_0 - 1) - 3bA^2B \\ -3c_1D = 0,\end{aligned} \tag{2.46}$$

$$\begin{aligned}-aAD^2 - 2aBD + 4(AD - B)D(2m_0 - 1) + 6(AD - B)m_0 - 3bAB^2 \\ -3c_1D^2 = 0,\end{aligned} \tag{2.47}$$

$$-aBD^2 - 2(AD - B)Dm_0 - bB^3 - c_1D^3 = 0. \tag{2.48}$$

For different values of m_0, we can obtain different types of travelling wave solutions.

Periodic solution

For $m_0 = 0$ and $A = 0$, Eq. (2.40) admits the non-singular periodic solution of the following type

$$\alpha(\xi) = \frac{2c_1}{a}\left(\frac{\cos^2\xi}{1-\frac{2}{3}\cos^2\xi}\right), \tag{2.49}$$

where $a = 4$ and ${c_1}^2 = (-128/27b)$. Intensity profile for periodic solution for typical values of parameters is shown in Fig. (2.7).

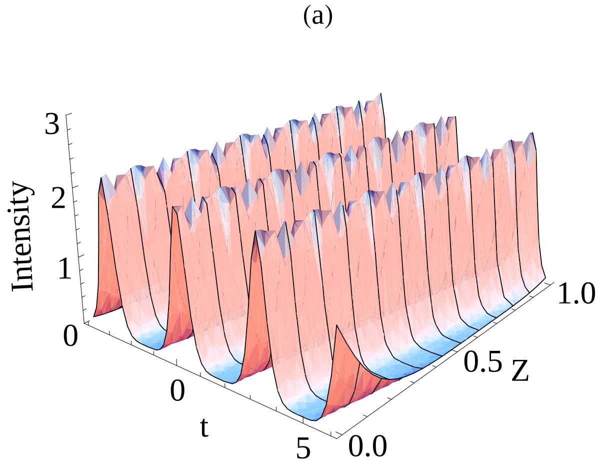

Figure 2.7: Typical intensity profiles for (a) periodic and (b) solitary wave solutions.

Dark/bright solitary wave solution

We found general localized solution for the case when the Jacobian elliptic modulus $m = 1$. The set of Eqs. (2.45) to Eq. (2.48) can be solved consistently for the unknown parameters A, B, D and for a particular value of c_1. The generic profile of the solution reads

$$\alpha(\xi) = \frac{A + B\ \mathrm{sech}^2\xi}{1 + D\ \mathrm{sech}^2\xi}. \tag{2.50}$$

Since the analytical form of solution is known, a simple maxima-minima analysis can be done to distinguish parameter regimes supporting dark and bright soliton solutions. In this case, when $AD < B$ one gets a bright soliton, whereas if $AD > B$ then a dark soliton exists. Intensity profile for dark and bright solutions is as shown in Fig solution for typical values of parameters is shown in Fig. 2.8.

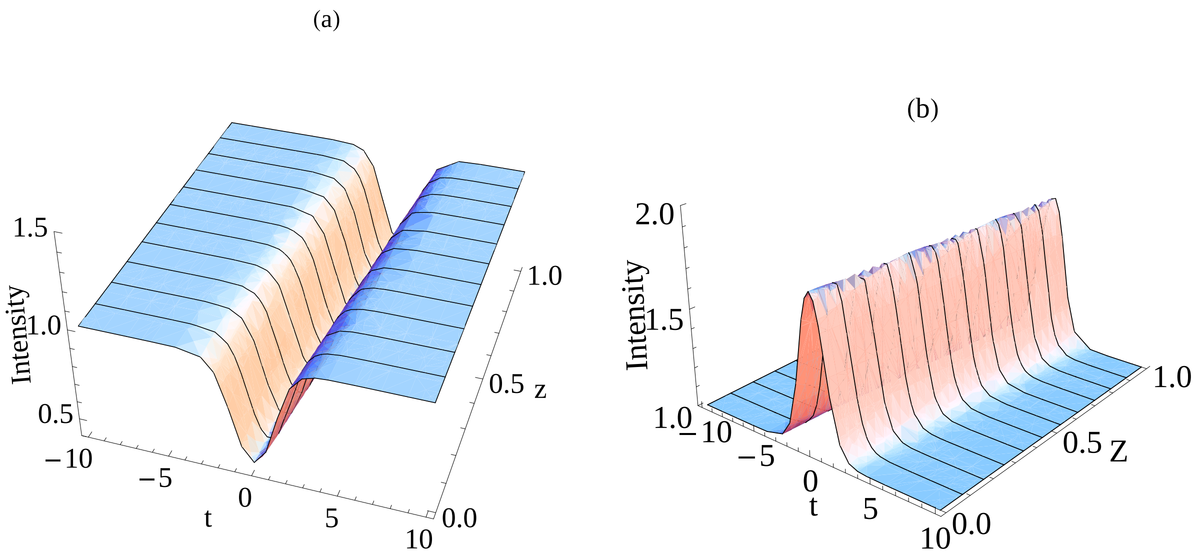

Figure 2.8: Typical intensity profiles for (a) dark and (b) bright solitary wave solutions.

2.4.3 Conclusion

We have also explored periodic, dark and bright solitary wave solutions for NIMs in presence of external source. The obtained solutions are necessarily fractional type. The study of pulse propagation in NIMs in presence of external source is a exciting field of research. Because NIMs are artificial materials and so we might have the flexibility of controlling these pulses.

The work discussed in second sub-section appeared in [38].

2.5 Chirped pulses in NIMs for coupled propagation equation

In this section, we consider the coupled pulse propagation equation in NIMs in the presence of electric and magnetic self-steepening effects, and obtain exact chirped soliton and periodic solutions for this model. These solutions are found for different choices of dispersion and other model parameters. It is shown that nonlinear chirp associated with each of these solutions is directly proportional to the intensity of the wave and saturates at some finite value as the retarded time approaches its asymptotic value.

2.5.1 Chirped wave

We have already discussed that NLSE admits bright and dark solitons depending on the signs of nonlinearity and dispersion. Such pulses are free of chip because chirp produced by Kerr nonlinearity is balanced by the chirp produced GVD [39]. If we include higher order terms, gain/loss term or variable coefficients in NLSE then chirped solitons are possible in optical medium [40, 41, 42]. A chirped wave is a signal in which the frequency increases (up-chirp) or decreases (down-chirp) with time. The chirp signal are also known as sweep signal and quadratic-phase signal. The chirp play a significant role in the pulse evolution. Such signals are commonly used in sonar and radar. In optics, ultrashort laser pulses also exhibit chirp, which, in optical transmission systems interacts with the dispersion properties of the materials, increasing or decreasing total pulse dispersion as the signal propagates. The chirped pulses finds application in pulse compression and pulse amplification. The case of linear chirp frequency was first investigated by Hmurcik *et al.* [43] for a sech-shaped pulse with quadratic variation of phase in time. Desaix *et al.* [44] investigated the effect of the linear and nonlinear chirp on the subsequent pulse development. Large number of research groups has done a lot of work on the existence of chirped solitons in nonlinear optical systems [45, 40, 41, 42, 46]. They have found that the properties of chirped solitons depend not only on the amplitude, but also on the form, of the initial chirp. A typical chirp signal is shown in Fig. (2.9).

2.5.2 Model equation

Earlier researchers have derived the mathematical model describing pulse propagation in NIMs created from split-ring resonators and arrays of wires embedded in a Kerr medium, exhibiting both electric and magnetic nonlinearity of Kerr-type. Sarma et al. [47] derived a new generalized model by assuming that the unit cell size of the NIMs is considerably smaller than the operating wavelength and thereby

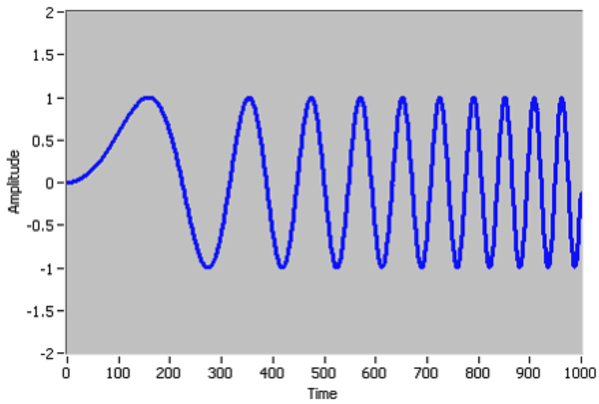

Figure 2.9: Chirp Signal

took an effective medium approach [48]. Unlike other authors, they invoked the electric and magnetic Kerr effect quite early into the derivation. Using this model, they studied the modulational instability for pulse propagation in NIMs in the presence of both electric and magnetic self-steepening effects. We have considered the same model and obtained exact soliton and periodic solutions for coupled generalized NLSE. In order to make the paper self contained, we sketch the essential steps of derivation of coupled equations, Ref. [47], for pulse propagation in nonlinear NIMs. The coupled generalized NLSE for a nonlinear NIM exhibiting Kerr-type electric and magnetic nonlinear polarization is

$$\frac{\partial A}{\partial Z} = \frac{i}{2k_0}\nabla_\perp^2 A - \frac{i\beta_2}{2}\frac{\partial^2 A}{\partial T^2} + iP_{nl}\left(1 + iP_S\frac{\partial}{\partial T}\right)|A|^2 A + iQ_{nl}|B|^2\left(A + iP_{se}\frac{\partial A}{\partial T}\right),$$
$$\frac{\partial B}{\partial Z} = \frac{i}{2k_0}\nabla_\perp^2 B - \frac{i\beta_2}{2}\frac{\partial^2 B}{\partial T^2} + iQ_{nl}\left(1 + iQ_S\frac{\partial}{\partial T}\right)|B|^2 B + iP_{nl}A^2\left(B + iQ_{sh}\frac{\partial B}{\partial T}\right), \tag{2.51}$$

where $P_{nl} = \frac{\omega_0^2\mu(\omega_0)\epsilon_0\chi_E^{(3)}}{2k_0}$, $P_s = \left[\frac{1}{\omega_0}\left(1 + \frac{\gamma}{\mu(\omega_0)}\right) - \frac{1}{k_0 V}\right]$, $P_{se} = \frac{1}{\omega_0}\left(1 + \frac{\alpha}{\epsilon(\omega_0)}\right)$, $Q_{nl} = \frac{\omega_0^2\epsilon(\omega_0)\mu_0\chi_M^{(3)}}{2k_0}$, $Q_s = \left[\frac{1}{\omega_0}\left(1 + \frac{\alpha}{\epsilon(\omega_0)}\right) - \frac{1}{k_0 V}\right]$, $Q_{sh} = \frac{1}{\omega_0}\left(1 + \frac{\gamma}{\mu(\omega_0)}\right)$,
with
$\beta_2 = [(\alpha\gamma + \omega_0\mu(\omega_0)\alpha'/2 + \omega_0\epsilon(\omega_0)\gamma'/2 - 1/V^2)]$, $\gamma = \partial\left[\omega\mu(\omega)\right]/\partial\omega|_{\omega=\omega_0}$,
$\gamma' = \partial^2\left[\omega\mu(\omega)\right]/\partial^2\omega|_{\omega=\omega_0}$, $\alpha = \partial\left[\omega\epsilon(\omega)\right]/\partial\omega|_{\omega=\omega_0}$,
$\alpha' = \partial^2\left[\omega\epsilon(\omega)\right]/\partial^2\omega|_{\omega=\omega_0}$ and $V = 2k_0/\left[\omega_0\epsilon(\omega_0)\gamma + \omega_0\mu(\omega_0)\alpha\right]$.

Here P_{nl}, P_s and P_{se} are the nonlinear, self-steepening and coupling coefficients for the electric field, respectively; Q_{nl}, Q_s and Q_{sh} are the nonlinear, self-steepening and coupling coefficients for the magnetic field, respectively. The dielectric permittivity (ϵ) and magnetic permeability (μ) are dispersive in NIMs and their frequency dispersion is given by the lossy Drude model [5], as $\mu(\omega) = \mu_0 \left(1 - \frac{(\omega_{pm}/\omega_{pe})^2}{\omega(\omega+i\gamma_m)}\right)$, $\epsilon(\omega) = \epsilon_0 \left(1 - \frac{1}{\omega(\omega+i\gamma_e)}\right)$, where $\omega = \omega_0/\omega_{pe}$, ω_{pe} and ω_{pm} are the respective electric and magnetic plasma frequencies. $\omega_{pe} = \frac{2\pi c}{\lambda_{pe}}$ where λ_{pe} is corresponding plasma wavelength and c is velocity of light. $k_0 = \frac{\omega_0 \ n(\omega_0)}{c}$ is wave number at the central frequency of electromagnetic pulse, $n(\omega_0)$ is the refractive index of material at ω_0. γ_e and γ_m denotes electric and magnetic loss respectively normalized with respect to electric and magnetic plasma frequencies. For lossless medium $\gamma_e = \gamma_m = 0$. ϵ_0 and μ_0 the free space electric permittivity and magnetic permeability respectively. To observe the properties of negative refraction in metamaterials, the values and range of ω_{pm} and ω_{pe} has to be chosen carefully. Various research groups have done theoretical and experimental analysis for $\omega_{pm}/\omega_{pe} = 0.8$. For this specific choice, the refractive index is negative only if $0 < \omega/\omega_{pe} < 0.8$. The Eq. (2.51) is the generalized coupled NLSE for pulse propagation through NIMs embedded into a Kerr medium. The Fig. 2.10(a) shows the variation of n, P_{nl}, P_s and P_{se} with normalized frequency ω/ω_{pe} for $\omega_{pm}/\omega_{pe} = 0.8$, and the Fig. 2.10(b) shows the variation of n, Q_{nl}, Q_s and Q_{se} with normalized frequency ω/ω_{pe} for $\omega_{pm}/\omega_{pe} = 0.8$.

In order to write Eq. (2.51) in normalized form, the normalized variables are [47], $\zeta = Z/L_D$, $\tau = T/T_0$, $\Psi_1 = \frac{A}{A_0}$, $\Psi_2 = \frac{B}{B_0}$, $X = \frac{x}{L_\perp}$ $Y = \frac{y}{L_\perp}$, $\psi_1 = N_E\Psi_1$ and $\psi_2 = N_H\Psi_2$, where $L_D = T_0^2/|sgn(\beta_2)|$ is the dispersion length and T_0 is pulse width which is of the order of femtosecond (fs). The terms, $sgn(\beta_2)$ define the sign of group velocity dispersion term (GVD). A_0 and B_0 are the initial amplitudes of the electric and magnetic fields. N_E and N_H may be termed as the order of soliton for the electric and magnetic fields, defined as $N_E^2 = L_D/L_{pnl}$, $N_H^2 = L_D/L_{Mnl}$. Here we have taken $N_E = N_H = N$. It is also defined that nonlinear polarization length for electric and magnetic field are $L_{Pnl} = 1/P_{nl}A_0^2$ and $L_{Mnl} = 1/Q_{nl}B_0^2$. A characteristic length $L_\perp = \sqrt{|L_D/k_0|}$. Hence, Eq. (2.51) can be transformed into

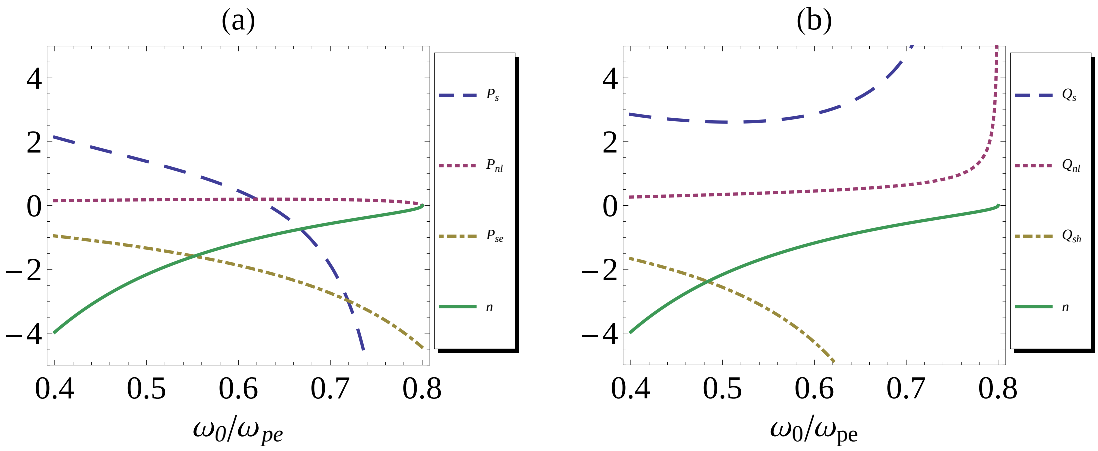

Figure 2.10: (a) Variation of refractive index n, electric nonlinear coefficients P_{nl}, electric self-steepening parameter P_s, electric coupling coefficients P_{se} with normalized frequency ω_0/ω_{pe}. P_{nl} is calculated in the unit of $\omega_{pe}\chi_E^{(3)}/c$, while P_s and P_{se} are calculated in the units of $1/\omega_{pe}$. (b) Variation of refractive index n, magnetic nonlinear coefficients Q_{nl}, magnetic self-steepening parameter Q_s, magnetic coupling coefficients Q_{sh} with normalized frequency ω_0/ω_{pe}. Q_{nl} is calculated in the unit of $\omega_{pe}\chi_M^{(3)}/c$, while Q_s and Q_{sh} are calculated in the units of $1/\omega_{pe}$. For both plots, $\gamma_e = \gamma_m = 0$.

normalized form as

$$\begin{aligned}\frac{\partial\psi_1}{\partial\zeta} &= \frac{isgn(k_0)}{2}\nabla_\tau^2\psi_1 - \frac{isgn(\beta_2)}{2}\frac{\partial^2\psi_1}{\partial\tau^2} + i\left(1 + iS_E\frac{\partial}{\partial\tau}\right)|\psi_1|^2\psi_1 + i|\psi_2|^2\psi_1 \\ &- C_E|\psi_2|^2\frac{\partial\psi_1}{\partial\tau}, \\ \frac{\partial\psi_2}{\partial\zeta} &= \frac{isgn(k_0)}{2}\nabla_\tau^2\psi_2 - \frac{isgn(\beta_2)}{2}\frac{\partial^2\psi_2}{\partial\tau^2} + i\left(1 + iS_H\frac{\partial}{\partial\tau}\right)|\psi_2|^2\psi_2 + i|\psi_1|^2\psi_2 \\ &- C_H|\psi_1|^2\frac{\partial\psi_2}{\partial\tau}, \end{aligned} \tag{2.52}$$

where $\nabla_\perp^2 = \partial^2/\partial X^2 + \partial^2/\partial Y^2$ is the transverse Laplacian, ψ_1 and ψ_2 are the slowly varying envelops in the direction of propagation of electric and magnetic fields, respectively. $S_E = |P_s|/T_0$ is electric self-steepening parameter and $S_H = |Q_s|/T_0$ is the magnetic self steepening parameters in the normalized unit. $C_E = |P_{se}|/T_0$ is electric coupling coefficients and $C_H = |Q_{sh}|/T_0$ is the magnetic coupling coefficient in the normalized unit. In this work, we are interested in the role of magnetic self- steepening S_H and electric self-steepening S_E in soliton formation. Hence, we neglect the diffraction and the last term in the generalized model. Hence, the modified coupled Eq. (2.52) reads [47]

$$\frac{\partial \psi_1}{\partial \zeta} = -\frac{isgn(\beta_2)}{2}\frac{\partial^2 \psi_1}{\partial \tau^2} + i\left(1 + iS_E\frac{\partial}{\partial \tau}\right)|\psi_1|^2\psi_1 + i|\psi_2|^2\psi_1,$$
$$\frac{\partial \psi_2}{\partial \zeta} = -\frac{isgn(\beta_2)}{2}\frac{\partial^2 \psi_2}{\partial \tau^2} + i\left(1 + iS_H\frac{\partial}{\partial \tau}\right)|\psi_2|^2\psi_2 + i|\psi_1|^2\psi_2. \qquad (2.53)$$

2.5.3 Travelling wave solutions

It is already discussed that for this coupled equation, MI have been studied by Sarma et al. [47]. In Ref. [10], authors have studied the same form of coupled equation in the absence of self-steepening coefficients S_E and S_H, and obtained dark solitons for the choice of $\psi_2 = \psi_1$. Our interest is to obtain the exact analytical solutions for this equation in the presence of self-steepening coefficients. As it is quiet complicated to solve the coupled equation for a particular system, so in order to obtain analytical solutions of Eq. (2.53), we have also restricted ourselves to the scalar choice $\psi_2 = a\ \psi_1$, where a is a constant. On substituting it into Eq. (2.53), and using $S_E = a^2 S_H = S$ and $\psi_1 = \psi$, the set of coupled equation reduces to one equivalent equation given as

$$\frac{\partial \psi}{\partial \zeta} + \frac{isgn(\beta_2)}{2}\frac{\partial^2 \psi}{\partial \tau^2} + S\frac{\partial}{\partial \tau}|\psi|^2\psi - i(a^2+1)|\psi|^2\psi = 0. \qquad (2.54)$$

To obtain the travelling solutions of Eq. (2.54), we consider the following ansatz

$$\psi(\zeta, \tau) = \alpha(\xi)e^{i\chi(\xi)}, \qquad (2.55)$$

where $\alpha(\xi)$, $\chi(\xi)$ are amplitude and phase, respectively, and $\xi = \zeta - v\tau$ is travelling frame of reference with v as the velocity of frame. For this form of the solution, the corresponding chirping can be found as $\delta\omega(\tau, \zeta) = -\frac{\partial}{\partial \tau}[\chi(\xi)] = v\chi'(\xi)$, where prime represent differentiation w.r.t. ξ. Substituting Eq. (2.55) into Eq. (2.54) and separating real and imaginary parts, we get a set of equations as

$$\alpha' - v^2 sgn(\beta_2)\chi'\alpha' - \frac{sgn(\beta_2)}{2}v^2\alpha\chi'' - 3vS\alpha^2\alpha' = 0, \tag{2.56}$$

$$\alpha\chi' + \frac{sgn(\beta_2)}{2}v^2\alpha'' - \frac{sgn(\beta_2)}{2}v^2\alpha(\chi')^2 - (a^2+1)\alpha^3 - vS\alpha^3\chi' = 0. \tag{2.57}$$

Assuming

$$\chi' = -\frac{3S}{2vsgn(\beta_2)}\alpha^2 + \frac{1}{sgn(\beta_2)v^2}, \tag{2.58}$$

Eqs. (2.56) and (2.57) are found to be consistent with the following equation

$$\alpha'' + p\alpha^5 + q\alpha^3 + r\alpha = 0, \tag{2.59}$$

where $p = \frac{3S^2}{4v^2(sgn(\beta_2))^2}$, $q = \frac{-2}{sgn(\beta_2)v^2}(a^2 + 1 + \frac{S}{sgn(\beta_2)v})$, $r = \frac{1}{(sgn(\beta_2))^2 v^4}$. Eq. (2.59) is an elliptic equation which admits a variety of solutions such as periodic, bright and dark solitons if certain relations among the coefficients are satisfied [25]. We observed that depending upon the sign of dispersion term and other model parameters, one can obtain different forms of soliton solutions for this equation. We found that unlike standard NLSE solitons, chirp does not cancel its effects. Here, the obtained solutions are chirped soliton solutions. The mathematical expression for chirp help to obtain its initial profile with which a pulse should be propagated through NIMs so that resulting pulse retains its solitary wave character. Apart from the soliton-like solutions, Eq. (2.59) also possess the chirped periodic solutions under different parametric conditions.

Bright and dark soliton solutions

For $sgn(\beta_2) = -1$, Eq. (2.59) has bell-shaped solution of the form

$$\alpha(\xi) = \sqrt{P(1 \pm \text{sech }(\eta\xi))}, \tag{2.60}$$

where $v = \frac{(\sqrt{5}-2)}{\sqrt{5}(a^2+1)}S$, $P = \frac{2}{\sqrt{5}vS}$ and $\eta = \sqrt{\frac{4}{5v^4}}$. For this case, the chirping is given by

$$\delta\omega = \frac{3S}{2}P\left(1 \pm \mathrm{sech}(\ \eta\xi)\right) - \frac{1}{v}. \tag{2.61}$$

The +ve and -ve sign in Eq. (2.60) corresponds to bright and dark solitons, respec-

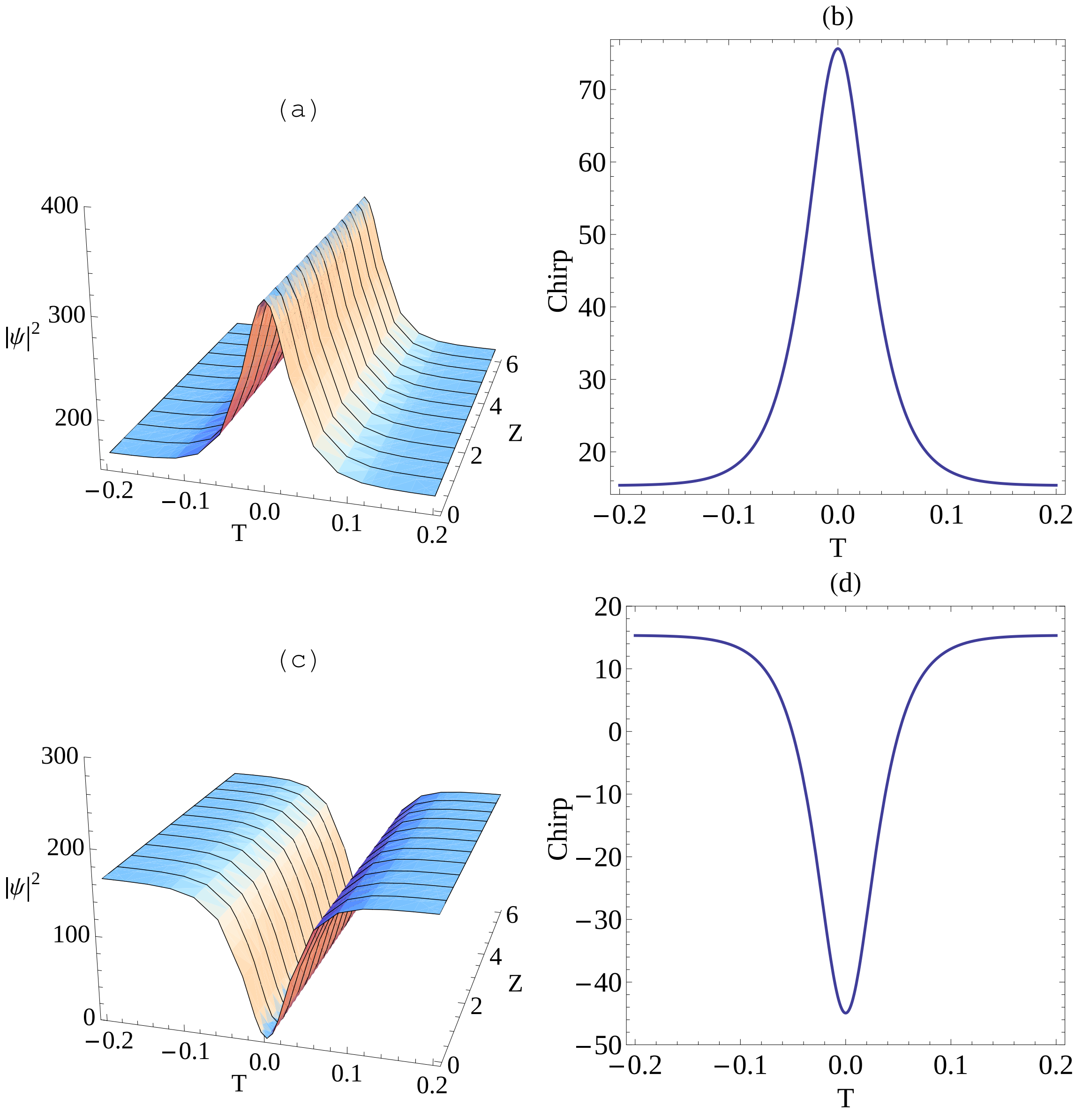

Figure 2.11: (a) Intensity profile and (b) chirp profile (for $Z = 0$) of bright soliton; (c) Intensity profile and (d) chirp profile (for $Z = 0$) of dark soliton; for $\omega/\omega_{pe} = 0.6, \omega_{pm}/\omega_{pe} = 0.8, T_0 = 1fs$ and $\lambda_{pe} = 1\mu m$. The other parameters are $S_E = 0.245$, $S_H = 1.524$, $a = 0.4007$, $v = 0.022$, $P = 164.29$ and $\eta = 1806.03$. Here, time (T) is in units of femtoseconds and distance (Z) is in the units of L_D.

tively. The values of the solution parameters are implicitly dependent on relative values of ω, ω_{pe} and ω_{pm}. Fixing these values amounts to unique value of velocity of the both bright and dark soliton pulse but having different initial chirp. The intensity profiles for bright and dark solitons, and corresponding chirp profiles for specific values of parameters are shown in Fig. 2.11, respectively. Here we choose $\omega_{pm}/\omega_{pe} = 0.8, T_0 = 1fs$ and $\lambda_{pe} = 1\mu m$. As stated earlier, all the equation parameters depend on the normalized frequency (ω/ω_{pe}), so once we fixed $\omega/\omega_{pe} = 0.6$, we obtain $S_E = 0.245$ and $S_H = 1.524$ and hence $a = 0.4007$. The value of velocity is also unique for each frequency, and for this case $v = 0.022$. The corresponding values of other parameters are $P = 164.29$ and $\eta = 1806.03$.

Fractional solutions

For $sgn(\beta_2) = +1$, Eq. (2.59) possesses fractional solutions of the form [49, 50],

$$\alpha(\xi) = \frac{n \sinh(m\xi)}{\sqrt{\epsilon + \sinh^2(m\xi)}}, \tag{2.62}$$

provided $n = \sqrt{\frac{-2r(2\epsilon-3)}{q(\epsilon-3)}}$, $m = \sqrt{\frac{-r\epsilon}{\epsilon-3}}$, $p = -\frac{3m^2}{n^4}\left(\frac{\epsilon-1}{\epsilon}\right)$. Depending upon the value of m (real or imaginary), these solutions would be either solitary or periodic. Analysis shows that for $\epsilon < 1$ these fractional solutions corresponds to solitary wave and for $\epsilon > 3$ these represents the periodic solutions. For these solutions, the chirping can be written as

$$\delta\omega = -\frac{3S}{2}\left(\frac{n^2 \sinh^2(m\xi)}{\epsilon + \sinh^2(m\xi)}\right) + \frac{1}{v}. \tag{2.63}$$

For negative value of $sgn(\beta_2)$, normalized frequency has to be adjusted accordingly. These solutions are obtained here for normalized frequency $\frac{\omega}{\omega_{pe}} = 0.55$, corresponding to this frequency, other parameters are, $S_H = 1.41$, $S_E = 0.518$ and hence $a = 0.606$.

Special Cases

Case I: $\epsilon < 1$

For this range of ϵ, m is found to be real and corresponding solutions are dark solitary wave. The amplitude and chirp profile of these solutions is shown in Fig. 2.12(a) and Fig. 2.12(b), respectively, for $\epsilon = 0.9, S = 0.5183$, $v = -0.875$, $m = 0.854$, $n = 0.981$. It is interesting to note that by changing the value of wave parameter ϵ, in the given range, one can vary the velocity of pulse for same frequency.

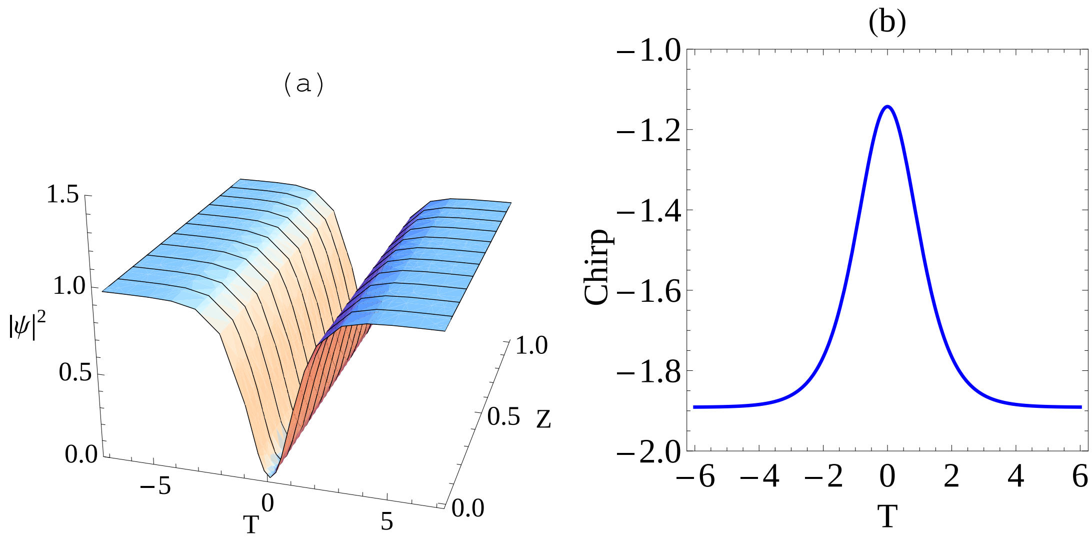

Figure 2.12: (a) Intensity profile (b) Chirp profile (for $Z = 0$) of dark soliton for $\frac{\omega}{\omega_{pe}} = 0.55$, $a = 0.606, S = 0.518$, $v = -0.875$, $m = 0.854$, $n = 0.981$ and $\epsilon = 0.9$. Time (T) is in the units of femtoseconds and distance (Z) is in the units of L_D.

Case II: $\epsilon > 3$

For this range of ϵ, m is imaginary and hence obtained solutions are periodic in nature. The amplitude and chirp profile of these periodic solutions is shown in Fig. 2.13(a) and Fig. 2.13(b), respectively, for $\epsilon = 10, S = 0.518$, $v = -0.785$, $m = 1.939i$, $n = 2.361$. Here also, it is possible to control the velocity of travelling periodic wave by varying the value of ϵ.

Periodic solutions

Eq. (2.59) possesses a another class of periodic solutions of the form, for $sgn(\beta_2) = +1$,

$$\alpha(\xi) = \frac{m}{\sqrt{1 + n\cos^2\ (\delta\ \xi)}}, \tag{2.64}$$

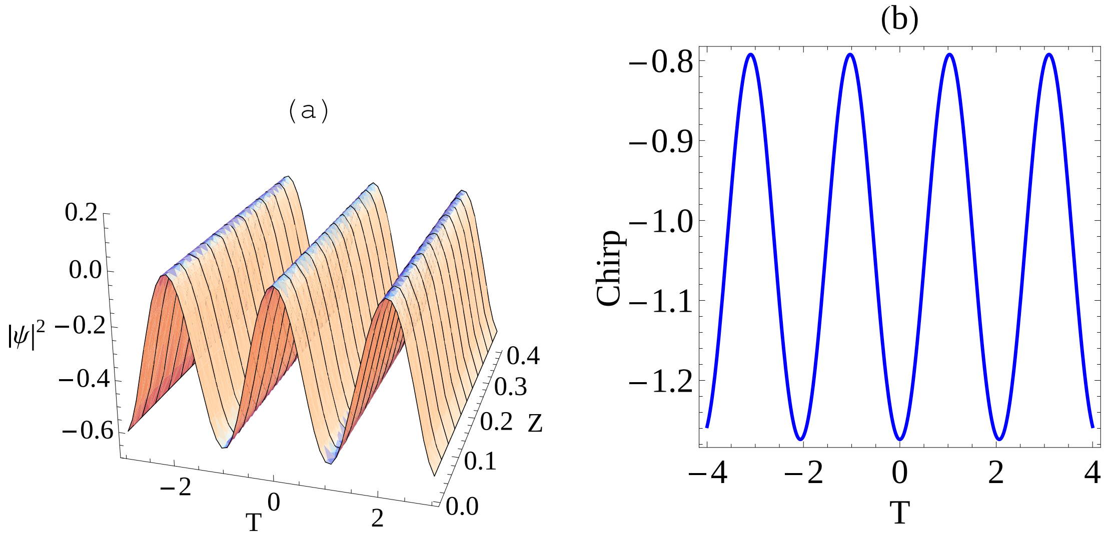

Figure 2.13: (a) Amplitude profile (b) Chirp profile (for $Z = 0$) of periodic solution for $\frac{\omega}{\omega_{pe}} = 0.55$, $a = 0.606$, $S = 0.518$, $v = -0.785$, $m = 1.939i$, $n = 2.361$ and $\epsilon = 10$. Time (T) is in the units of femtoseconds and distance (Z) is in the units of L_D.

where

$$
\begin{aligned}
m &= -\sqrt{2}\sqrt{\frac{1}{Sv} + \frac{a^2}{S^2} + \frac{1}{S^2} - \frac{\gamma}{S^2v^2}},\\
\gamma &= \sqrt{(a^2+1)v^3(2S + a^2v + v)}, \quad \delta = -\frac{1}{v^2},\\
n &= 2(\frac{2v}{S} + \frac{2a^2v}{S} + \frac{v^2}{S^2} + \frac{a^4v^2}{S^2} + \frac{2a^2v^2}{S^2} - \frac{\gamma}{Sv} - \frac{a^2\gamma}{S^2} - \frac{\gamma}{S^2}).
\end{aligned}
\tag{2.65}
$$

For this case, the chirping can be written as

$$
\delta\omega = -\frac{3S}{2}\left(\frac{m^2}{1 + n\cos^2\ (\delta\ \xi)}\right) + \frac{1}{v}. \tag{2.66}
$$

As clear from the its expression, similar to the intensity profile chirp also vary periodically. The typical intensity and chirp profile for periodic solutions for $\frac{\omega}{\omega_{pe}} = 0.71$, is shown in Fig. 2.14(a) and Fig. 2.14(b) respectively. For this frequency $S_H = 2.759$, $S_E = 1.265$ and hence $a = 0.677$. The values of other parameters are $S = 1.265$, $m = -0.624$, $n = -0.939$ and $\delta = -1$. This solution is applicable for any positive values of v.

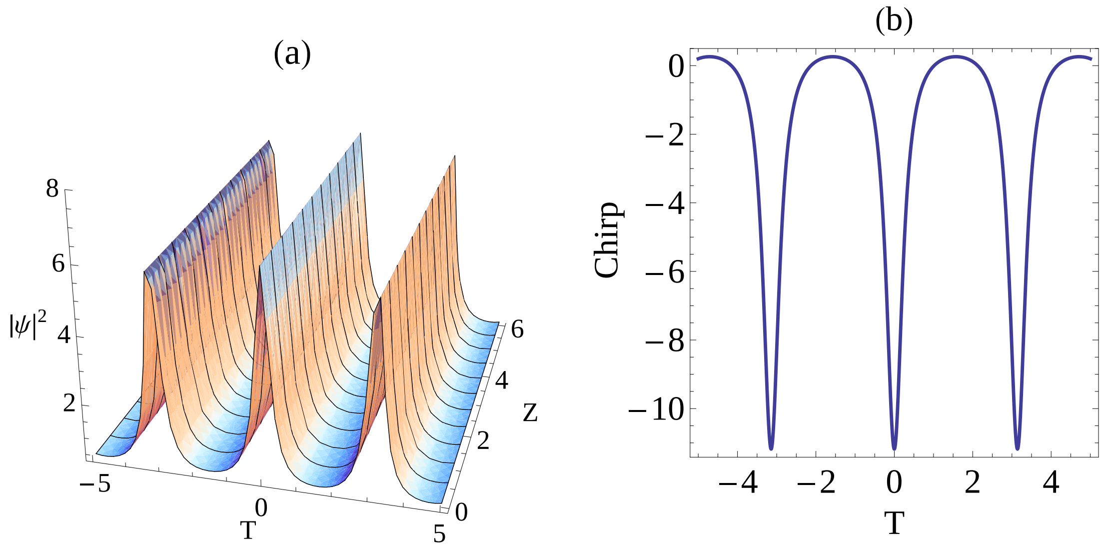

Figure 2.14: (a) Intensity profiles and (b) chirp profile (for $Z = 0$) of periodic solitons for $\frac{\omega}{\omega_{pe}} = 0.71$. The other parameters are $S = 1.26$, $a = 0.677$, $m = -0.6241$, $n = -0.939$, $v = 1$ and $\delta = -1$. Here, time (T) is in units of femtoseconds and distance (Z) is in units of L_D.

2.5.4 Conclusion

Our work encourages the study of the propagation of chirped periodic and soliton pulses through NIMs. NIMs are artificially designed materials, so we have freedom to vary the parameters in order to control the nature of these travelling waves. For the normal dispersion, we obtained the bright and dark soliton solutions having unique velocity but different initial chirp for same normalized frequency; on the other hand for the anomalous dispersion, it possesses the fractional solutions having different velocity for a particular normalized frequency. Moreover there is also a possibility of obtaining the periodic nonlinear waves in NIMs in anomalous dispersion regime. We have plotted these solutions for different normalized frequencies. It is shown that nonlinear chirp associated with each of these solutions is directly proportional to the intensity of the pulse and saturates at some finite value as the retarded time approaches its asymptotic value. Hence we represent the soliton-like solutions in NIMs for frequency dependent parameters. These solutions can find applications in nonlinear optics of NIMs.

Bibliography

[1] VG Veselago. Electrodynamics of materials both permittivity and permeability being negative. *Uspekhi Fizicheskikh Nauk (in Russian)*, 92(7):517–526, 1967.

[2] A Chowdhury and JA Tataronis. Nonlinear wave mixing and susceptibility properties of negative refractive index materials. *Physical Review E*, 75(1):016603, 2007.

[3] SA Ramakrishna. Comment on"negative refraction at optical frequencies in nonmagnetic two-component molecular media". *Physical Review Letters*, 98(5):59701, 2007.

[4] Y Liu, G Bartal, DA Genov, and X Zhang. Subwavelength discrete solitons in nonlinear metamaterials. *Physical Review Letters*, 99(15):153901, 2007.

[5] G D'Aguanno, N Mattiucci, M Scalora, and MJ Bloemer. Bright and dark gap solitons in a negative index fabry-perot etalon. *Physical Review Letters*, 93(21):213902, 2004.

[6] M Scalora, MS Syrchin, N Akozbek, EY Poliakov, Giuseppe DAguanno, N Mattiucci, MJ Bloemer, and AM Zheltikov. Generalized nonlinear Schrödinger equation for dispersive susceptibility and permeability: application to negative index materials. *Physical Review Letters*, 95(1):013902, 2005.

[7] NL Tsitsas, N Rompotis, I Kourakis, PG Kevrekidis, and DJ Frantzeskakis. Higher-order effects and ultrashort solitons in left-handed metamaterials. *Physical Review E*, 79(3):037601, 2009.

[8] P Li, R Yang, and Z Xu. Gray solitary-wave solutions in nonlinear negative-index materials. *Physical Review E*, 82(4):046603, 2010.

[9] VK Sharma, A Goyal, TS Raju, and CN Kumar. Periodic and solitary wave solutions for ultrashort pulses in nims. *Journal of Modern Optics*, 60(1):836–840, 2013.

[10] N Lazarides and GP Tsironis. Coupled nonlinear Schrödinger field equations for electromagnetic wave propagation in nonlinear left-handed materials. *Physical Review E*, 71(3):036614, 2005.

[11] I Kourakis and PK Shukla. Nonlinear propagation of electromagnetic waves in negative-refraction-index composite materials. *Physical Review E*, 72(1):016626, 2005.

[12] AK Popov and VM Shalaev. Compensating losses in negative-index metamaterials by optical parametric amplification. *Optics Letters*, 31(14):2169–2171, 2006.

[13] S Wen, Y Wang, W Su, Y Xiang, X Fu, and D Fan. Modulation instability in nonlinear negative-index material. *Physical Review E*, 73(3):036617, 2006.

[14] AD Boardman, P Egan, L Velasco, and N King. Control of planar nonlinear guided waves and spatial solitons with a left-handed medium. *Journal of Optics A: Pure and Applied Optics*, 7(2):S57–S67, 2005.

[15] PP Banerjee and G Nehmetallah. Spatial and spatiotemporal solitary waves and their stabilization in nonlinear negative index materials. *Journal of Optical Society of America B*, 24(10):a69–a76, 2007.

[16] I Shadrivov, N Zharova, A Zharov, and Y Kivshar. Nonlinear transmission and spatiotemporal solitons in metamaterials with negative refraction. *Optics Express*, 13(4):1291–1298, 2005.

[17] A Joseph, K Porsezian, and M Wadati. Small amplitude solitons on a pedestal in the modified nonlinear Schrödinger equation for negative index materials. *Journal of the Physical Society of Japan*, 78(4):044402, 2009.

[18] W Cui, Y Zhu, H Li, and S Liu. Dark solitons and their head-on collisions in nonlinear metamaterials. *Physics Letters A*, 374(2):380–385, 2009.

[19] LD Landau, JS Bell, MJ Kearsley, LP Pitaevskii, EM Lifshitz, and JB Sykes. *Electrodynamics of continuous media*, volume 8. Elsevier, 1984.

[20] MS Syrchin, AM Zheltikov, and M Scalora. Analytical treatment of self-phase modulation beyond the slowly varying envelpe approximation. *Physics Review A*, 69(5):053803, 2004.

[21] AD Boardman, O Hess, RC Mitchell-Thomas, YG Rapport, and Velasco L. Temporal solitons in magneto-optic and metamaterial waveguides. *Photonics and Nanostructures-Fundamentals and Applications*, 8(4):228–243, 2010.

[22] AK Sarma. Solitary waves in a negative index material with dispersive permittivity and permeability. *The European Physical Journal D-Atomic, Molecular, Optical and Plasma Physics*, 62(3):421–424, 2011.

[23] G Dolling, C Enkrich, M Wegener, CM Soukoulis, and S Linden. Low-loss negative-index metamaterial at telecommunication wavelengths. *Optics Letters*, 31(12):1800–1802, 2006.

[24] T Lepetit, É Akmansoy, and JP Ganne. Experimental measurement of negative index in an all-dielectric metamaterial. *Applied Physics Letters*, 95(12):121101, 2009.

[25] W Alka, A Goyal, and CN Kumar. Nonlinear dynamics of DNA–Riccati generalized solitary wave solutions. *Physics Letters A*, 375(3):480–483, 2011.

[26] VM Vyas, TS Raju, CN Kumar, and PK Panigrahi. Soliton solutions of driven nonlinear Schrödinger equation. *Journal of Physics A: Mathematical and General*, 39(29):9151–9159, 2006.

[27] A Goyal, Alka, TS Raju, and CN Kumar. Lorentzian-type soliton solutions of ac-driven complex Ginzburg-Landau equation. *Applied Mathematics and Computation*, 218(24):11931–11937, 2012.

[28] IV Barashenkov, MM Bogdan, and VI Korobov. Stability diagram of the phase-locked solitons in the parametrically driven, damped nonlinear Schrödinger equation. *Europhysics Letters*, 15(2):113, 1991.

[29] D Cai, AR Bishop, N Grønbech-Jensen, and BA Malomed. Bound solitons in the ac-driven, damped nonlinear Schrödinger equation. *Physical Review E*, 49(2):1677–1679, 1994.

[30] BA Malomed. Bound solitons in a nonlinear optical coupler. *Physical Review E*, 51(2):R864–R866, 1995.

[31] G Cohen. Soliton interaction with an external traveling wave. *Physical Review E*, 61(1):874–879, 2000.

[32] TS Raju, CN Kumar, and PK Panigrahi. Exact solitary wave solutions of the nonlinear Schrödinger equation with a source. *Journal of Physics A: Mathematical and General*, 38:L271–L276, 2005.

[33] TS Raju, PK Panigrahi, and K Porsezian. Nonlinear compression of solitary waves in asymmetric twin-core fibres. *Physical Review E*, 71:026608, 2005.

[34] TS Raju, PK Panigrahi, and K Porsezian. Self-similar propagation and compression of chirped self-similar waves in asymmetric twin-core fibers with nonlinear gain. *Physical Review E*, 72(4):046612, 2005.

[35] TS Raju and PK Panigrahi. self-similar propagation in graded-index nonlinear-fiber amplifier with an external source. *Physical Review A*, 81:043820, 2010.

[36] TS Raju and PK Panigrahi. Optical similaritons in a tapered graded-index nonlinear-fiber amplifier with an external source. *Physical Review A*, 84(3):033807, 2011.

[37] TS Raju, PK Panigrahi, and CN Kumar. Compression and propagation of dispersive and rectangular similaritons in asymmetric twin-core fibers. *Journal of Optical Society of America B*, 30:934, 2013.

[38] VK Sharma, A Goyal, CN Kumar, and J Goswamy. Travelling wave solutions in negative index materials in the presence of external source. In *Proceeding of international conference on recent trends in applied physics and material science: RAM 2013*, volume 1536, pages 717–718. AIP Publishing, 2013.

[39] YS Kivshar and GP Agrawal. *Optical solitons: from fibers to photonic crystals*. Academic Press, 2003.

[40] VI Kruglov, AC Peacock, and JD Harvey. Exact self-similar solutions of the generalized nonlinear Schrödinger equation with distributed coefficients. *Physical Review Letters*, 90(11):113902, 2003.

[41] J Wang, L Li, and S Jia. Exact chirped gray soliton solutions of the nonlinear Schrödinger equation with variable coefficients. *Optics Communications*, 274(1):223–230, 2007.

[42] Alka, A Goyal, R Gupta, CN Kumar, and TS Raju. Chirped femtosecond solitons and double-kink solitons in the cubic-quintic nonlinear Schrödinger equation with self-steepening and self-frequency shift. *Physical Review A*, 84(6):63830, 2011.

[43] LV Hmurcik and DJ Kaup. Solitons created by chirped initial profiles in coherent pulse propagation. *Journal of the Optical Society of America*, 69(4):597–604, 1979.

[44] M Desaix, L Helczynski, D Anderson, and M Lisak. Propagation properties of chirped soliton pulses in optical nonlinear kerr media. *Physical Review E*, 65(5):56602, 2002.

[45] GP Agrawal. Optical pulse propagation in doped fiber amplifiers. *Physical Review A*, 44(11):7493–7501, 1991.

[46] K Senthilnathan, K Nakkeeran, Q Li, and PKA Wai. Pedestal free pulse compression of chirped optical solitons. *Optics Communications*, 285(6):1449–1455, 2012.

[47] AK Sarma and M Saha. Modulational instability of coupled nonlinear field equations for pulse propagation in a negative index material embedded into a kerr medium. *Journal of Optical Society of America B*, 28(4):944–948, 2011.

[48] SA Ramakrishna and TM Grzegorczyk. *Physics and applications of negative refractive index materials*, volume 186. CRC Press, 2009.

[49] NH Christ and TD Lee. Quantum expansion of soliton solutions. *Physical Review D*, 15(6):1606–1627, 1975.

[50] A Goyal, VK Sharma, TS Raju, and CN Kumar. Chirped double-kink and fractional-transform solitons in an optical gain medium with two-photon absorption. *Journal of Modern Optics*, 61(4):315–321, 2014.

Chapter 3

Spatial, temporal, and spatio-temporal modulational instabilities in twin-core optical fibers

3.1 Introduction

In this chapter, we study Modulational instability (MI) in the context of twin-core fiber. Three different types of MI — spatial, temporal, and spatiotemporal have been studied by the method of linear stability analysis. We have investigated the variation of spatial MI with quintic nonlinearity for self-focusing and self-defocusing materials. For the temporal case, the impact of various parameters such as CCD, FOD, SS, and quintic nonlinearity on the MI gain in normal as well as anomalous dispersion regimes has been studied.

3.2 Modulation instability

In nonlinear dynamics, much attention has been devoted to the investigations of modulational instability (MI) in the framework of nonlinear Schrödinger equation. MI is a characteristic feature of a wide class of nonlinear dispersive systems. This phenomenon arises due to interplay between nonlinearity and dispersion. It is a fundamental nonlinear phenomenon [1, 2, 3] in which a weak perturbation imposed on a continuous wave (cw) state grows exponentially, which results in the break up of cw into a train of ultra-short pulses. Hence MI considered as a basic process that classifies the quantitative behavior of modulated waves and may initialize the formation of stable entities such as envelope of solitons. In general, MI typically occurs in the same parameter region where soliton-like phenomenon occurs. The relation between MI and solitons is best observed in the fact that the trains of pulses that emerge from the MI process are actually trains of almost ideal solitons. Hence it can be loosely considered as a precursor to soliton formation. MI can be classified into three main categories—spatial [4, 5], temporal [6, 7] and spatiotemporal [8, 9]. The spatial MI occurs due to the interaction between the nonlinearity and diffraction which results into the breaks up of homogeneous beam into numerous small filaments. The temporal MI occurs due to interplay between the group velocity dispersion(GVD) and nonlinearity and manifests itself as break-up of cw into a train of ultrashort pulses. In temporal MI the anomalous GVD plays the same role as is played by diffraction term in spatial MI. However in spatiotemporal MI all the three terms—nonlinearity, dispersion and diffraction are nonzero and it occurs due to the simultaneous presence of spatial and temporal MI in nonlinear medium. To study the MI of any nonlinear evolution equation (NLEE), following steps have to be followed:-

- Steady state solution of the equation is considered.
- The beginning of instability can be investigated by perturbing the steady state solution of NLEE, by applying some weak perturbation.

- As perturbation is assumed as small so the resultant equation is linearized in perturbation term by neglecting the terms containing higher order perturbation.

- This equation can be easily solved in frequency domain. However, the equation contain the term having complex conjugate of perturbation hence the Fourier components at frequencies Ω and $-\Omega$ are coupled. Therefore perturbation term is splitted into two parts.

- The dispersion relation for MI gain is obtained from resultant equation.

MI plays an important role in many nonlinear phenomenon such as cross phase modulation [2, 10], four-wave mixing [11], parametric oscillators [12], polarization and birefringence [13, 14, 15, 16], temporal solitons in fibers [17, 18, 19], supercontinuum generation [20] and Bragg's grating [3, 21]. MI has been studied since 1960s and has been extensively explored in different areas such as negative refractive index materials (NIMs) [22, 23], silicon photonic nanowires [24], single core optical fiber [17, 25], and plasma [26, 27]. Some recent works related to study of MI in twin-core fiber appeared in [28, 29].

3.3 Twin core fiber (TCF)

The twin-core fiber (TCF) is a fiber that consists of two linearly coupled identical parallel cores as shown in Fig. 3.1. In TCF optical power can be transferred between two cores periodically [30]. This phenomenon of periodic optical power transfer between the two cores along a TCF is widely used in many practical optical devices. The evolution of slowly varying envelope in twin-core fiber is governed by a set of linearly coupled NLSE. The coupling coefficient for linear coupling between the two equations dictates the strength of the power transfer. The magnitude of coupling constant depends upon the design and operation condition of the optical fiber. In general, the coupling coefficient depends on the optical wavelength. The effect of

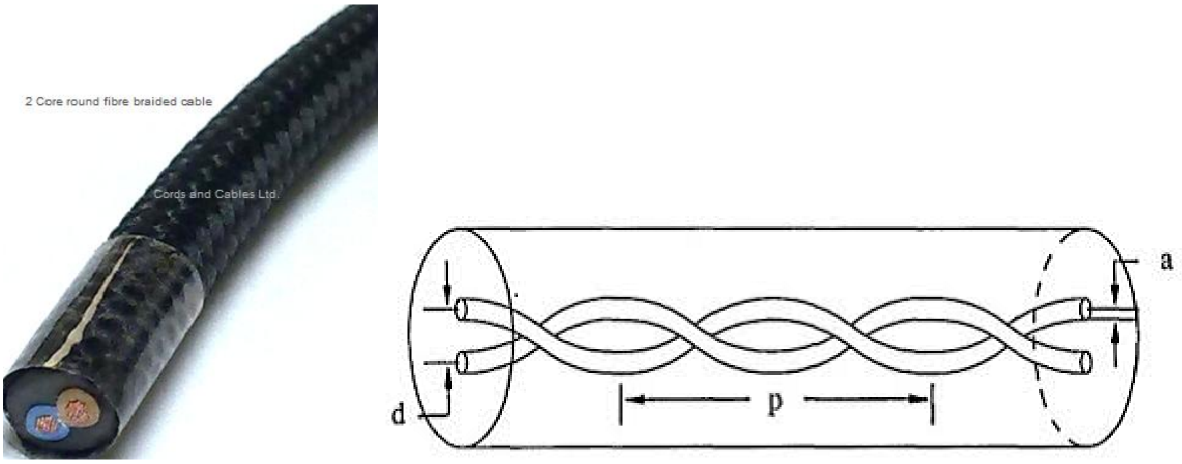

Figure 3.1: Twin-core fiber.

a dispersive coupling coefficient on the propagation of pulses in a twin-core fiber is considered recently [31, 32, 33, 34, 35, 36, 37, 38]. The coupling coefficient dispersion (CCD) plays an important role in pulse distortion and it can also results into the pulse breakup and thus effect nonlinear pulse switching [32, 33]. In twin-core fiber the pulse break-up effect has been observed experimentally [37] and this effect has been applied to the generation of high-speed pulse trains [38].

Recently Li et. al. [39] have investigated the effect of CCD on temporal MI for pulse propagation in twin-core fiber in the presence of GVD and cubic nonlinearity. Motivated by this work we considered the pulse propagation with higher order effects such as FOD, SS, quintic nonlinearity and investigated MI in twin-core fiber. In particular, we have studied three different types of MI — spatial, temporal, and spatiotemporal MI. We have investigated the variation of spatial MI with quintic nonlinearity for self-focusing and self-defocusing materials. For the temporal case we have studied the impact of various parameters such as CCD, FOD, SS, and quintic nonlinearity on the MI gain in normal as well as anomalous dispersion regimes.

3.4 Mathematical model for pulse propagation in twin-core fiber

In twin-core fiber each core supports only a single mode. The evolution of the electric-field envelopes along the fiber is described by pair of generalized linearly coupled nonlinear Schrödinger equation given by

$$\begin{aligned}\frac{\partial\Psi_1}{\partial\xi} &= \frac{i}{2k_0}\nabla_\perp^2\Psi_1 - \frac{i\beta_2}{2}\frac{\partial^2\Psi_1}{\partial\tau^2} + iC_{nl}(1+iC_s\frac{\partial}{\partial\tau})|\Psi_1|^2\Psi_1 - \delta_3\frac{\partial^3\Psi_1}{\partial\tau^3}\\ &+ i\delta_4\frac{\partial^4\Psi_1}{\partial\tau^4} + iC_q|\Psi_1|^4\Psi_1 + P\frac{\partial\Psi_2}{\partial\tau},\\ \frac{\partial\Psi_2}{\partial\xi} &= \frac{i}{2k_0}\nabla_\perp^2\Psi_2 - \frac{i\beta_2}{2}\frac{\partial^2\Psi_2}{\partial\tau^2} + iD_{nl}(1+iD_s\frac{\partial}{\partial\tau})|\Psi_2|^2\Psi_2 - \delta_3\frac{\partial^3\Psi_2}{\partial\tau^3}\\ &+ i\delta_4\frac{\partial^4\Psi_2}{\partial\tau^4} + iD_q|\Psi_2|^4\Psi_2 + P\frac{\partial\Psi_1}{\partial\tau},\end{aligned} \tag{3.1}$$

where ξ and τ are the propagation distance and time respectively. Ψ_1 and Ψ_2 are the slowly varying pulse envelops in two cores, β_2, measures the GVD at the carrier frequency ($\beta_2 < 0$ for anomalous dispersion and $\beta_2 > 0$ for normal dispersion). C_{nl} and D_{nl} are the coefficients of cubic nonlinearity in two cores of the fibers. $C_{nl}C_s$ and $D_{nl}D_s$ self-steepening coefficients in two cores. δ_3, δ_4 are the coefficient of TOD and FOD respectively. C_q, D_q are the coefficients of quintic nonlinearity in two cores and P is the coupling coefficients dispersion term.

3.5 Analysis of modulaional instability

For analysis of MI, introducing the normalized units,
$Z = \frac{\xi}{L_D}$, $t = \frac{\tau}{T_0}$, $U = \frac{\Psi_1}{\Psi_{01}}$, $V = \frac{\Psi_2}{\Psi_{02}}$, $X = \frac{x}{L_\perp}$, $Y = \frac{y}{L_\perp}$, $u = N_E U$, $v = N_H V$, where T_0 is the pulse width, $L_D = T_0^2/|\beta_2|$ is the dispersion length, and Ψ_{01} and Ψ_{02} are the initial amplitudes of the slowly varying envelope in two cores of the fiber. N_E and N_H may be termed the order of solitons and are defined as $N_E^2 = L_D/L_{C_{nl}}$, $N_H^2 = L_D/L_{M_{nl}}$, and we assume that $N_E = N_H = N$. We

define nonlinear polarization length as $L_{C_{nl}} = 1/C_{nl}\Psi_{01}^2$ and $L_{M_{nl}} = 1/D_{nl}\Psi_{02}^2$. Let $g_E = \Psi_{01}^2 C_{qnl}/(C_{nl}N^2)$ and $g_H = \Psi_{02}^2 D_{qnl}/(D_{nl}N^2)$ and characteristics length $L_\perp = \sqrt{|L_D/k_0|}$ is also introduced. $\beta_3 = \delta_3/T_0|\beta_2|$, $\beta_4 = \delta_4/T_0^2|\beta_2|$ and $C_1 = P\Psi_{02}/\Psi 01|\beta_2|$. Thus Eq. (3.1) can be transformed into the following form

$$\begin{aligned}\frac{\partial u}{\partial Z} &= \frac{isgn(k_0)}{2}\nabla_\perp^2 u - \frac{isgn(\beta_2)}{2}\frac{\partial^2 u}{\partial t^2} + if(1+iS_E\frac{\partial}{\partial t})|u|^2u - \beta_3\frac{\partial^3 u}{\partial t^3}\\ &+ i\beta_4\frac{\partial^4 u}{\partial t^4} + ig_E|u|^4u + C_1\frac{\partial v}{\partial t},\\ \frac{\partial v}{\partial Z} &= \frac{isgn(k_0)}{2}\nabla_\perp^2 v - \frac{isgn(\beta_2)}{2}\frac{\partial^2 v}{\partial t^2} + if(1+iS_E\frac{\partial}{\partial t})|v|^2v - \beta_3\frac{\partial^3 v}{\partial t^3}\\ &+ i\beta_4\frac{\partial^4 v}{\partial t^4} + ig_H|v|^4v + C_1\frac{\partial u}{\partial t}.\end{aligned} \tag{3.2}$$

Here $S_E = |C_s|/T_0$, $S_H = |D_s|/T_0$ also $\nabla_\perp = \frac{\partial^2}{\partial X^2} + \frac{\partial^2}{\partial Y^2}$ is the transverse Laplacian. The continuous steady state solution of Eq. (3.2) is given by

$$u = a_0\exp(i\Omega_{0a}Z), \tag{3.3}$$

and

$$v = b_0\exp(i\Omega_{0b}Z), \tag{3.4}$$

where a_0 and b_0 are the normalized amplitude, Ω_{0a} and Ω_{0b} are corresponding nonlinear phase shift. On substituting Eq. (3.3) and Eq. (3.4) in Eq. (3.2), we obtain

$$\Omega_{0a} = fa_0^2 + b_0^2 + g_E a_0^4, \tag{3.5}$$

and

$$\Omega_{0b} = a_0^2 + fb_0^2 + g_H b_0^4. \tag{3.6}$$

If continuous wave solution is slightly perturbed from the steady state,

$$u(X,Y,Z,T) = [a_0 + a(X,Y,Z,T)]\exp(i\Omega_{0a}Z), \tag{3.7}$$

$$v(X,Y,Z,T) = [b_0 + b(X,Y,Z,T)]\exp(i\Omega_{0b}Z), \tag{3.8}$$

where $a(X,Y,Z,T)$ and $b(X,Y,Z,T)$ are the perturbations such that $a, b << 1$. Substituting Eq. (3.7) and Eq. (3.8) into Eq. (3.2), we obtain the following equations

$$\begin{aligned}
\frac{\partial a}{\partial Z} &= p\frac{i}{2}\nabla_\perp^2 a - \frac{i\delta}{2}\frac{\partial^2 a}{\partial T^2} + if(a_0^2 a + a_0^2 a^* + a^2 a^* + a^2 a_0 + 2a_0 a a^*) - \beta_3\frac{\partial^3 a}{\partial T^3} + i\beta_4\frac{\partial^4 a}{\partial T^4}\\
&- fS_E(2a_0^2\frac{\partial a}{\partial T} + \frac{\partial a^*}{\partial T} + 2a_0 a\frac{\partial a}{\partial T} + 2a^2 a\frac{\partial a^*}{\partial T} + 2aa^*\frac{\partial a}{\partial T} + 2aa_0\frac{\partial a^*}{\partial T} + 2a_0 a^*\frac{\partial a}{\partial T})\\
&+ 2ig_E(a_0^4 a + a_0^4 a^* + a_0^2 a^3 + 3a_0^3 a^2 + 2a_0 a^3 a^* + 6a_0^2 a^2 a^* + 6a_0^3 a a^* + a^3(a^*)^2\\
&+ 3a_0 a^2(a^*)^2 + 3a_0^2 a(a^*)^2 + a_0^3(a^*)^2) + C_1\frac{\partial a}{\partial T},\\
\frac{\partial b}{\partial Z} &= p\frac{i}{2}\nabla_\perp^2 b - \frac{i\delta}{2}\frac{\partial^2 b}{\partial T^2} + if(b_0^2 b + b_0^2 b^* + b^2 b^* + b^2 b_0 + 2b_0 b b^*) - \beta_3\frac{\partial^3 b}{\partial T^3} + i\beta_4\frac{\partial^4 b}{\partial T^4}\\
&- fS_H(2b_0^2\frac{\partial b}{\partial T} + \frac{\partial b^*}{\partial T} + 2b_0 b\frac{\partial b}{\partial T} + 2b^2 b\frac{\partial b^*}{\partial T} + 2bb^*\frac{\partial a}{\partial T} + 2bb_0\frac{\partial b^*}{\partial T} + 2b_0 b^*\frac{\partial b}{\partial T})\\
&+ 2ig_H(b_0^4 b + b_0^4 b^* + b_0^2 b^3 + 3b_0^3 b^2 + 2b_0 b^3 b^* + 6b_0^2 b^2 b^* + 6b_0^3 b b^* + b^3(b^*)^2\\
&+ 3b_0 b^2(b^*)^2 + 3b_0^2 b(b^*)^2 + b_0^3(b^*)^2) + C_1\frac{\partial b}{\partial T}. \qquad (3.9)
\end{aligned}$$

On linearizing Eq. (3.9) in a and b and neglecting terms with $a^2, aa^*, a\frac{\partial a}{\partial T}, a^*\frac{\partial a}{\partial T}, a\frac{\partial a^*}{\partial T}, b^2, bb^*, b\frac{\partial b}{\partial T}, b^*\frac{\partial b}{\partial T}, b\frac{\partial b^*}{\partial T}$ and other higher order terms of a and b we obtain

$$\begin{aligned}
\frac{\partial a}{\partial Z} &= p\frac{i}{2}\nabla_\perp^2 a - \frac{i\delta}{2}\frac{\partial^2 a}{\partial T^2} + ifa_0^2(a + a^*) - fS_E a_0^2(2\frac{\partial a}{\partial T} + \frac{\partial a^*}{\partial T}) - \beta_3\frac{\partial^3 a}{\partial T^3}\\
&+ i\beta_4\frac{\partial^4 a}{\partial T^4} + 2ig_E b_0^4(a + a^*) + C_1\frac{\partial a}{\partial T},\\
\frac{\partial b}{\partial Z} &= p\frac{i}{2}\nabla_\perp^2 b - \frac{i\delta}{2}\frac{\partial^2 b}{\partial T^2} + ifb_0^2(b + b^*) - fS_H b_0^2(2\frac{\partial b}{\partial T} + \frac{\partial b^*}{\partial T}) - \beta_3\frac{\partial^3 b}{\partial T^3}\\
&+ i\beta_4\frac{\partial^4 b}{\partial T^4} + 2ig_H a_0^4(b + b^*) + C_1\frac{\partial a}{\partial T}. \qquad (3.10)
\end{aligned}$$

Now substituting

$$a = a_1\exp(i(kZ - \Omega T + q_X X + q_Y Y)) + a_2\exp(-i(kZ - \Omega T + q_X X + q_Y Y)), \quad (3.11)$$

and

$$b = b_1 \exp(i(kZ - \Omega T + q_X X + q_Y Y)) + b_2 \exp(-i(kZ - \Omega T + q_X X + q_Y Y)), \quad (3.12)$$

where k is wave number, Ω is frequency and $q^2 = q_X^2 + q_Y^2$ is transverse wave number of the perturbation respectively. Now substituting $S_H b_0^2 = S_E a_0^2 = s$ and $g_H b_0^4 = g_E a_0^4 = G$ in Eq. (3.10), we obtain

$$\Big(ika_1 + \frac{iq^2}{2}a_1 - \frac{i\delta}{2}\Omega^2 a_1 - ifa_0^2 a_1 - ifa_0^2 a_2 - 2ifM\Omega a_1 + 2ifM\Omega a_2 + iQ\Omega^3 a_1 - iR\Omega^4 a_1$$
$$- 2iGa_1 - 2iGa_2 + isa_0^2\Omega a_1 + iP\Omega b_1 - ia_0b_0b_1 - ia_0b_0b_2 - iC_1\Omega a_1\Big)\exp(i\chi) + (-ika_2$$
$$+ \frac{iq^2}{2}a_2 - \frac{i\delta}{2}\Omega^2 a_2 - ifa_0^2 a_2 - ifa_0^2 a_1 - 2ifM\Omega a_1 + 2ifM\Omega a_2 - iQ\Omega^3 a_2 - iR\Omega^4 a_2 - 2iGa_2$$
$$- 2iGa_1 + isa_0^2\Omega a_2 + iP\Omega b_2 - ia_0b_0b_2 - ia_0b_0b_1 + iC_1\Omega a_2 = 0\Big)\exp(-(i\chi)) = 0, \quad (3.13)$$

$$\Big(ikb_1 + \frac{iq^2}{2}b_1 - \frac{i\delta}{2}\Omega^2 b_1 - ifb_0^2 b_1 - ifb_0^2 b_2 - 2ifM\Omega b_1 + 2ifM\Omega b_2 + iQ\Omega^3 b_1 - iR\Omega^4 b_1$$
$$- 2iGb_1 - 2iGb_2 + isb_0^2\Omega b_1 + iP\Omega a_1 - ia_0b_0a_1 - ia_0b_0a_2 - iC_1\Omega b_1\Big)\exp(i\chi) + (-ikb_2$$
$$+ \frac{iq^2}{2}b_2 - \frac{i\delta}{2}\Omega^2 b_2 - ifb_0^2 b_2 - ifb_0^2 b_1 - 2ifM\Omega b_1 + 2ifM\Omega b_2 - iQ\Omega^3 b_2 - iR\Omega^4 b_2 - 2iGb_2$$
$$- 2iGb_1 + isb_0^2\Omega b_2 - iP\Omega a_2 - ia_0b_0a_2 - ia_0b_0a_1 + iC_1\Omega b_2\Big)\exp(-(i\chi)) = 0, \quad (3.14)$$

where $\chi = kZ - \Omega T + q_X X + q_Y Y$, equating the coefficients of $\exp(i\chi)$ and $\exp(-i\chi)$ from Eq. (3.13) and Eq. (3.14) equal to zero separately, we obtain

$$ika_1 + \frac{iq^2}{2}a_1 - \frac{i\delta}{2}\Omega^2 a_1 - ifa_0^2 a_1 - ifa_0^2 a_2 - 2ifM\Omega a_1 + 2ifM\Omega a_2 + iQ\Omega^3 a_1 - iR\Omega^4 a_1$$
$$- 2iGa_1 - 2iGa_2 + isa_0^2\Omega a_1 + iP\Omega b_1 - ia_0b_0b_1 - ia_0b_0b_2 - iC_1\Omega a_1 = 0, \quad (3.15)$$

$$-ika_2 + \frac{iq^2}{2}a_2 - \frac{i\delta}{2}\Omega^2 a_2 - ifa_0^2 a_2 - ifa_0^2 a_1 - 2ifM\Omega a_1 + 2ifM\Omega a_2 - iQ\Omega^3 a_2 - iR\Omega^4 a_2$$
$$- 2iGa_2 - 2iGa_1 + isa_0^2\Omega a_2 + iP\Omega b_2 - ia_0b_0b_2 - ia_0b_0b_1 + iC_1\Omega a_2 = 0, \quad (3.16)$$

$$ikb_1 + \frac{iq^2}{2}b_1 - \frac{i\delta}{2}\Omega^2 b_1 - ifb_0^2 b_1 - ifb_0^2 b_2 - 2ifM\Omega b_1 + 2ifM\Omega b_2 + iQ\Omega^3 b_1 - iR\Omega^4 b_1 - 2iGb_1 - 2iGb_2 + isb_0^2\Omega b_1 + iP\Omega a_1 - ia_0b_0a_1 - ia_0b_0a_2 - iC_1\Omega b_1 = 0, \quad (3.17)$$

$$-ikb_2 + \frac{iq^2}{2}b_2 - \frac{i\delta}{2}\Omega^2 b_2 - ifb_0^2 b_2 - ifb_0^2 b_1 - 2ifM\Omega b_1 + 2ifM\Omega b_2 - iQ\Omega^3 b_2 - iR\Omega^4 b_2 - 2iGb_2 - 2iGb_1 + isb_0^2\Omega b_2 - iP\Omega a_2 - ia_0b_0a_2 - ia_0b_0a_1 + iC_1\Omega b_2 = 0. \quad (3.18)$$

We can write Eq. (3.15)–Eq. (3.18) in matrix form as follows

$$\begin{pmatrix} A_{11} & A_{12} + w\Omega {a_0}^2 & 0 & 0 \\ A_{21} - w\Omega {a_0}^2 & A_{22} + w\Omega {a_0}^2 & -\Omega P & A_{24} \\ 0 & 0 & A_{11} & A_{12} + w\Omega {b_0}^2 \\ -P\Omega & A_{24} & A_{21} - w\Omega {b_0}^2 & A_{22} + w\Omega {b_0}^2 \end{pmatrix} \begin{pmatrix} a_1 \\ a_2 \\ b_1 \\ b_2 \end{pmatrix} = \begin{pmatrix} 0 \\ 0 \\ 0 \\ 0 \end{pmatrix},$$

where

$A_{11} = -pq^2 + \delta\Omega^2 + 2R\Omega^4,$

$A_{12} = -k + p\frac{q^2}{2} - \frac{\delta\Omega^2}{2} + 3fs\Omega - Q\Omega^3 - R\Omega^4 + C\Omega + P\Omega,$

$A_{21} = -k + p\frac{q^2}{2} - \delta\frac{\Omega^2}{2} + fs\Omega - Q\Omega^3 - R\Omega^4 - C\Omega,$

$A_{22} = k - p\frac{q^2}{2} - 2fs\Omega + \delta\frac{\Omega^2}{2} + f{a_0}^2 + Q\Omega^3 + R\Omega^4 - C\Omega + 2G,$

$A_{24} = \Omega P + \Gamma a_0 b_0.$

Hence

$$\begin{pmatrix} A_{11} & A_{12} + w\Omega {a_0}^2 & 0 & 0 \\ A_{21} - w\Omega {a_0}^2 & A_{22} + w\Omega {a_0}^2 & -\Omega P & A_{24} \\ 0 & 0 & A_{11} & A_{12} + w\Omega {b_0}^2 \\ -P\Omega & A_{24} & A_{21} - w\Omega {b_0}^2 & A_{22} + w\Omega {b_0}^2 \end{pmatrix} = 0,$$

from above matrix, we obtain following dispersion relations

$$
\begin{aligned}
k = \frac{1}{2} & \left(2\gamma \pm 2 \left(-4G^2 + \alpha^2 + C_1^2\Omega^2 + f^2s^2\Omega^2 - 2fGa_0^2 + f\alpha a_0^2 - 2fGb_0^2 + f\alpha b_0^2\right.\right. \\
& - \left(-16G^2C_1^2\Omega^2 + 4C_1^2\alpha^2\Omega^2 + 4f^2C_1^2s^2\Omega^4 - 8fGC_1^2\Omega^2a_0^2 + 4fC_1^2\alpha\Omega^2a_0^2 + 4f^2G^2a_0^4\right. \\
& - \ 4f^2G\alpha a_0^4 + f^2\alpha^2a_0^4 - 8fGC_1^2\Omega^2b_0^2 + 4fC_1^2\alpha\Omega^2b_0^2 - 8f^2G^2a_0^2b_0^2 + 8f^2G\alpha a_0^2b_0^2 \\
& - \left.\left.\left. 2f^2\alpha^2a_0^2b_0^2 + 4f^2G^2b_0^4 - 4f^2G\alpha b_0^4 + f^2\alpha^2b_0^4\right)^{\frac{1}{2}}\right)^{\frac{1}{2}}\right), \qquad (3.19)
\end{aligned}
$$

where $\alpha = -p\frac{q^2}{2} + \delta\frac{\Omega^2}{2} + \beta_3\Omega^4 + 2G, \gamma = 2fs\Omega - \beta_4\Omega^3$. The steady-state solution become unstable when k becomes imaginary, because then the perturbation grows exponentially. The general expression for the MI gain g_{MI} is

$$g_{MI} = 2Im(k), \qquad (3.20)$$

hence

$$
\begin{aligned}
g_{MI} = \pm & \left(- \left(-4G^2 + \alpha^2 + C_1^2\Omega^2 + f^2s^2\Omega^2 - 2fGa_0^2 + f\alpha a_0^2 - 2fGb_0^2 + f\alpha b_0^2\right.\right. \\
& - \left(-16G^2C_1^2\Omega^2 + 4C_1^2\alpha^2\Omega^2 + 4f^2C_1^2s^2\Omega^4 - 8fGC_1^2\Omega^2a_0^2 + 4fC_1^2\alpha\Omega^2a_0^2\right. \\
& + \ 4f^2G^2a_0^4 - 4f^2G\alpha a_0^4 + f^2\alpha^2a_0^4 - 8fGC_1^2\Omega^2b_0^2 + 4fC_1^2\alpha\Omega^2b_0^2 - 8f^2G^2a_0^2b_0^2 \\
& + \left.\left.\left. 8f^2G\alpha a_0^2b_0^2 - 2f^2\alpha^2a_0^2b_0^2 + 4f^2G^2b_0^4 - 4f^2G\alpha b_0^4 + f^2\alpha^2b_0^4\right)^{\frac{1}{2}}\right)^{\frac{1}{2}}\right), \qquad (3.21)
\end{aligned}
$$

from gain expression it is clear that MI is independent of third order dispersion. We study three different types of MI - spatial, temporal and spatiotemporal.

3.5.1 Spatial MI analysis

Spatial modulation instability can be studied by substituting $\Omega = 0$ in Eq. (3.21) which reduces the expression to

$$g_{MI} = \pm\frac{1}{2}\sqrt{-(-8Gpq^2 + p^2q^4 - 4fpq^2a_0^2)}, \qquad (3.22)$$

MI will occurs only if $q^2 > \frac{8G+4fa_0^2}{p}$. Now from Eq. (3.22), it is clear that spatial MI gain is dependent of quintic nonlinearity only. The variation of gain with quintic nonlinearity as shown in Fig. (3.2). It can be clearly observed that the MI gain

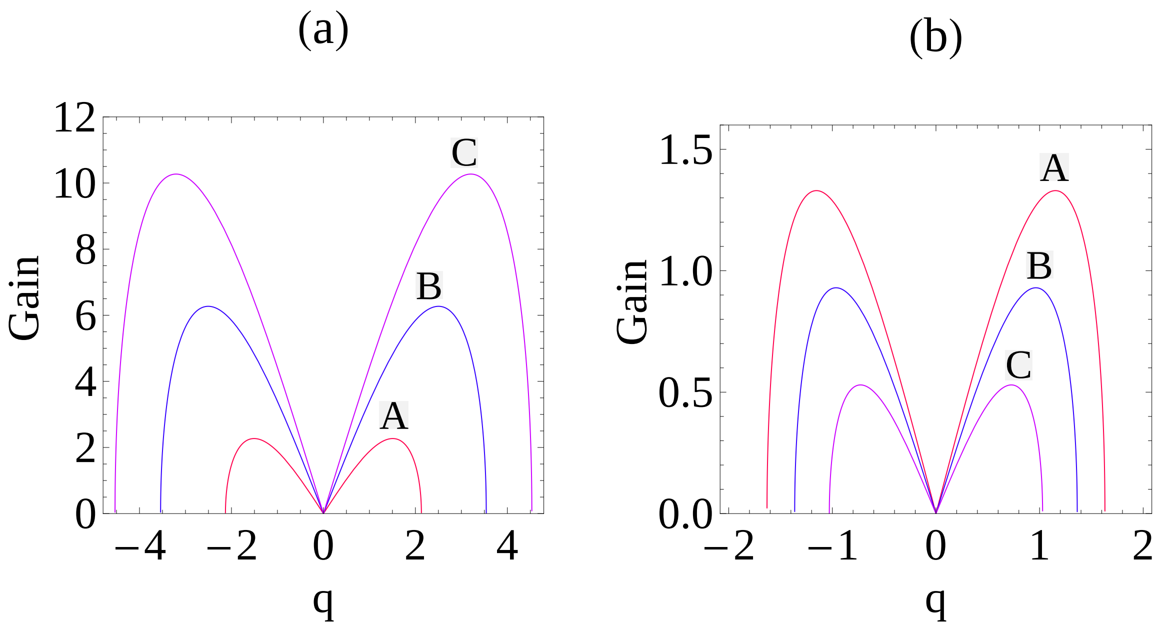

Figure 3.2: Gain profile for the spatial MI (a)for self-focussing medium taking $f = +1$; $(A; B; C$; for $G = -1, -2, -3)$ (b) for defocussing medium taking $f = -1$; $(A; B; C$; for $G = 0.1, 0.2, 0.3)$ and the values of other parameters are $a_0 = 0.93, b_0 = 0.676, p = -1$.

spectrum is symmetric with respect to $q = 0$. From Fig. 3.2(a) it is clear that for judicious choice of various parameters of the gain profile for self-focusing medium (f=+1) increases with decrease in the value of quintic nonlinearity— G. Eventually, due to MI gain, the continuous wave beam would break up spontaneously into a periodic pulse train, known as solitons. Such soliton pulses would exist if the following condition is met: $q^2 > \frac{8G+4fa_0^2}{p}$. Similarly the variation of MI gain profile for defocusing medium (f=-1) with normalized frequency Ω is depicted in Fig. 3.2(b). It is clear from this figure, that the MI gain decreases with the increase in the value of G.

3.5.2 Temporal MI analysis

The temporal MI can be studied by substituting $q = 0$ in Eq. (3.21), hence it reads

$$
\begin{aligned}
g_{MI} = \Big(- \big(&-4\mathrm{G}^2 + \alpha^2 + C_1^2\Omega^2 + f^2\mathrm{s}^2\Omega^2 - 2f\mathrm{G}a_0^2 + f\alpha a_0^2 - 2f\mathrm{G}b_0^2 + f\alpha b_0^2 \\
&- \big(-16\mathrm{G}^2C_1^2\Omega^2 + 4C_1^2\alpha^2\Omega^2 + 4f^2C_1^2s^2\Omega^4 - 8f\mathrm{G}C_1^2\Omega^2a_0^2 + 4fC_1^2\alpha\Omega^2a_0^2 \\
&+ 4f^2\mathrm{G}^2a_0^4 - 4f^2\mathrm{G}\alpha a_0^4 f^2\alpha^2a_0^4 - 8f\mathrm{G}C_1^2\Omega^2b_0^2 + 4fC_1^2\alpha\Omega^2b_0^2 - 8f^2\mathrm{G}^2a_0^2b_0^2 \\
&+ \ 8f^2\mathrm{G}\alpha a_0^2b_0^2 - 2f^2\alpha^2a_0^2b_0^2 + 4f^2\mathrm{G}^2b_0^4 - 4f^2\mathrm{G}\alpha b_0^4 + f^2\alpha^2b_0^4\big)^{\frac{1}{2}}\big)^{\frac{1}{2}}\Big), \qquad (3.23)
\end{aligned}
$$

where $\alpha = \delta\frac{\Omega^2}{2} + \beta_3\Omega^4 + 2G$.

The temporal MI gain is a function of quintic nonlinearity, FOD term, CCD term and SS term. We can study the impact of each parameter on MI. MI for this case occur normal dispersion with self-focusing, and anomalous dispersion with self-defocusing properties and vice-versa. The variation of MI with quintic nonlinearity G for all the four cases is depicted in Fig. (3.3). From Fig. 3.3(a) it is clear that for focusing medium with anomalous dispersion as the value of G decreases the MI gain increase and at $G = -0.4$ the MI gain become so much high that pulse breaks up into shorter pulses. In Fig. 3.3(b) plot is shown for focusing medium with anomalous dispersion, the plot shows that as the value of G decreases MI gain increases and at $G = -0.5$ shorter pulses are formed. In Fig. 3.3(c) the MI gain is plotted for defocusing medium and normal dispersion, the diagram clearly shows that at lower value of G, MI is high and it decreases as the value of G increases. In Fig. 3.3(d) the MI gain is plotted for defocusing medium and anomalous dispersion, again the same effect appear as the value of G decreases the MI increases and at $G = -1.2$ pulse breaks up into shorter pulses. So it is clear that with judicious choice of G and other parameters we can control MI.

Impact of various parameters on MI in normal dispersion regime

Now we shall discuss the effect of various parameters on modulation instability in focussing region and with normal dispersion. The effect of CCD term on the MI is

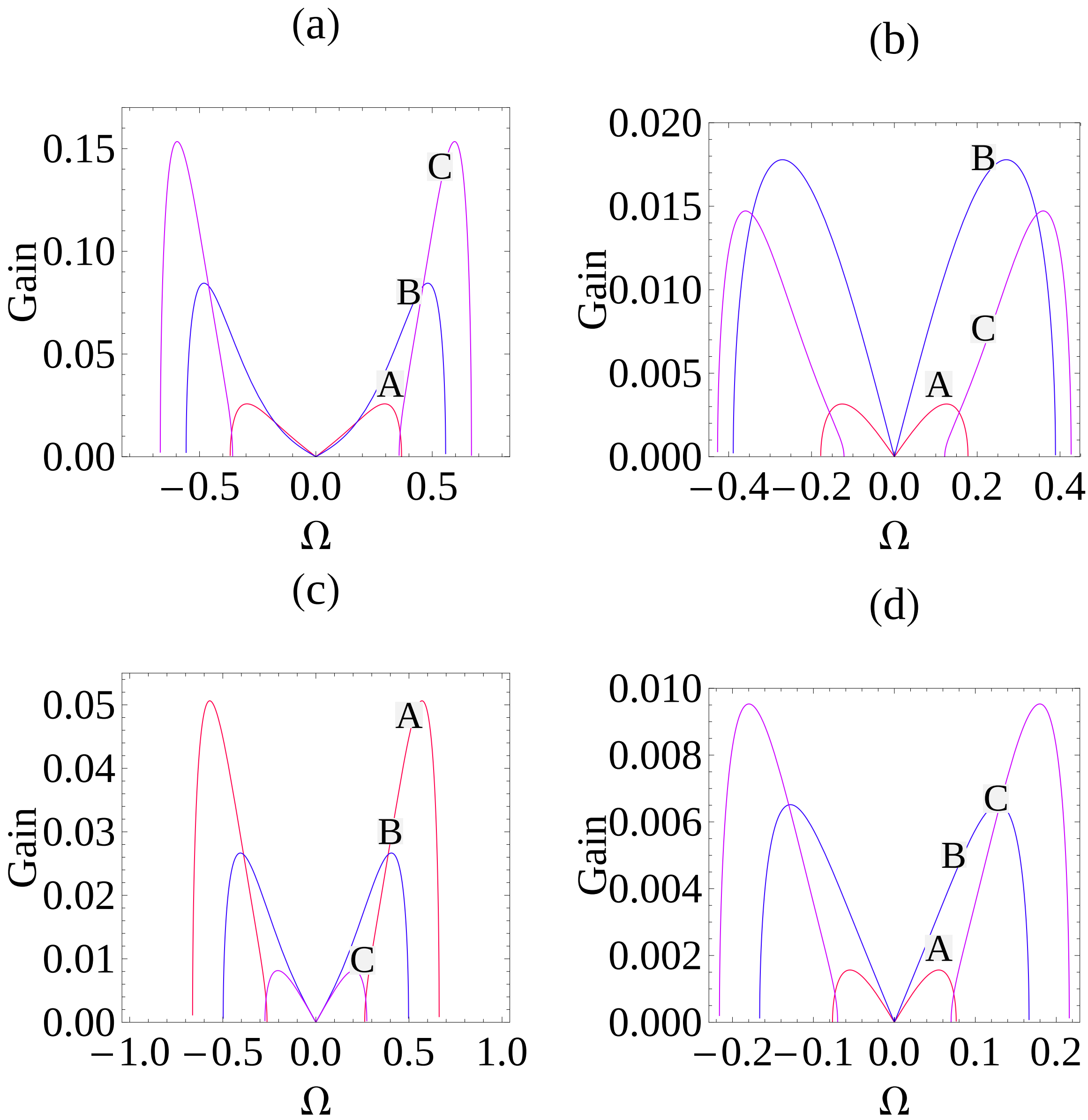

Figure 3.3: Gain profile of temporal Modulation instability in medium with following properties (a) focussing, normal dispersion is plotted with $G = -0.2, -0.3, -0.4$ for A, B, C respectively and $\beta_4 = 2.9; C_1 = 1.1; s = 1$ (b) focussing and anomalous dispersion is plotted with $G = -0.3, -0.4, -0.5; \beta_4 = 2.1; C_1 = 1.063; s = 1$ (c) defocussing, normal dispersion is plotted with $G = 0.5, 0.6, 0.7; \beta_4 = 1; C_1 = 1.7; s = 1.5$ (d) defocussing anomalous dispersion is plotted with $G = -1, -1.1, -1.2; \beta_4 = 1.5; C_1 = 1.69; s = 0.2$. The values of other parameters are $a_0 = 0.93$ and $b_0 = 0.676$.

shown in Fig. (3.4). From Fig. 3.4(a) and Fig. 3.4(b) it is clear that there is only single MI band for particular set of parameters. As the value of CCD parameter

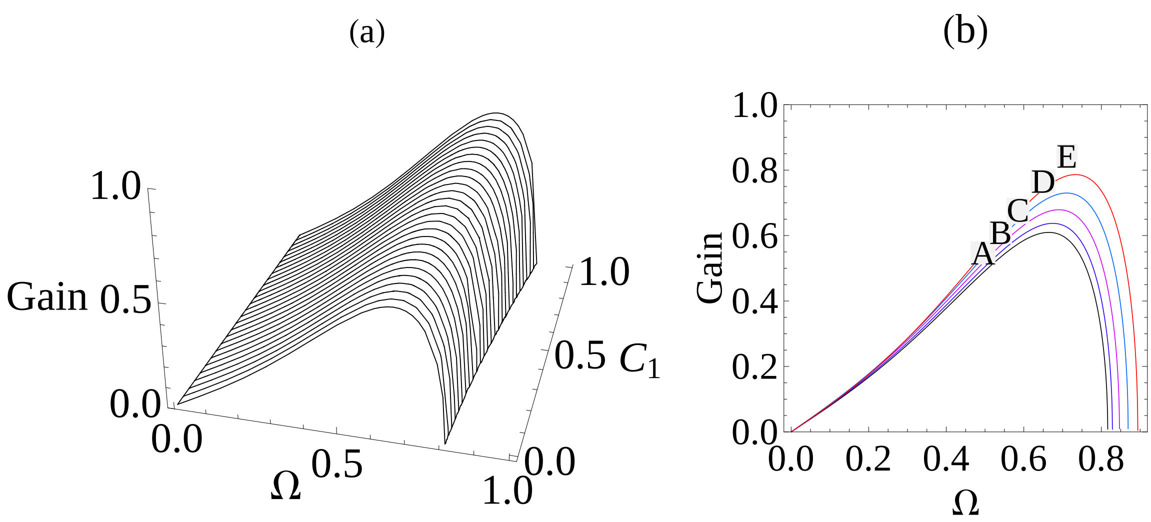

Figure 3.4: (a) 3D plot and (b) 2D plot ($A; B; C; D; E$ for $C_1 = 0.2; 0.4; 0.6; 0.8; 1$) showing the variation of the temporal MI gain spectrum with CCD parameter C_1 in focussing, normal dispersion regime. Other parameters used are $G = -0.3, s = 0.001, a_0 = 1.93, b_0 = 0.00676$, and $\beta_4 = 2$

increases, the MI gain increases and MI side band shifts toward higher frequency.

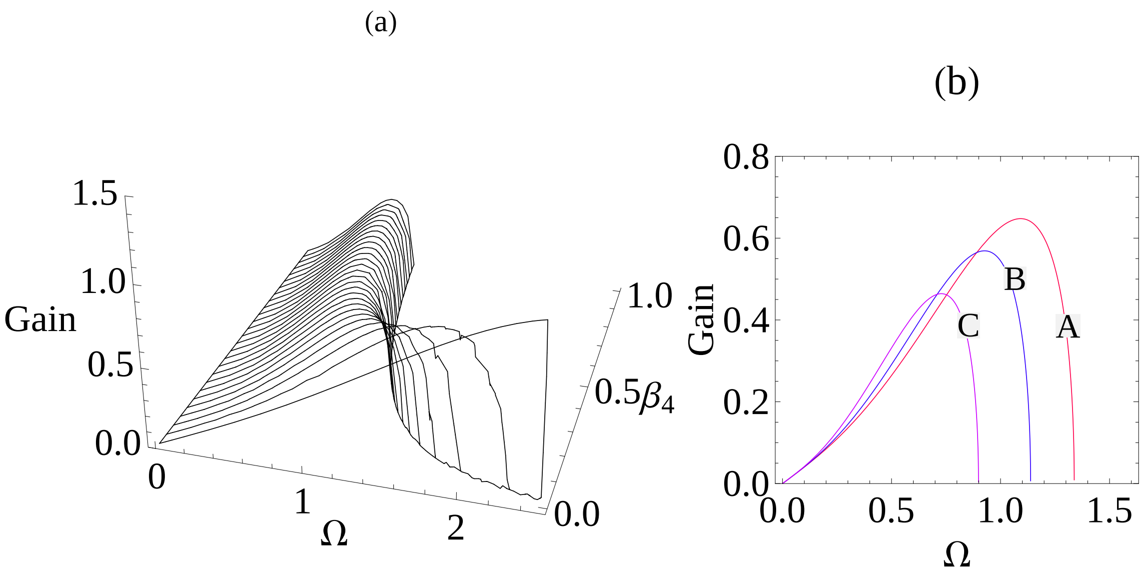

Figure 3.5: (a) 3D plot and (b) 2D plot ($A; B; C$ for $\beta_4 = 0.3; 0.5; 1$) plots showing the variation of the temporal MI gain spectrum with FOD parameter β_4 in focussing, normal dispersion regime. The other parameters are $G = 0.5, s = 0.01, a_0 = 1.93, b_0 = 0.00676$ and $C_1 = 2$

Fig. (3.5) shows the variation of gain spectrum with FOD for various set of parameters in normal dispersion regime. From Fig. 3.5(a) and Fig. 3.5(b) it is clear that there is only single MI band for particular set of parameters. As the value of FOD increases the MI gain decreases and with increase in FOD the MI side band shifts toward lower frequency side. The variation of MI gain with self steepening parameter is shown in Fig. (3.6).

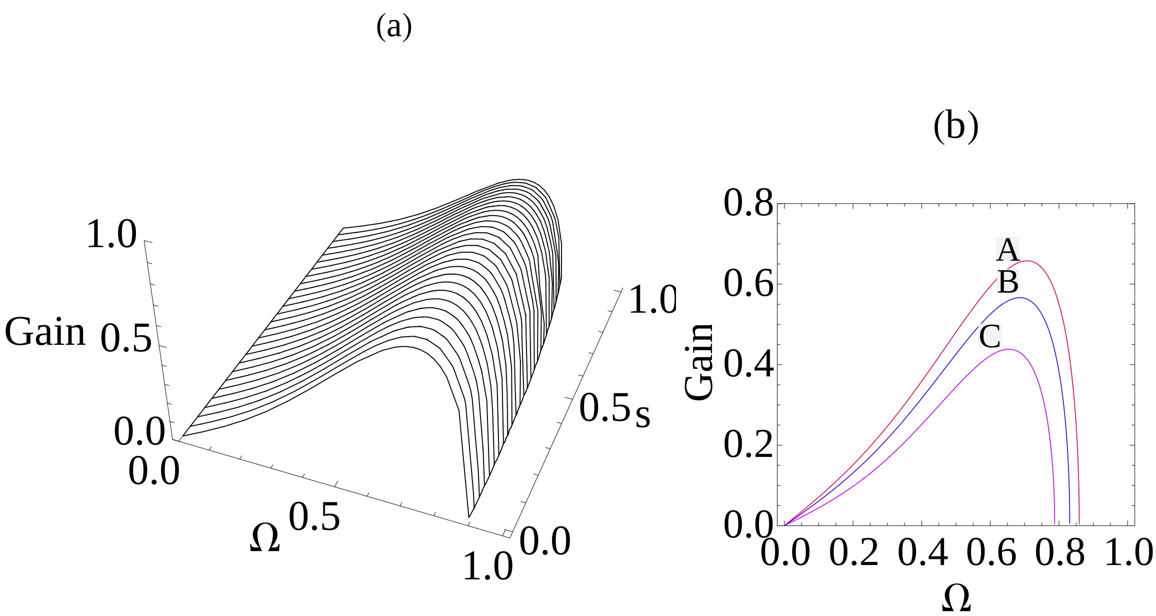

Figure 3.6: (a) 3D plot and (b) 2D plot ($A; B; C$ for $s = 0.1, 0.2, 0.3$) showing the variation of the temporal MI gain spectrum with SS parameter s in focussing, normal dispersion regime. The other parameters are $G = 0.5, s = 0.01, a_0 = 1.93, b_0 = 0.00676$ and $C_1 = 2$

The Fig. 3.6(a) and Fig. 3.6(b) shows that the MI gain decreases with increase in SS parameter and it leads to the slight shifting of MI gain band towards the higher frequency side.

Impact of various parameters on MI in anomalous dispersion regime

Now we shall discuss the effect of various parameters on modulation instability in focussing region and with anomalous dispersion. The effect of CCD term on the

MI is shown in fig. (3.7). From the Fig. 3.7(a) and Fig. 3.7(b) it is clear that

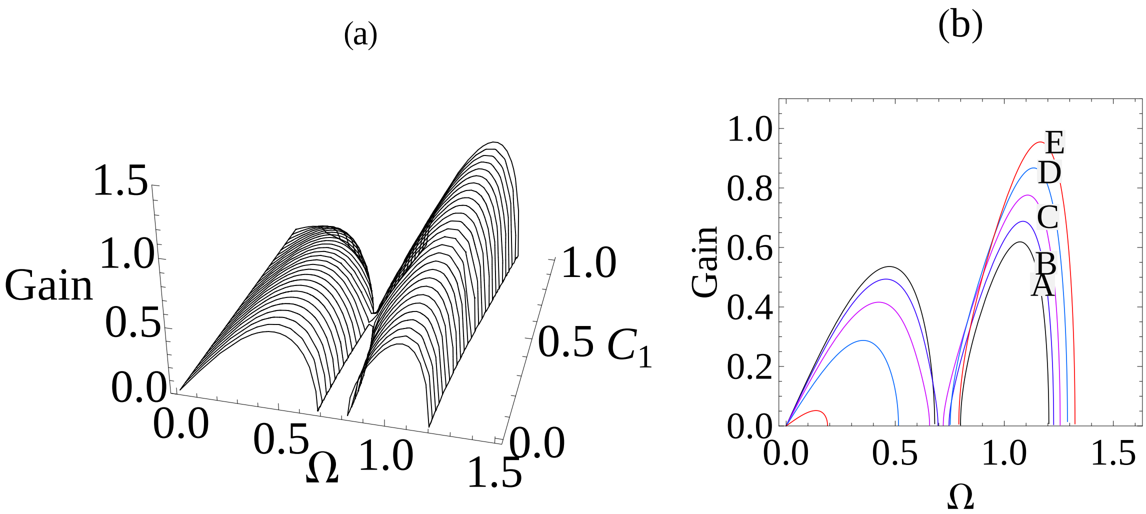

Figure 3.7: (a) 3D plot and (b) 2D plot (A; B; C; D; E for $C_1 = 0.2; 0.4; 0.6; 0.8; 1$) showing the variation of the temporal MI gain spectrum with CCD parameter C_1 in focussing,anomalous dispersion regime. Other parameters used are $G = -0.4, s = 0.5, a_0 = 1.93, b_0 = 0.00676$, and $\beta_4 = 1$

in anomalous dispersion regime there are two bands; one with high amplitude is on higher frequency side and other is on the lower frequency side. Analysis shows that with increase in the value of CCD parameter the gain of lower frequency band decreases and gain of higher frequency sideband increases. It further shows that at very large value of CCD parameter lower frequency band vanishes and only higher frequency band persists. The two bands will remain up to the critical value of C_1 and as earlier as the the C_1 crosses this value only the higher frequency band will remain. This new feature of MI is introduced by CCD term. These results suggest the possibility of switching of the dominant MI from low-frequency band to a high-frequency band.

The variation of MI gain with FOD in anomalous dispersion regime is shown in Fig. 3.8(a) and Fig. 3.8(b). It can be clearly seen that initially there exists two sidebands due to the variation of MI gain with FOD term, namely, lower band on lower frequency side and higher band on higher frequency side. As the value of FOD increases, the MI gain for higher frequency band decreases and it starts shifting toward lower frequency side and for lower frequency band MI gain decreases and it also shifts toward lower frequency side.

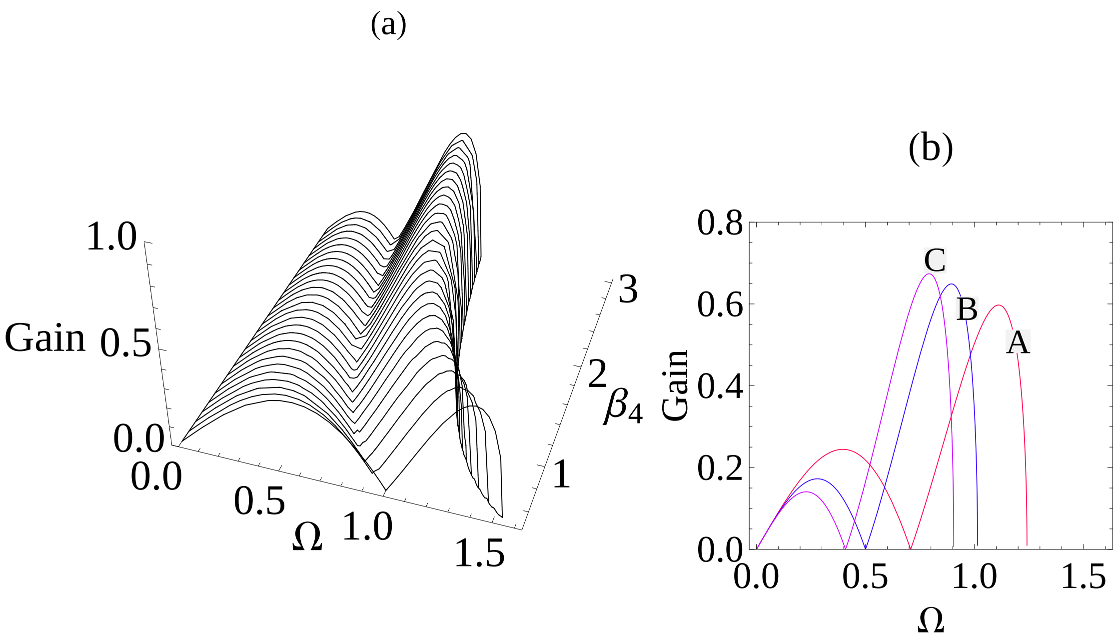

Figure 3.8: (a)3D plot and (b) 2D plot ($A; B; C$ for $\beta_4 = 1, 2, 3$) showing the variation of the MI gain spectrum with FOD parameter β_4 in focussing, anomalous dispersion regime. The values of other parameters are $G = -0.4, s = 1, a_0 = 1.93, b_0 = 0.00676$ and $C_1 = 1$.

Similarly Fig. (3.9) shows that there are two side bands formed in the MI gain, due to the variation of SS parameter. One band lies on the lower frequency side which is having lower MI gain and other on the higher frequency side which is having higher MI gain. Analysis shows that with increase in value of SS parameter the MI gain for lower frequency sideband increases and it shifts toward higher frequency side, however MI gain for higher frequency side decrease with increase in the value of SS parameter, and it slightly shifts toward lower frequency side. Similarly the impact of various parameters on MI gain can be studied in defocussing case.

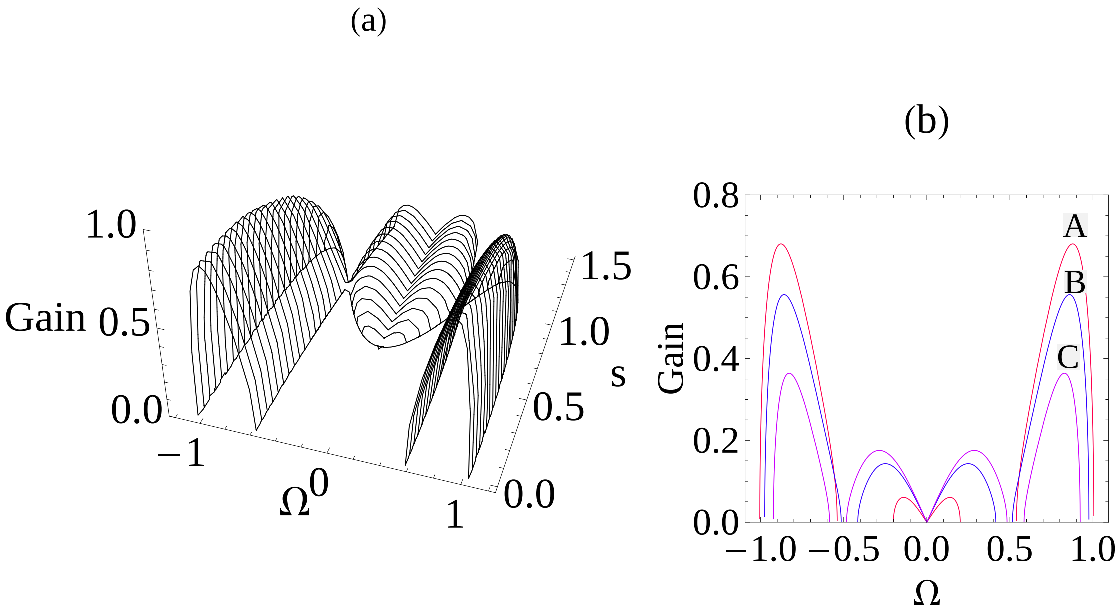

Figure 3.9: (a)3D plot and (b) 2D plot $(A; B; C$ for $s = 0.7, 0.9, 1.1)$ showing the variation of the MI gain spectrum with self-steepening parameter s in focussing, anomalous dispersion regime. The values of other parameters are $G = -0.3, a_0 = 1.93, b_0 = 0.00676, \beta_4 = 1$ and $C_1 = 1$.

3.5.3 Spatiotemporal MI analysis

To study spatiotemporal MI we consider $q \neq 0$ and $\Omega \neq 0$ in Eq. (3.21). Here we carry out a study on the spatiotemporal MI for focusing case with normal and anomalous dispersion, and MI for defocusing case with normal and anomalous dispersion regimes. The results for the spatiotemporal MI for twin-core fibers are summarized in the plots of gain versus temporal frequency Ω and spatial frequency q, which are shown in Fig. (3.10).

3.6 Conclusion

In this work, we have studied the modulational instability for a twin-core fibers in the presence of higher order effects such as quintic nonlinearity, SS, TOD, FOD, and CCD term in both normal and anomalous dispersion regimes discussed. It

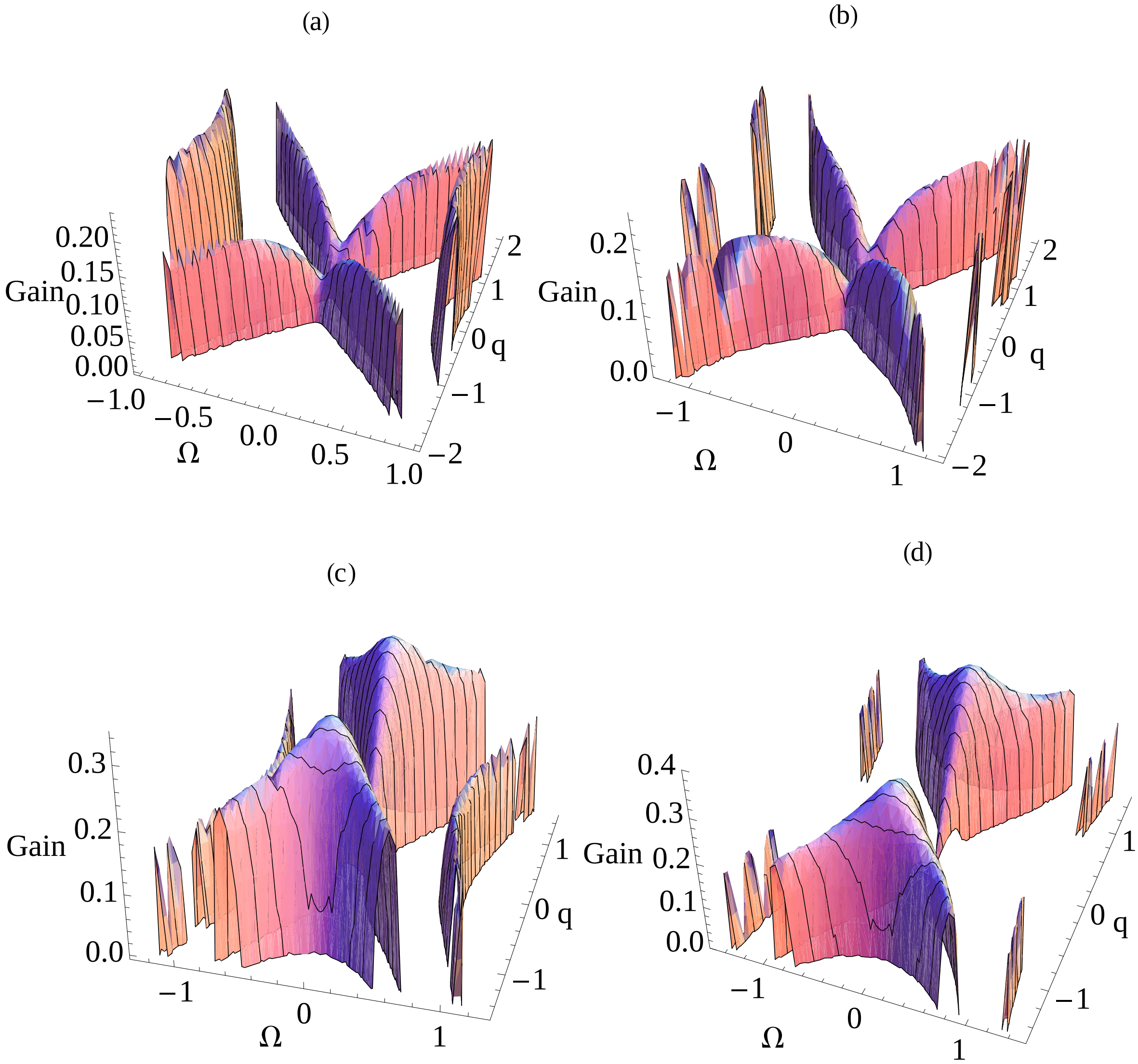

Figure 3.10: spatiotemporal Modulation instability for (a) focussing, normal dispersion (b) focussing anomalous dispersion (c) defocussing, normal dispersion (d) defocussing anomalous dispersion case for $G = -0.4, s = 0.01, a_0 = 0.93, b_0 = 0.676$ and $C_1 = 1$.

is observed that impact of TOD is minimal on MI gain. We have discussed the characteristic of three kinds of MI—spatial, temporal, spatiotemporal. It is found that the spatial MI gain is independent of SS, FOD, CCD terms. We have further investigated the impact of quintic nonlinearity, CCD, FOD, SS on temporal MI gain separately. It is observed that all these terms play vital role in MI gain and none of the terms can be ignored. A judicious choice of all these parameters provides us a freedom to control the MI gain spectrum. To sum up, the MI in twin-core fiber occurs for all combinations of nonlinearity and dispersion. Since the solitons and MI occur in the same parameter regime, this detailed MI analysis suggests the generation of ultrashort pulses in twin-core optical fibers for different parameter domains.

The work presented above is submitted to Journal of Optical Fiber Technology for publication as an article [40].

Bibliography

[1] VI Bespalov and VI Talanov. Filamentary structure of light beams in nonlinear liquids. *ZhETF Pisma Redaktsiiu*, 3:471, 1966.

[2] GP Agrawal. Modulation instability induced by cross-phase modulation. *Physical Review Letters*, 59(8):880–883, 1987.

[3] CM de Sterke. Theory of modulational instability in fiber bragg gratings. *Journal of Optical Society of America B*, 15(11):2660–2667, 1998.

[4] NC Kothari and SC Abbi. Instability growth and filamentation of very intense laser beams in self-focusing media. *Progress of Theoretical Physics*, 83(3):414–442, 1990.

[5] RA Fuerst, DM Baboiu, B Lawrence, WE Torruellas, GI Stegeman, S Trillo, and S Wabnitz. Spatial modulational instability and multi-soliton-like generation in a quadratically nonlinear optical medium. *Physical Review Letters*, 78:2756–2759, 1997.

[6] GP Agrawal. *Applications of nonlinear fiber optics*. Academic Press, 2001.

[7] MJ Potasek. Modulation instability in an extended nonlinear Schrödinger equation. *Optics Letters*, 12(11):921–923, 1987.

[8] LW Liou, XD Cao, CJ McKinstrie, and GP Agrawal. Spatiotemporal instabilities in dispersive nonlinear media. *Physical Review A*, 46(7):4202–4208, 1992.

[9] S Wen and D Fan. Spatiotemporal instabilities in nonlinear kerr media in the presence of arbitrary higher-order dispersions. *Journal of Optical Society of America B*, 19(7):1653–1659, 2002.

[10] T Tanemura and K Kikuchi. Unified analysis of modulational instability induced by cross-phase modulation in optical fibers. *Journal of Optical Society of America B*, 20(12):2502–2514, 2003.

[11] JM Boggio, S Tenenbaum, and HL Fragnito. Amplification of broadband noise pumped by two lasers in optical fibers. *Journal of Optical Society of America B*, 18(10):1428–1435, 2001.

[12] CR Phillips and MM Fejer. Stability of the singly resonant optical parametric oscillator. *Journal of Optical Society of America B*, 27(12):2687–2699, 2010.

[13] G Millot, S Pitois, and PT Dinda. Modulational instability processes in optical isotropic fibers under dual-frequency circular polarization pumping. *Journal of Optical Society of America B*, 19(3):454–460, 2002.

[14] ME Marhic, KKY Wong, and LG Kazovsky. Fiber optical parametric amplifiers with linearly or circularly polarized waves. *Journal of Optical Society of America B*, 20(12):2425–2433, 2003.

[15] C Mckinstrie, S Radic, and C Xie. Parametric instabilities driven by orthogonal pump waves in birefringent fibers. *Optics Express*, 11(20):2619–2633, 2003.

[16] HS Chiu and KW Chow. Effect of birefringence on the modulation instabilities of a system of coherently coupled nonlinear schrödinger equations. *Physical Review A*, 79(6):065803, 2009.

[17] YS Kivshar and GP Agrawal. *Optical solitons: from fibers to photonic crystals.* Academic Press, 2003.

[18] A Höök and M Karlsson. Ultrashort solitons at the minimum-dispersion wavelength: effects of fourth-order dispersion. *Optics Letters*, 18(17):1388–1390, 1993.

[19] T Tanemura, Y Ozeki, and K Kikuchi. Modulational instability and parametric amplification induced by loss dispersion in optical fibers. *Physical Review Letters*, 93(16):163902, 2004.

[20] JM Dudley, G Genty, F Dias, B Kibler, and N Akhmediev. Modulation instability, Akhmediev breathers and continuous wave supercontinuum generation. *Optics Express*, 17(24):21497–21508, 2009.

[21] A Parini, G Bellanca, S Trillo, M Conforti, A Locatelli, and CD Angelis. Self-pulsing and bistability in nonlinear Bragg gratings. *Journal of Optical Society of America B*, 24(9):2229–2237, 2007.

[22] AK Sarma and M Saha. Modulational instability of coupled nonlinear field equations for pulse propagation in a negative index material embedded into a kerr medium. *Journal of Optical Society of America B*, 28(4):944–948, 2011.

[23] R Gupta, TS Raju, CN Kumar, and PK Panigrahi. Modulational instability of copropagating light beams induced by cubic–quintic nonlinearity in nonlinear negative-index material. *Journal of Optical Society of America B*, 29(12):3360–3366, 2012.

[24] NC Panoiu, X Chen, RM Osgood Jr, et al. Modulation instability in silicon photonic nanowires. *Optics Letters*, 31(24):3609–3611, 2006.

[25] K Tai, A Hasegawa, and A Tomita. Observation of modulational instability in optical fibers. *Physical Review Letters*, 56(2):135–138, 1986.

[26] AA Galeev, RZ Sagdeev, Iu S Sigov, VD Shapiro, and VI Shevchenko. Nonlinear theory for the modulation instability of plasma waves. *Soviet Journal of Plasma Physics*, 1:5–10, 1975.

[27] P Sprangle, J Krall, and E Esarey. Hose-modulation instability of laser pulses in plasmas. *Physical Review Letters*, 73(26):3544–3547, 1994.

[28] JH Li, KS Chiang, BA Malomed, and KW Chow. Modulation instabilities in birefringent two-core optical fibres. *Journal of Physics B: Atomic, Molecular and Optical Physics*, 45(16):165404, 2012.

[29] RS Tasgal and BA Malomed. Modulational instabilities in the dual-core nonlinear optical fiber. *Physica Scripta*, 60(5):418, 1999.

[30] AW Snyder. Coupled-mode theory for optical fibers. *Journal of Optical Society of America B*, 62(11):1267–1277, 1972.

[31] KS Chiang. Propagation of short optical pulses in directional couplers with kerr nonlinearity. *Journal of Optical Society of America B*, 14(6):1437–1443, 1997.

[32] KS Chiang. Coupled-mode equations for pulse switching in parallel waveguides. *IEEE Journal of Quantum Electronics*, 33(6):950–954, 1997.

[33] P Shum, KS Chiang, and WA Gambling. Switching dynamics of short optical pulses in a nonlinear directional coupler. *IEEE Journal of Quantum Electronics*, 35(1):79–83, 1999.

[34] PM Ramos and CR Paiva. All-optical pulse switching in twin-core fiber couplers with intermodal dispersion. *IEEE Journal of Quantum Electronics*, 35(6):983–989, 1999.

[35] V Rastogi, KS Chiang, and NN Akhmediev. Soliton states in a nonlinear directional coupler with intermodal dispersion. *Physics Letters A*, 301(1):27–34, 2002.

[36] SC Tsang, KS Chiang, and KW Chow. Soliton interaction in a two-core optical fiber. *Optics Communications*, 229(1):431–439, 2004.

[37] KS Chiang, YT Chow, DJ Richardson, D Taverner, L Dong, L Reekie, and KM Lo. Experimental demonstration of intermodal dispersion in a two-core optical fibre. *Optics Communications*, 143(4):189–192, 1997.

[38] P Peterka, P Honzatko, J Kanka, V Matejec, and I Kasik. Generation of high-repetition-rate pulse trains in a fiber laser through a twin-core fiber. In *Photonics, Devices, and Systems II*, pages 376–381. International Society for Optics and Photonics, 2003.

[39] JH Li, KS Chiang, and KW Chow. Modulation instabilities in two-core optical fibers. *Journal of Optical Society of America B*, 28(7):1693–1701, 2011.

[40] VK Sharma, A Goyal, TS Raju, CN Kumar, and PK Panigrahi. Spatial, temporal, and spatio-temporal modulational instabilities in twin-core optical fibers, submitted to. *Optical Fibre Technology*, 2014.

Chapter 4

Study of modulational instability and solitary wave solutions of variant of nonlinear Schrödinger equation

4.1 Introduction

In this chapter we discuss about the MI and solitary wave solutions for a class of NLSEs. This chapter is divided into two sections. In first section we discuss about bright and dark solitary wave solutions and other localized solutions for higher order NLSE in the presence of non-Kerr terms. In second section we study the modulation instability for NLSE phase locked with an external source. In this section we have studied the impact of variation of source term on MI for focussing as well as defocussing nonlinearity.

4.2 Ultrashort soliton-like solutions GNLSE in the presence of non-Kerr terms

In first chapter we have dicussed that in optical fiber communication, a major role is played by the NLSE [1]. This equation provide a canonical description of the dynamics of quasi monochromatic pulses in weakly nonlinear media and hence is encountered in a variety of fields such as hydrodynamics, plasma physics, optics and in the description of Bose-Einstein condensates. The waveguides which are used for the propagation of pecosecond pulses in nonlinear optical communication systems are usually of Kerr type. The dynamics of such pulses are described by NLSE with cubic nonlinear terms [2, 3, 4]. To enlarge the information carrying capacity, it is necessary to transmit ultrashort optical pulse of subpicosecond and femtosecond size. Now a days in telecommunication and ultrafast signal routing systems, due to the strong intensity of incident light, nonlinearity of non-Kerr type comes into play, the results of which is the change in the stability and physical features of the NLSE solitons. The influences of non-Kerr nonlinearity is described by the NLSE family of equations which include the higher order terms [5, 6, 7, 8, 9]. The higher order nonlinear terms arise from the expansion of the refractive index in terms of light intensity 'I' of the pulse $n = n_0 + n_2 I + n_4 I_2 + \ldots\ldots\ldots\ldots$ here n_0 is the linear refractive index coefficient, n_2 and n_4 are the nonlinear refractive index coefficients which originate from the third and fifth order susceptibilities, respectively. The polarizations induced through third and fifth order susceptibilities give rise to the cubic (Kerr) and quintic (non-Kerr) terms in the NLSE equation, respectively. This type of nonlinearity which originates from third and fifth order susceptibilities can be obtained in optical materials such as semiconductors, glasses doped with semiconductors, calcogenide glasses, polydiacctylene toluene sulfonate (PTS), and some transparent organic materials.

Recently Chaudhuri et. al, [10] considered a generalized NLSE model with non-Kerr terms and presented the existence of dipole solitons. We considered the same model for ultrashort pulse propagation and explored a variety of optical solitons for different parametric conditions. We show the existence of bell and kink type solitons including double-kink and algebraic solitons. The algebraic solitons are necessarily of the Lorentzian type.

4.2.1 Governing Equation

We considered the generalized NLSE for ultrashort pulse propagation through non-Kerr medium, as

$$\psi_z - i\psi_{tt} - i|\psi|^2\psi - \psi_{ttt} - \alpha_1(|\psi|^2\psi)_t - \alpha_2\psi(|\psi|^2)_t - i\alpha_3|\psi|^4\psi - \alpha_4(|\psi|^4\psi)_t - \alpha_5\psi(|\psi|^4)_t = 0, \tag{4.1}$$

where t is the normalized time and z is the normalized distance along the fiber. The terms ψ_{tt}, ψ_{ttt} and $|\psi|^2\psi$ are group velocity dispersion (GVD), third-order dispersion (TOD) and self phase modulation(SPM) respectively. The coefficients α_1, α_2 denotes self-steepening and self-frequency shift due to stimulated Raman scattering (SRS). The coefficients α_3, α_4 and α_5 are the quintic non-Kerr terms. These non-Kerr terms are crucial when shorter pulses of femtosecond width are produced by increasing intensity of incident light. The nonlinear absorption during propagation in highly nonlinear material is compensated by these terms and these terms play an important role for the post-soliton compression to get highly stable compressed optical pulses. If α_3, α_4 and α_5 are all equal to zero then Eq. (4.1) reduce to higher order NLSE which is analyzed by many authors from different points of view [11, 12].

4.2.2 Soliton-like solutions

In order to find exact solitary wave solutions of Eq. (4.1), we have chosen the following form for the complex envelope travelling wave solution

$$\psi(z,t) = \rho(\xi)\ e^{i(\chi(\xi) - kz)}, \tag{4.2}$$

where $\xi = t - uz$ is the travelling coordinate with $\frac{1}{u}$ as velocity. ρ, χ are real functions of ξ.

Substituting Eq. (2) in Eq. (1) and separating real and imaginary part of equation, we obtain following equations

$$-u\rho'+2\rho'\chi'+\rho\chi''-\rho'''+3\rho'(\chi')^2+3\rho\chi'\chi''-3\alpha_1\rho^2\rho'-2\alpha_2\rho^2\rho'-5\alpha_4\rho^4\rho'-4\alpha_5\rho^4\rho'=0, \tag{4.3}$$

$$-u\chi'\rho-k\rho-\rho''+\rho(\chi')^2-\rho^3-3\rho''\chi'-3\rho'\chi''-\rho\chi'''+\rho(\chi')^3-\alpha_1\rho^3\chi'-\alpha_3\rho^5-\alpha_4\chi'\rho^5=0. \tag{4.4}$$

Assume

$$\chi'=m \tag{4.5}$$

Using Eq. (4.5) in Eq. (4.3) and integrating we get

$$\rho''+a\rho+b\rho^3+c\rho^5=0, \tag{4.6}$$

where $a=(u-2m-3m^2)$, $b=\frac{3\alpha_1+2\alpha_2}{3}$ and $c=\frac{5\alpha_4+4\alpha_5}{5}$
Substituting Eq. (4.5) and Eq. (4.6) in Eq. (4.4) and equating the various coefficients to zero, we obtained a set of equations

$$3m+1=0, \tag{4.7}$$

$$-um-k+m^2+m^3=0, \tag{4.8}$$

$$1+\alpha_1 m=0, \tag{4.9}$$

$$\alpha_3+m\alpha_4=0. \tag{4.10}$$

Solving these equations, we obtain $m=-\frac{1}{3}$, $\alpha_1=3$, $\alpha_4=3\ \alpha_3$ and $k=\frac{9u+2}{27}$. Hence, using these expressions, the coefficients in Eq. (4.6) reads as $a=u+\frac{1}{3}$, $b=\frac{9+2\alpha_2}{3}$ and $c=\frac{5\alpha_4+4\alpha_5}{5}$.

Eq. (4.6) is an elliptic equation and is known to admit a variety of solutions. In this paper, we report various localized solution for different parametric conditions. It is interesting to note that if $c=0$, then Eq. (4.6) reduces to a cubic nonlinear equation which admits bright and dark soliton solutions. Also for the case $a=0$, we obtained Lorentzian-type algebraic solutions [13]. In the most general case, when all the coefficients are non-zero, Eq. (4.6) can be mapped into a ϕ^6 field equation to obtain double-kink solutions, [14] and bright and dark soliton solutions [15].

In the following, we describe the parametric conditions for which various soliton-like solutions exist for this model.

Kink-type soliton

For $c = 0.$, we get $\alpha_4 = -\frac{4}{5}\,\alpha_5$. In this situation two subcases are possible which yields soliton solutions.
For $b < 0$ and $a > 0$, we obtain dark soliton of the form

$$\psi(\xi) = \sqrt{\frac{-a}{b}}\tanh\left(\sqrt{\frac{a}{2}}\xi\right)\; e^{i(m\xi - kz)}, \tag{4.11}$$

provided $\alpha_2 < -\frac{9}{2}$ and $u > -\frac{1}{3}$.

The amplitude profile for dark soliton for $\alpha_2 = -5$ and $u = -\frac{1}{4}$ is shown in Fig. 4.1a and corresponding intensity profile is shown in Fig. 4.1b.

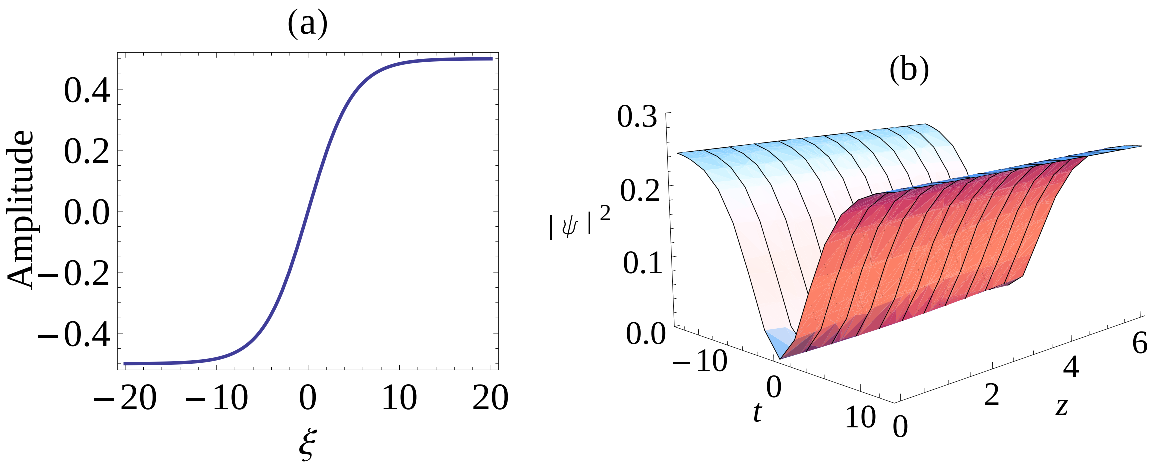

Figure 4.1: (a) Amplitude and (b) intensity of soliton is given in Eq. (4.11) for $\alpha_2 = -5$ and $u = -\frac{1}{4}$.

For $b > 0$ and $a < 0$, we obtain bright soliton of the form

$$\psi(\xi) = \sqrt{-\frac{2a}{b}}\operatorname{sech}\left(\sqrt{-a}\xi\right)\; e^{i(m\xi - kz)}, \tag{4.12}$$

provided $\alpha_2 > -\frac{9}{2}$ and $u < -\frac{1}{3}$.

The the plot of amplitude profile for bright soliton for $\alpha_2 = -4$ and $u = -\frac{2}{3}$ is shown in Fig. 4.2a and corresponding intensity profile is shown in Fig. 4.2b.

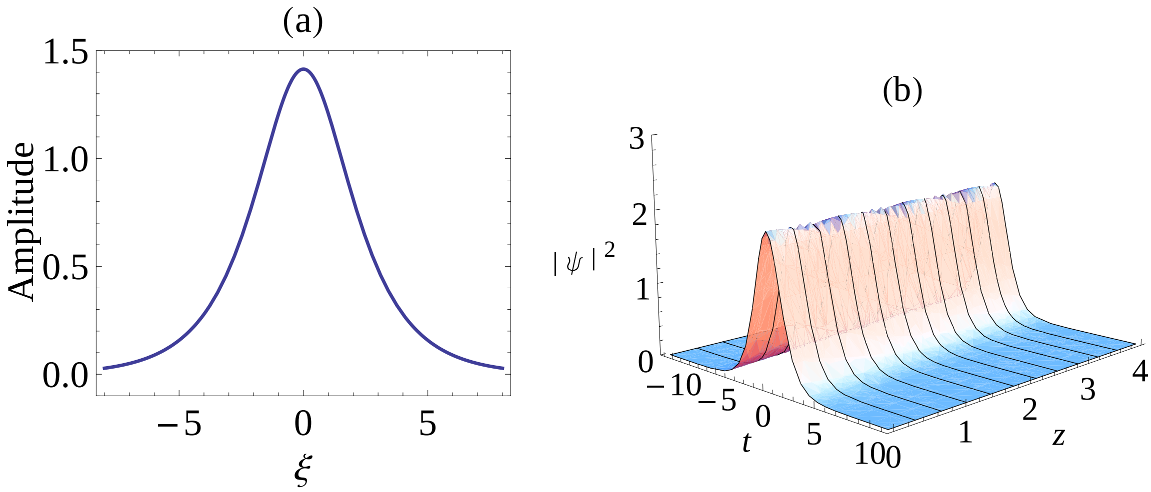

Figure 4.2: (a) Amplitude and (b) intensity of bright soliton given in Eq. (4.12) for $\alpha_2 = -4$ and $u = -\frac{2}{3}$.

Algebraic soliton

For $a = 0$, we obtain another interesting algebraic soliton-like solutions. In particular for $b < 0$ and $c > 0$, the Eq. (4.6) have following solutions, [13]

$$\psi(\xi) = \frac{1}{\sqrt{M + N\xi}}\, e^{i(m\xi - kz)}, \tag{4.13}$$

where $M = -\frac{2c}{3b}$, $N = -\frac{b}{2}$. For $\alpha_2 = -5, \alpha_4 = -3, \alpha_5 = 5, u = -\frac{1}{3}$ the corresponding value of $M = 2, N = 0.167$. The amplitude profile for algebraic solution given in Eq. (4.13) for $\alpha_2 = -5, \alpha_4 = -3, \alpha_5 = 5, u = -\frac{1}{3}$ is shown in Fig. 4.3a and corresponding intensity profile is shown in Fig. 4.3b.

Double-kink soliton

For $a \neq 0, \quad b \neq 0, \quad c \neq 0.$, Eq. (4.6) can be solved for different solitary wave solutions, like double-kink, bell and kink type solution for different parametric conditions

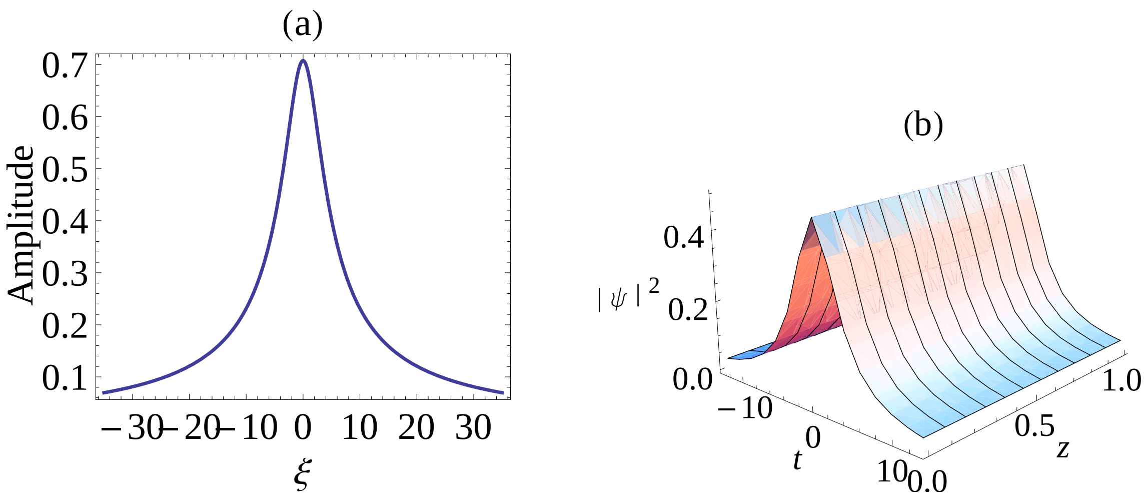

Figure 4.3: (a) Amplitude and (b) intensity plot of bright algebraic soliton-like solution given in Eq. (4.13) for $\alpha_2 = -5, \alpha_4 = -3, \alpha_5 = 5, u = -\frac{1}{3}$.

a) Eq. (4.6) possesses double-kink solutions given as, [14, 16]

$$\psi(\xi) = \frac{P\sinh(q\xi)}{\sqrt{\epsilon + \sinh^2(q\xi)}}\, e^{i(m\xi - kz)}, \tag{4.14}$$

where $a = -q^2\left(\frac{\epsilon-3}{\epsilon}\right), b = \frac{2q^2}{p^2}\left(\frac{2\epsilon-3}{\epsilon}\right), c = -\frac{3q^2}{p^4}\left(\frac{\epsilon-1}{\epsilon}\right)$. Using the expression for a, b, c we can calculate the various unknown parameters P, q and u for different value of ϵ. For $\alpha_2 = 1, \alpha_4 = -1, \alpha_5 = -2$, the value of various unknown parameters can be calculated for different ϵ. The double-kink feature will be more prominent for large value of ϵ. For $\epsilon = 10, 100, 1000$, these parameters are found to be $u = -1.17876, q = 1.09897, P = 1.05826$; $u = -1.29297, q = 0.994642, P = 1.03105$; $u = -1.30191, q = 0.985644, P = 1.0287$ respectively. The amplitude profile for double-kink solution given in Eq. (4.14) for $\alpha_2 = 1, \alpha_4 = -1, \alpha_5 = -2$ and for different values of ϵ is shown in Fig.4.4a and corresponding intensity profile for double-kink solution is shown in Fig.4.4b.

b) It is interesting to note that for $a < 0$ and $b > 0$, Eq. (4.6) has both bright and dark soliton solutions depending upon the value of c [15].

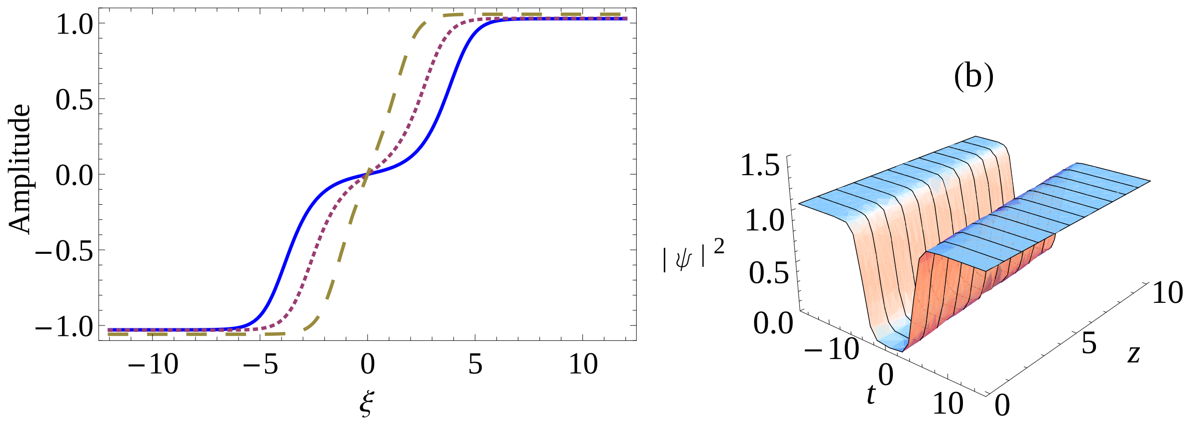

Figure 4.4: (a) Amplitude profile of double-kink solution given in Eq. (4.14) for $\alpha_2 = 1, \alpha_4 = -1, \alpha_5 = -2$ and $\epsilon = 10$ (solid line), $\epsilon = 100$ (dotted line), $\epsilon = 1000$ (dashed line), (b) corresponding intensity profile for $\epsilon = 1000$.

If $c < |\frac{3b^2}{16a}|$, then Eq. (4.6) has a bright soliton-like solution, which is given as

$$\psi(\xi) = \frac{P}{\sqrt{1 + r\cosh(q\xi)}}\, e^{i(m\xi - kz)}, \tag{4.15}$$

where $p^2 = -\frac{4a}{b}, q^2 = -4a, r^2 = 1 - \frac{16ca}{3b^2}$. Using the expression for a, b, c we can calculate the P, q, r. For $\alpha_2 = 5, \alpha_4 = -1, \alpha_5 = -2, u = -2$ the corresponding values of $P = 1.02598, q = 2.58199, r = 0.651017$. The amplitude profile for bright soliton solution given in Eq. (4.15) for $\alpha_2 = 5, \alpha_4 = -1, \alpha_5 = -2, u = -2$ is shown in Fig. 4.5a and corresponding intensity profile is shown in Fig. 4.5b.

If $c = |\frac{3b^2}{16a}|$ then Eq. (4.6) has a kink solution, which is given as

$$\psi_\pm(\xi) = \pm P\sqrt{1 \pm \tanh(q\xi)}\, e^{i(m\xi - kz)}, \tag{4.16}$$

where $P^2 = \frac{-2a}{b}, q^2 = -a$. Using a and b we can calculate the value of P and q. For $\alpha_2 = 5, \alpha_4 = -1, \alpha_5 = -2, u = -2$ the corresponding value of $P = 0.725476$ and $q = 1.29099$. The amplitude profile for solution given in Eq. (4.16) is shown in Fig. 4.6a for $\alpha_2 = 5, \alpha_4 = -1, \alpha_5 = -2, u = -2$ and corresponding intensity profile for solution is shown in Fig. 4.6b.

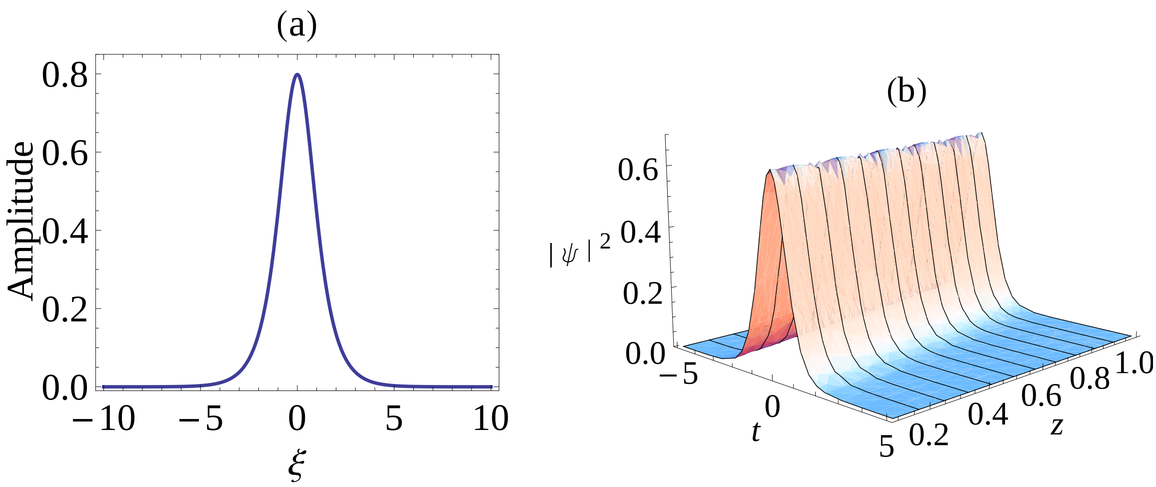

Figure 4.5: (a) Amplitude and (b) intensity of bright soliton given in Eq. (4.15) for $\alpha_2 = 5, \alpha_4 = -1, \alpha_5 = -2$ and $u = -2$.

4.2.3 Conclusion

In this work, we studied the GNLSE with non-Kerr terms, which is short wave equation. We demonstrated that the non-Kerr terms induces different types of bright and dark solitons, which are subjected to constraint relations among the parameters. The higher order terms are responsible for compensation of the nonlinear absorption when pulse propagate through highly nonlinear media and play an important role for the post-soliton compression to get stable compressed optical pulse. These femtosecond pulses are useful to increase the capacity of carrying information in order to make ultra fast communication which is useful for trans-continental and trans-ocean

The work discussed in this section appeared in [17].

4.3 Modulation instability of NLSE phase locked with an external source

4.3.1 Introduction

We have already discussed in second chapter that, MI is a process in which a small amplitude and phase perturbation grows rapidly under the effect of dispersion and nonlinearity

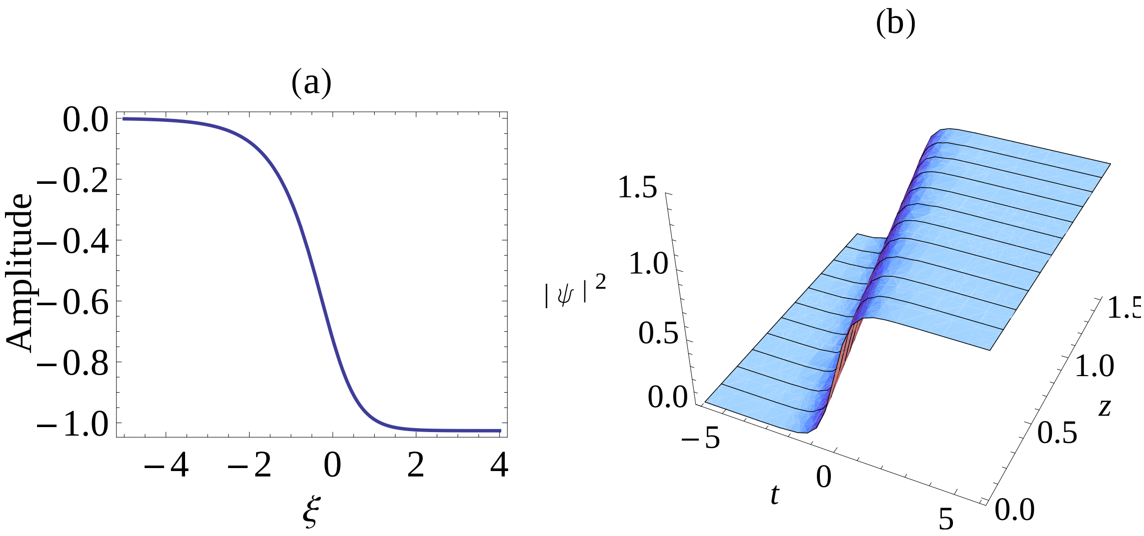

Figure 4.6: (a) Amplitude and (b) intensity of kink soliton solution given in Eq. (4.16) for $\alpha_2 = 5, \alpha_4 = -1, \alpha_5 = -2, u = -2$.

and results into breakup of continuous wave (cw) into pulse train during propagation [18]. MI was first predicted by Bespalov and Talanov [18] for electromagnetic waves in nonlinear media with cubic nonlinearity. Later on Benjamin and Feir predicted MI for deep water waves [19]. Since then MI has been studied in various fields such as fluid dynamics [20, 21], plasma physics [22, 23] and nonlinear optics [24, 25, 26]. In optics MI is of fundamental importance for the formation of temporal and spatial solitons. MI results into the chain of ultrashort pulses which are helpful for high-bit-rate data transmission through an optical fiber [27, 28]. We know the propagation through an optical fiber is described by NLSE. MI for various structure of NLSE has been extensively studied in different context by many research groups [29, 30, 31]. However for NLSE driven by an external source MI has not been studied so far.

In fist chapter we have already discussed that external tunable driving acts as a source of energy and helps in stabilizing the dynamical system against dispersive losses. Externally driven NLSE has been firstly proposed in the seminal work of Kaup and Newell [32]. This equation features prominently in the problem of pulse propagation in asymmetric, twin-core optical fibers [33, 34, 35, 36, 37, 38, 39, 40, 41]. The important applications of externally driven NLSE are to long Josephson junctions [42], charge density waves [43], plasmas driven by radio frequency fields [44] and chaotic phenomena [45]. Although, different novel localized wavepackets signifying similaritons, fractional-transform solitons, and Möbius-transform solitons and their dynamical behaviors are quiet explored for this dynamical system [46, 47, 48, 49], a formal study of MI does not exist so far. In this work we study the MI in case of externally driven NLSE. We explore various regions where MI is possible for self-focussing as well as self-defocussing nonlinearity. We observed that for self-defocussing case MI does not exist for negative source term coefficient. However for self-focussing case MI exist for both positive and negative source term coefficients. We also observed that in self-focussing as well as self-defocussing nonlinearity, MI varies with variation in both nonlinear coefficient and source term coefficient.

4.3.2 Analysis of MI for NLSE, phase locked to an external source

NLSE phase locked to an external source is expressed as

$$i\frac{\partial u}{\partial z}+\frac{\beta_2}{2}\frac{\partial^2 u}{\partial T^2}+\Gamma|u|^2u=\Phi\ e^{i(\delta Z)}, \tag{4.17}$$

where first term is time evolution term, β_2 is the coefficients of group velocity dispersion term, Γ is the coefficient of nonlinear term and Φ is the coefficient of source term. In normalized units $Z=\beta_2 z$, $\gamma=\frac{\Gamma}{\beta_2}$ and $\phi=\frac{\Phi}{\beta_2}$, the Eq. (4.17) reduce to

$$i\frac{\partial u}{\partial Z}+\frac{1}{2}\frac{\partial^2 u}{\partial T^2}+\gamma|u|^2u=\phi\ e^{i(\delta Z)}. \tag{4.18}$$

The steady state solution of Eq. (4.18) is given by

$$u=\sqrt{P_0}\ e^{i(\delta Z)}, \tag{4.19}$$

where P_0 is the initial power and δ is the phase shift. on substituting Eq. (4.19) in Eq. (4.18) we obtain

$$\delta=\gamma P_0-\frac{\phi}{\sqrt{P_0}}, \tag{4.20}$$

If the continuous wave solution is slightly perturbed from steady state,

$$u=\left(\sqrt{P_0}+a(Z,T)\right)\ e^{i(\delta Z)}, \tag{4.21}$$

where $a(Z,T)$ is the perturbation such that $a < 1$. On substituting Eq. (4.21) in Eq. (4.18) we obtain the following evolution equation for the perturbation:

$$i\frac{\partial a}{\partial Z} + \frac{1}{2}\frac{\partial^2 a}{\partial T^2} + \gamma P_0(a + a^*) + \frac{\phi\ a}{\sqrt{P_0}} = 0. \tag{4.22}$$

This equation can be easily solved in frequency domain. However, because of the a^* term, the Fourier components at frequencies Ω and $-\Omega$ are coupled. Thus we should consider its solution in the form

$$a(Z,T) = a_1 \exp[i(KZ - \Omega T)] + a_2 \exp[-i(KZ - \Omega T)], \tag{4.23}$$

where K is the longitudinal wave number and Ω is the frequency of the perturbation. on substituting Eq. (4.23) in Eq. (4.22) we obtain

$$\begin{aligned}&\left(-Ka_1 + \gamma a_0^2 a_1 + \gamma a_0^2 a_2 + \frac{\phi}{a_0}a_1 - \frac{\beta}{2}\Omega^2 a_1\right)\exp[i(KZ - \Omega T)]\\ &+\left(Ka_2 + \gamma a_0^2 a_2 + \gamma a_0^2 a_1 + \frac{\phi}{a_0}a_2 - \frac{\beta}{2}\Omega^2 a_2\right)\exp[-i(KZ - \Omega T)],\end{aligned} \tag{4.24}$$

separation the coefficients of $\exp[i(KZ - \Omega T)]$ and $\exp[-i(KZ - \Omega T)]$, we get

$$\begin{aligned}-Ka_1 + \gamma a_0^2 a_1 + \gamma a_0^2 a_2 + \frac{\phi}{a_0}a_1 - \frac{\beta}{2}\Omega^2 a_1 = 0,\\ Ka_2 + \gamma a_0^2 a_2 + \gamma a_0^2 a_1 + \frac{\phi}{a_0}a_2 - \frac{\beta}{2}\Omega^2 a_2 = 0,\end{aligned} \tag{4.25}$$

we can write Eq. (4.25) in the matrix form as

$$\begin{pmatrix} -k + A_{11} & \gamma a_0^2 \\ \gamma a_0^2 & K + A_{11}\end{pmatrix}\begin{pmatrix} a_1 \\ a_2\end{pmatrix} = \begin{pmatrix} 0 \\ 0\end{pmatrix},$$

where $A_{11} = \gamma a_0^2 + \frac{\phi}{a_0} - \frac{\beta}{2}\Omega^2$, hence

$$\begin{pmatrix} -k + A_{11} & \gamma a_0^2 \\ \gamma a_0^2 & K + A_{11}\end{pmatrix}=0,$$

from above matrix, we obtain dispersion relation for K which is given by

$$K = \pm\frac{1}{2}\sqrt{\Omega^4 - 4\left(\gamma\sqrt{P_0} + \frac{\phi}{\sqrt{P_0}}\right)\Omega^2 + \frac{4\phi^2}{\sqrt{P_0}} + 8\phi\gamma\sqrt{P_0}}, \tag{4.26}$$

$$K = \pm\frac{1}{2}\sqrt{\left(\Omega^2 - \frac{2\phi}{\sqrt{P_0}}\right)\left(\Omega^2 - \frac{2\phi}{\sqrt{P_0}} - 4\gamma P_0\right)}. \tag{4.27}$$

The steady-state solution becomes unstable if K becomes imaginary, because then perturbation grows exponentially. The general expression of the MI gain is

$$g(\Omega) = 2Im(K) = \sqrt{-\left(\Omega^2 - \frac{2\phi}{\sqrt{P_0}}\right)\left(\Omega^2 - \frac{2\phi}{\sqrt{P_0}} - 4\gamma P_0\right)}. \tag{4.28}$$

It is clear from the gain expression that MI gain depends upon source term coefficient ϕ, nonlinear term coefficient γ and the perturbed normalized frequency Ω. The region where MI is possible for both self-focussing and self-defocussing nonlinearity is shown in Fig. (4.7). It is clear from Fig. 4.7 that MI is possible for all set of values ϕ and γ except when ϕ and γ both are less than zero simultaneously. It is instructive to note that the solitary wave solutions obtained for NLSE phase locked to an external source in the ref. [35], also lies in the same range of k and g, which corresponds to ϕ and γ respectively in our work. The analysis of this work [35] shows that solitary waves solution for NLSE with an external source are possible everywhere except where $k < 0$ and $g < 0$ simultaneously. On the basis of this, we have shown the variation of MI gain with frequency in Fig.(4.8), Fig.(4.9) and Fig.(4.10).

4.3.3 Special cases

For Self-defocussing nonlinearity ($\gamma < 0$)

Case-I: For $\phi > 0$

Fig. (4.8) shows the variation of MI with nonlinearity γ and source terms coefficient ϕ for self-defocussing nonlinearity. It is clear from Fig. 4.8(a)–4.8(d) that as the value of γ decreases from -0.009 to -0.015, the amplitude of gain profile increases for $\phi = 20, 25, 30$. For $\phi = 20$ splitting occurs at $\gamma = -0.009$, for $\phi = 25$ and $\phi = 30$, the splitting of side-band occurs at $\gamma = -0.012$. Analysis shows that with increase in nonlinearity, gain

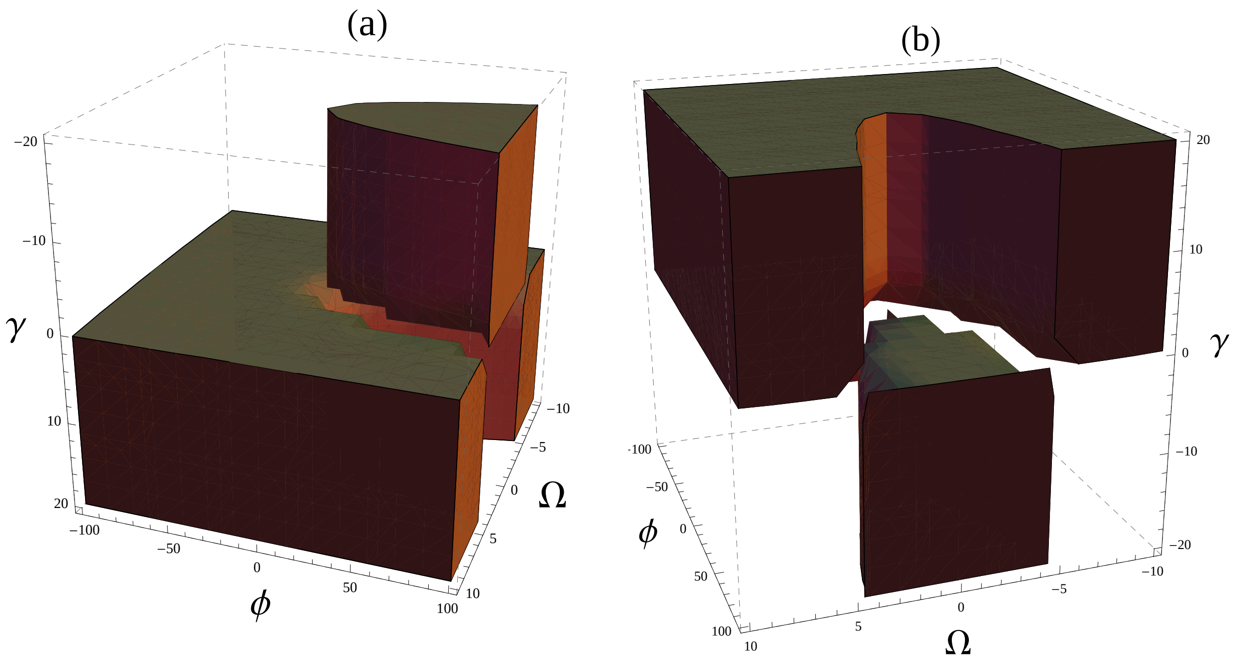

Figure 4.7: Region where MI is possible for $P_0 = 100$ and for set of range of ϕ, γ and Ω.

increases however the increase in source term coefficient leads to the shifting of side-bands towards higher frequency side.

For Self-focussing nonlinearity ($\gamma > 0$)

Case-I: For $\phi > 0$

Fig. (4.9) shows the variation of MI gain with γ for different values of ϕ for self-focussing nonlinearity. It is clear from Fig. 4.9(a)–4.9(d) that as the value of γ increases from 0.005 to 1, the amplitude of gain profile increases for all values of ϕ. When $\gamma = 1$ the gain profile for all values of ϕ coincides and splitting reduces. We analyzed that for self-focussing nonlinearity with increase in value of nonlinearity MI gain increases. We further observed that at lower value of nonlinearity as the source parameter increases MI side-bands shifts towards higher frequency side. With increase in value nonlinearity the impact of source parameter on MI reduces and at higher value the MI sideband coincides for all values of source parameter.

Case-II: For $\phi < 0$

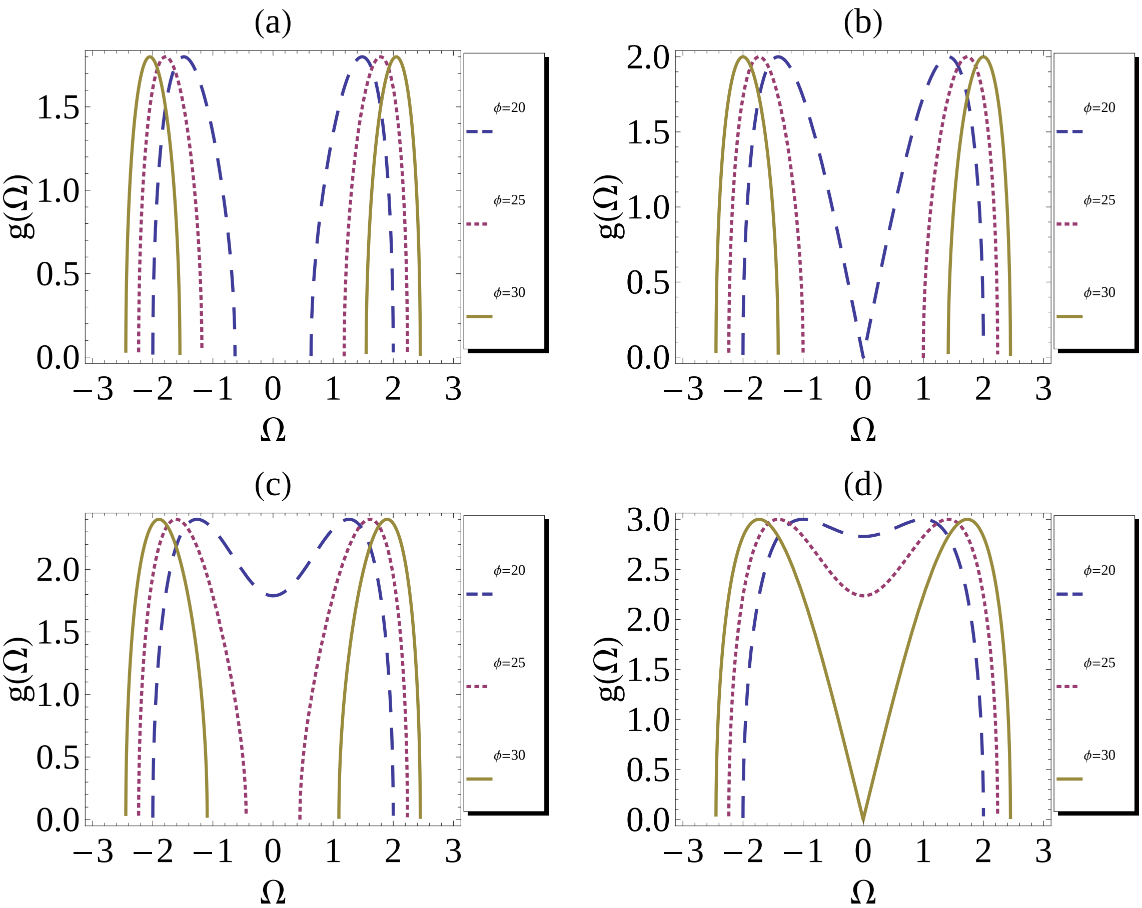

dc

Figure 4.8: Gain profile of MI for (a)$\gamma = -0.009$ (b)$\gamma = -0.01$ (c)$\gamma = -0.012$ (d)$\gamma = -0.015$ respectively at initial power of $P_0 = 100$.

Fig. (4.10) shows the variation of MI gain with γ for different values of ϕ for self-focussing nonlinearity. It is clear from Fig. 4.10(a)–4.10(d) that as the value of γ increases from 0.005 to 10, the amplitude of gain profile increases for all values of ϕ. Hence it is clear that at lower value of nonlinear parameter as the value of source term coefficient increases, MI sidebands shift towards higher frequency side. However for higher value of nonlinearity, the effect of source term coefficient on MI reduces and MI side band for all value of ϕ overlap.

4.3.4 Conclusion

In conclusion, a number of interesting features have emerged from the study of MI of NLSE driven with external source. Analysis shows that MI exist for all regions except

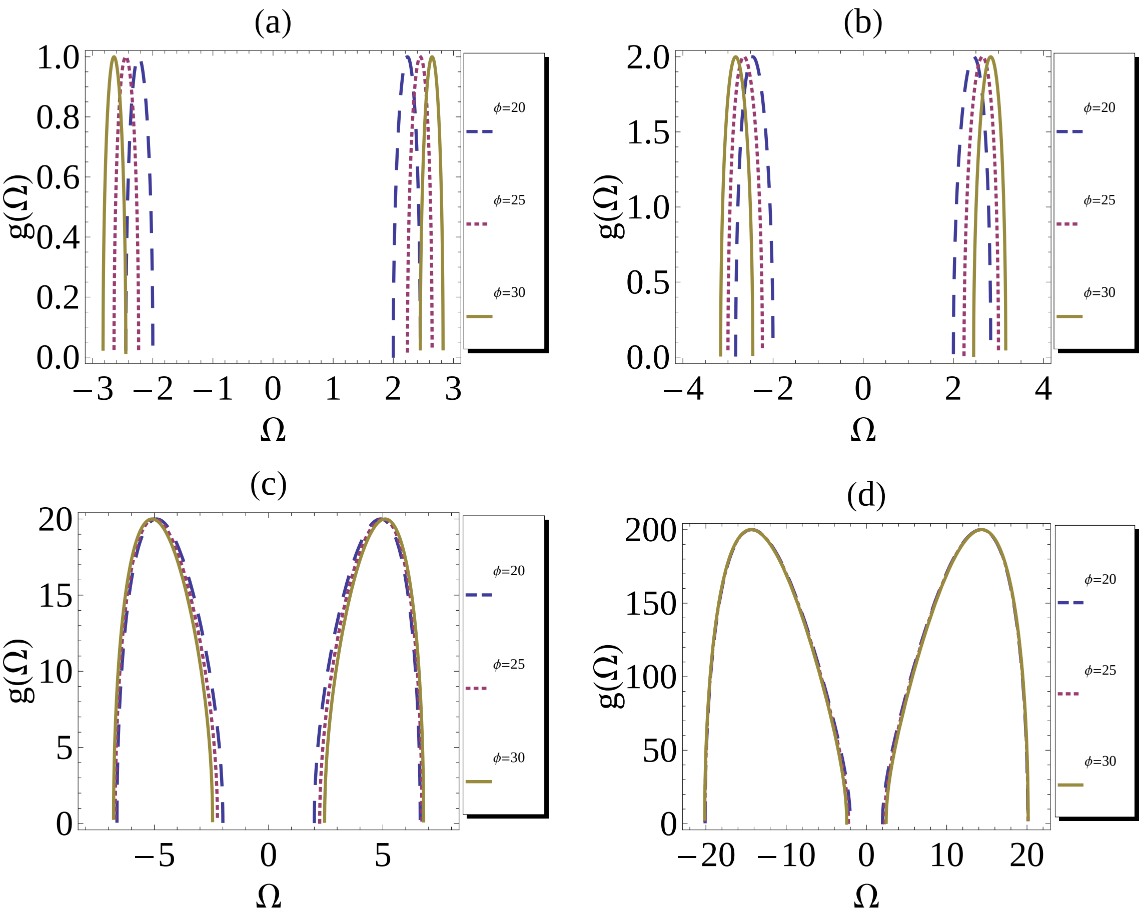

Figure 4.9: Gain profile of MI for (a)$\gamma = 0.005$ (b)$\gamma = 0.01$ (c)$\gamma = 0.1$ (d)$\gamma = 1$ respectively and at initial power of $P_0 = 100$.

the region where nonlinearity is self-defocussing in nature and source term coefficient is negative. The results of ref. [35] indicate that soliton-like solutions are also possible for all parametric regime except the region where nonlinearity and source term both are negative. This may be the answer for well established question that whether splitting of MI side-bands results into the solitons formation. It is observed that for all cases MI gain increases with increase in nonlinearity. For self-defocussing case, with increase in nonlinearity, MI gain increases and increase of source term coefficient leads to shifting of sidebands towards higher frequency side. We further observed that for lower value of self-focussing nonlinearity and positive source term coefficient, with increase in source term coefficient, MI side-bands shifts towards higher frequency side. It is further observed that with increase in value nonlinearity the impact of source parameter on MI reduces

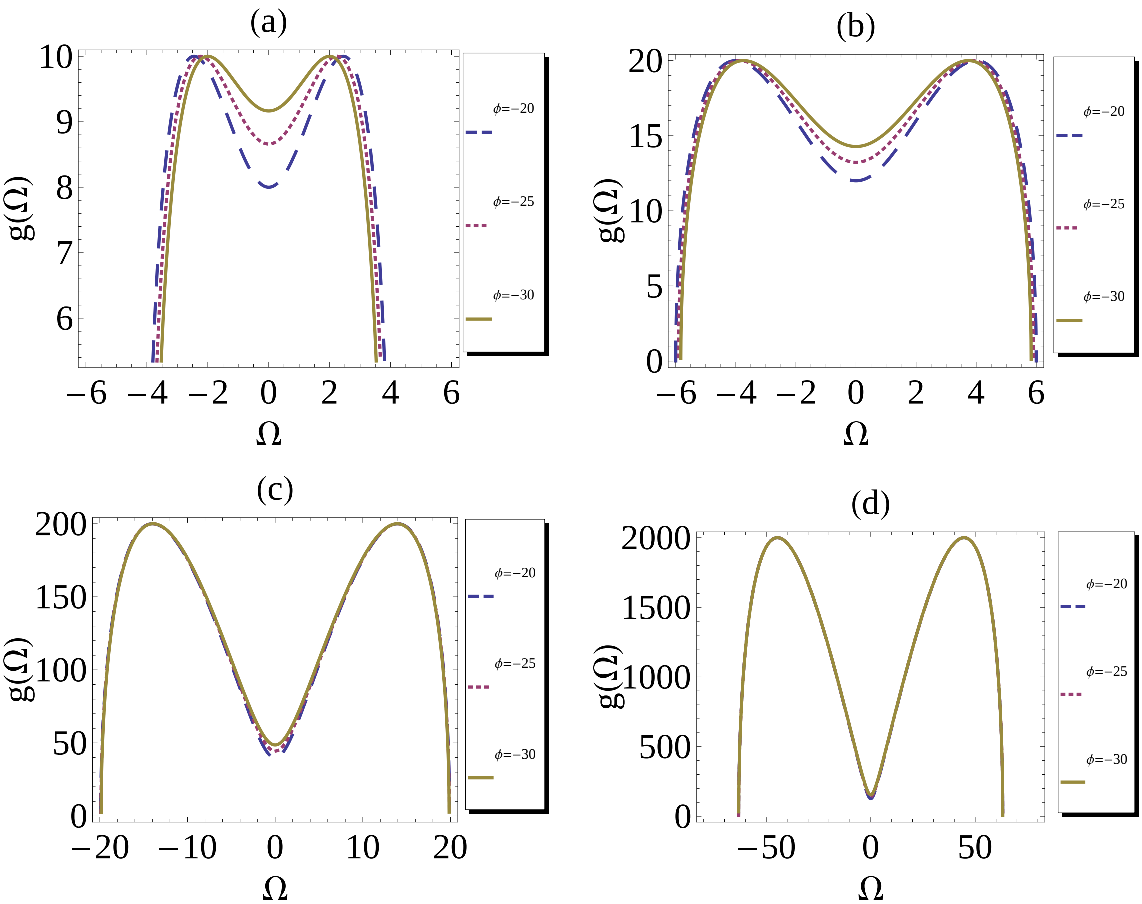

Figure 4.10: Gain profile of MI for (a)$\gamma = 0.005$ (b)$\gamma = 0.1$ (c)$\gamma = 1$ (d)$\gamma = 10$ respectively at initial power $P_0 = 100$.

and at higher nonlinear coefficient the MI sideband coincides for all values of source term coefficients. For self-focussing nonlinearity and negative source term coefficient, at lower value of nonlinear parameter as the value of source term increases, MI sidebands shift towards higher frequency side. However with increase in value of nonlinearity, the effect of source parameter on MI reduces and for high nonlinearity, MI side band for all value of source parameter overlap.

The work discussed above in submitted for publication as regular article in Journal of Mathematics and Computers with Applications [50].

Bibliography

[1] A Hasegawa. *Optical solitons in fibers.* Springer, 1989.

[2] YS Kivshar and GP Agrawal. *Optical solitons: from fibers to photonic crystals.* Academic Press, 2003.

[3] VI Kruglov, AC Peacock, and JD Harvey. Exact self-similar solutions of the generalized nonlinear Schrödinger equation with distributed coefficients. *Physical Review Letters*, 90(11):113902, 2003.

[4] VN Serkin and A Hasegawa. Novel soliton solutions of the nonlinear Schrödinger equation model. *Physical Review Letters*, 85(21):4502–4505, 2000.

[5] CN Kumar and P Durganandini. New phase modulated solutions for a higher-order nonlinear Schrödinger equation. *Pramana–J. Phys*, 53(2):271–277, 1999.

[6] R Radhakrishnan, A Kundu, and M Lakshmanan. Coupled nonlinear Schrödinger equations with cubic-quintic nonlinearity: Integrability and soliton interaction in non-kerr media. *Physical Review E*, 60(3):3314–3323, 1999.

[7] WP Hong. Optical solitary wave solutions for the higher order nonlinear Schrödinger equation with cubic-quintic non-kerr terms. *Optics Communications*, 194(1):217–223, 2001.

[8] A Choudhuri and K Porsezian. Impact of dispersion and non-kerr nonlinearity on the modulational instability of the higher-order nonlinear Schrödinger equation. *Physical Review A*, 85(3):033820, 2012.

[9] VK Sharma, A Goyal, TS Raju, and CN Kumar. Periodic and solitary wave solutions for ultrashort pulses in nims. *Journal of Modern Optics*, 60(1):836–840, 2013.

[10] A Choudhuri and K Porsezian. Dark-in-the-bright solitary wave solution of higher-order nonlinear Schrödinger equation with non-kerr terms. *Optics Communications*, 285(3):364–367, 2012.

[11] M Gedalin, TC Scott, and YB Band. Optical solitary waves in the higher order nonlinear Schrödinger equation. *Physical Review Letters*, 78(3):448–451, 1997.

[12] Z Li, L Li, H Tian, and G Zhou. New types of solitary wave solutions for the higher order nonlinear Schrödinger equation. *Physical Review Letters*, 84(18):4096–4099, 2000.

[13] A Goyal, R Gupta, CN Kumar, and TS Raju. Chirped femtosecond solitons and double-kink solitons in the cubic-quintic nonlinear Schrödinger equation with self-steepening and self-frequency shift. *Physical Review A*, 84(6):063830, 2011.

[14] NH Christ and TD Lee. Quantum expansion of soliton solutions. *Physical Review D*, 15(6):1606–1627, 1975.

[15] SN Behera and A Khare. Classical φ^6-field theory in (1+ 1) dimensions. A model for structural phase transitions. *Pramana-Journal of Physics*, 15(3):245–269, 1980.

[16] A Goyal, VK Sharma, TS Raju, and CN Kumar. Chirped double-kink and fractional-transform solitons in an optical gain medium with two-photon absorption. *Journal of Modern Optics*, 61(4):315–321, 2014.

[17] VK Sharma and A Goyal. Ultrashort double-kink and algebraic solitons of generalized nonlinear schrödinger equation in the presence of non-kerr terms. *Journal of Nonlinear Optical Physics & Materials*, 23(03), 2014.

[18] VI Bespalov and VI Talanov. Filamentary structure of light beams in nonlinear liquids. *ZhETF Pisma Redaktsiiu*, 3:471, 1966.

[19] TB Benjamin and JE Feir. The disintegration of wave trains on deep water part 1. theory. *Journal of Fluid Mechanics*, 27(03):417–430, 1967.

[20] AI Dyachenko and VE Zakharov. Modulation instability of stokes wave or freak wave. *Journal of Experimental and Theoretical Physics Letters*, 81(6):255–259, 2005.

[21] H Hasimoto and H Ono. Nonlinear modulation of gravity waves. *Journal of the Physical Society of Japan*, 33(3):805–811, 1972.

[22] GP Agrawal. Modulation instability induced by cross-phase modulation. *Physical Review Letters*, 59(8):880–883, 1987.

[23] P Sprangle, J Krall, and E Esarey. Hose-modulation instability of laser pulses in plasmas. *Physical Review Letters*, 73(26):3544–3547, 1994.

[24] VI Karpman. Self-modulation of nonlinear plane waves in dispersive media. *Soviet Journal of Experimental and Theoretical Physics Letters*, 6:277, 1967.

[25] K Tai, A Hasegawa, and A Tomita. Observation of modulational instability in optical fibers. *Physical Review Letters*, 56(2):135–138, 1986.

[26] S Trillo and S Wabnitz. Dynamics of the nonlinear modulational instability in optical fibers. *Optics Letters*, 16(13):986–988, 1991.

[27] A Hasegawa. Generation of a train of soliton pulses by induced modulational instability in optical fibers. *Optics Letters*, 9(7):288–290, 1984.

[28] G Millot, S Pitois, and PT Dinda. Modulational instability processes in optical isotropic fibers under dual-frequency circular polarization pumping. *Journal of Optical Society of America B*, 19(3):454–460, 2002.

[29] D Anderson and M Lisak. Modulational instability of coherent optical-fiber transmission signals. *Optics Letters*, 9(10):468–470, 1984.

[30] S Liu. Four-wave mixing and modulation instability of continuous optical waves in single-mode optical fibers. *Applied Physics Letters*, 89(17):171118, 2006.

[31] GP Agrawal, PL Baldeck, and RR Alfano. Modulation instability induced by cross-phase modulation in optical fibers. *Physical Review A*, 39(7):3406–3413, 1989.

[32] DJ Kaup and AC Newell. Solitons as particles, oscillators, and in slowly changing media: a singular perturbation theory. *Proceedings of the Royal Society of London. A. Mathematical and Physical Sciences*, 361(1707):413–446, 1978.

[33] BA Malomed. Bound solitons in a nonlinear optical coupler. *Physical Review E*, 51(2):R864–R866, 1995.

[34] G Cohen. Soliton interaction with an external traveling wave. *Physical Review E*, 61(1):874–879, 2000.

[35] TS Raju, CN Kumar, and PK Panigrahi. Exact solitary wave solutions of the non-linear Schrödinger equation with a source. *Journal of Physics A: Mathematical and General*, 38:L271–L276, 2005.

[36] VM Vyas, TS Raju, CN Kumar, and PK Panigrahi. Soliton solutions of driven nonlinear Schrödinger equation. *Journal of Physics A: Mathematical and General*, 39(29):9151–9159, 2006.

[37] TS Raju, PK Panigrahi, and K Porsezian. Nonlinear compression of solitary waves in asymmetric twin-core fibres. *Physical Review E*, 71:026608, 2005.

[38] TS Raju, PK Panigrahi, and K Porsezian. Self-similar propagation and compression of chirped self-similar waves in asymmetric twin-core fibers with nonlinear gain. *Physical Review E*, 72(4):046612, 2005.

[39] TS Raju and PK Panigrahi. self-similar propagation in graded-index nonlinear-fiber amplifier with an external source. *Physical Review A*, 81:043820, 2010.

[40] TS Raju and PK Panigrahi. Optical similaritons in a tapered graded-index nonlinear-fiber amplifier with an external source. *Physical Review A*, 84(3):033807, 2011.

[41] TS Raju, PK Panigrahi, and CN Kumar. Compression and propagation of dispersive and rectangular similaritons in asymmetric twin-core fibers. *Journal of Optical Society of America B*, 30:934, 2013.

[42] PS Lomdahl and MR Samuelsen. Persistent breather excitations in an ac-driven sine-gordon system with loss. *Physical Review A*, 34(1):664–667, 1986.

[43] DJ Kaup and AC Newell. Theory of nonlinear oscillating dipolar excitations in one-dimensional condensates. *Physical Review B*, 18(10):5162–5167, 1978.

[44] K Nozaki and N Bekki. Chaos in a perturbed nonlinear Schrödinger equation. *Physical Review Letters*, 50(17):1226–1229, 1983.

[45] K Nozaki and N Bekki. Low-dimensional chaos in a driven damped nonlinear Schrödinger equation. *Physica D: Nonlinear Phenomena*, 21(2):381–393, 1986.

[46] IV Barashenkov, MM Bogdan, and VI Korobov. Stability diagram of the phase-locked solitons in the parametrically driven, damped nonlinear Schrödinger equation. *Europhysics Letters*, 15(2):113, 1991.

[47] D Cai, AR Bishop, N Grønbech-Jensen, and BA Malomed. Bound solitons in the ac-driven, damped nonlinear Schrödinger equation. *Physical Review E*, 49(2):1677–1679, 1994.

[48] F Cooper, A Khare, NR Quintero, FG Mertens, and A Saxena. Forced nonlinear Schrödinger equation with arbitrary nonlinearity. *Physical Review E*, 85(4):046607, 2012.

[49] FG Mertens, NR Quintero, and AR Bishop. Nonlinear Schrödinger solitons oscillate under a constant external force. *Physical Review E*, 87(3):032917, 2013.

[50] VK Sharma, TS Raju, and CN Kumar. Study of modulation instability for nonlinear Schrödinger equation phase locked with an external source, Submitted to. *Journal of Computers and Mathematics with Applications*, 2014.

Chapter 5

Summary and conclusion

This thesis deals with the study of solitary wave or soliton-like solutions for NLSE. In this thesis we have investigated MI for twin-core fiber which is physical system of considerable interest. MI is responsible for soliton pulses in different nonlinear media. We have illustrated the properties of negative index materials (NIMs) and studied the solitary wave solutions for higher order NLSE, NLSE with source and NLSE in coupled mode. We have also illustrated the the solitary wave solutions for HNLSE for ordinary nonlinear materials and also discussed the impact of source term on MI in case of NLSE with source.

In Chapter 2, is divided into three parts. In first section we have considered the wave propagation in Negative refractive index materials. There has been considerable interest, experimentally as well as theoretically, in the use of NIMs in optical communication systems, as these are artificially designed materials so we have flexibility of controlling the behavior of these materials. In first section we presented periodic and solitary waves, propagating through NIMs [Sharma *et al.*, J. Mod. Opt. 60 (2013) 836]. It has been accomplished by first by assuming an ansatz for the NLSE containing higher order effects like quintic nonlinearity, self-steepening and nonlinear dispersive terms which governs the pulse propagation through NIMs. We find the conditions for which the assumed ansatz satisfies the equation. In this we have explored dark and bright solitary wave solutions for some constraints. The evolution of dark solitary waves is shown for specific range of normalized frequency while the existence of bright solitary waves are possible under some conditions on model parameters which can be achieved through the structural changes in NIMs. We further studied fractional-transform solutions, containing periodic, hyperbolic and cnoidal solitary wave solutions for GNLSE, in absence of quintic and nonlinear dispersion terms. In second section we have studied solitary wave solutions for NLSE with source [Sharma *et al.*, AIP Conf. Proc. 1536 (2013) 717]. In this case we have obtained the periodic and solitary wave solution by using ansatz method. Third section deals with study of chirped pulses in NIMs. We have considered the coupled pulse propagation equation in NIMs in the presence of electric and magnetic self-steepening effects, and obtained exact chirped soliton and periodic solutions for this model for normal as well as anomalous dispersion. For the normal dispersion, we obtained the bright and dark soliton solutions having unique velocity but different initial chirp for same normalized frequency; on the other hand for the anomalous dispersion, it possesses the fractional solutions having different velocity for a particular normalized frequency. Moreover there is also a possibility of obtaining the periodic nonlinear waves in NIMs in anomalous dispersion regime. We have plotted these solutions for different normalized frequencies. It is shown that nonlinear chirp associated with each of these solutions is directly proportional to the intensity of the pulse and saturates at some finite value as the retarded time approaches its asymptotic value.

In Chapter 3, we studied the MI for a twin-core fibers in the presence of higher order effects such. We considered CNLSE containing higher order terms such as quintic nonlinearity, self-steepening (SS), third order dispersion (TOD), forth order dispersion (FOD) and coupling coefficient dispersion (CCD) term. We have applied linear stability analysis for the study of modulation instability. For study of MI we perturb the steady state solution of coupled equation slightly by applying weak perturbation. Then the resultant equation is linearized in perturbation term. We write perturbation term as a sum of positive exponential and negative exponential term in the resultant equation. Then a dispersion relation is obtained from the resultant equation. Imaginary part of dispersion relation will give gain expression for MI. It is observed that impact of TOD is minimal on MI gain. We have discussed the characteristic of three kinds of MI—spatial, temporal, spatiotemporal.

It is found that the spatial MI gain is independent of SS, FOD, CCD terms. We have further investigated the impact of quintic nonlinearity, CCD, FOD, SS on temporal MI gain separately. It is observed that all these terms play vital role in MI gain and none of the terms can be ignored. A judicious choice of all these parameters provides us a freedom to control the MI gain spectrum. To sum up, the MI in twin-core fiber occurs for all combinations of nonlinearity and dispersion. Since the solitons and MI occur in the same parameter regime, this detailed MI analysis suggests the generation of ultrashort pulses in twin-core optical fibers for different parameter domains.

Chapter 4 is divided into two parts. In first part, we studied the GNLSE with non-Kerr terms [Sharma *et al.*,J. Nonl. Opt. Phys. Mat. 23 (2014) 3], which is short wave equation. We demonstrated that the non-Kerr terms induces different types of bright and dark solitons, which are subjected to constraint relations among the parameters. These femtosecond pulses are useful to increase the capacity of carrying information in order to make ultra fast communication which is useful for trans-continental and trans-ocean. In second part we have investigated the MI for NLSE with source term by using linear stability analysis. A number of interesting features have emerged from this study. Analysis shows that MI exist for all regions except the region where nonlinearity is self-defocussing in nature and source term coefficient is negative. It is observed that for all cases gain increases with increase in nonlinearity. For self-defocussing case, with increase in nonlinearity, MI gain increases and increase of source term coefficient leads to shifting of sidebands towards higher frequency side. We further observed that for lower value of self-focussing nonlinearity and positive source term coefficient, with increase in source term coefficient, MI side-bands shifts towards higher frequency side. It is further observed that with increase in value nonlinearity the impact of source parameter on MI reduces and at higher nonlinear coefficient the MI sideband coincides for all values of source term coefficients. For self-focussing nonlinearity and negative source term coefficient, at lower value of nonlinear parameter as the value of source term increases, MI sidebands shift towards higher frequency side. However with increase in value of nonlinearity, the effect of source parameter on MI reduces and for high nonlinearity, MI side band for all value of source parameter overlap.

The work described in this thesis has led to some interesting results of wave propagation in the field of nonlinear optics regarding study of MI in the context of twin-core fiber and regarding solitary wave solutions in the context of NIMs, ordinary nonlinear materials. These solutions may be useful in communication networks and other optical processes. The study of propagation of waves in NIMs will be useful to understand the structure and fabrication of NIMs.

List of publications

Papers in refereed journals

1. **V. K. Sharma**, A. Goyal, T. S. Raju and C. N. Kumar, Periodic and solitary wave solutions for ultrashort pulses in negative-index materials, ***Journal of Modern Optics*** 60 (2013) 836–840.

2. A. Goyal, **V. K. Sharma**, T. S. Raju and C. N. Kumar, Chirped double-kink and fractional-transform solitons in an optical gain medium with two-photon absorption, Manuscript submitted to ***Journal of Modern Optics*** 61 (2013) 315–321.

3. **V. K. Sharma** and A. Goyal, Ultrashort double-kink and algebraic solitons of generalized nonlinear Schrödinger equation in the presence of non-Kerr terms, ***Journal of nonlinear Optical physics and materials*** 24 (2014) 1450034.

4. **V. K. Sharma**, A. Goyal, T. S. Raju, C. N. Kumar and P. K. Panigrahi, Spatial, temporal, and spatio-temporal modulational instabilities in twin-core optical fibers, Submitted to ***Journal of Optical Fibre Technology*** for publication as artical (2014).

5. **V. K. Sharma**, R. Gupta, A. Goyal, C. N. Kumar, A. K. Sarma, Chirped soliton-like solutions of coupled generalized nonlinear Schrödinger equation for pulse propagation in negative index material, Submitted to ***Journal of Modern Optics*** for publication as an article (2014).

6. **V. K. Sharma**, A. Goyal, T. S. Raju, C. N. Kumar, Study of Modulation instability for nonlinear Schrödinger equation phase locked with an external source, Submitted to ***Journal of Mathematics and computers with applications*** for publication as an article (2014).

Conference papers in refereed journals

1. A. Goyal, **V. K. Sharma** and C. N. Kumar, Optical solitons supported by localized gain in the presence of two-photon absorption, International Conference on Fiber Optics and Photonics, ***OSA Technical Digest*** (online) (Optical Society of America, 2012).

2. **V. K. Sharma**, A. Goyal, C. N. Kumar and J. Goswamy, Travelling wave solutions in negative index materials in the presence of external source, ***AIP Conference Proceedings*** 1536 (2013) 717.

3. **V. K. Sharma**, K. K. De, A. Goyal, Solitary wave solutions of higher-order nonlinear Schrödinger equation with derivative non-Kerr nonlinear terms, ***IEEE Xplore Conference Proceedings*** (2014) 1-2 DOI 10.1109/WRAP.2013.6917712.

Papers in conferences and workshops

1. **A. Goyal**, V. Sharma, J. Goswamy and C. N. Kumar, Soliton-like solutions for higher order nonlinear Schrödinger equation, 6^{th} ***Chandigarh Science Congress***, Panjab University, Feb. 26-28, 2012.

2. R. Gupta,**V. K. Sharma** and C. N. Kumar,Study of modulation instability in negative index metamaterials governed by cubic-quintic nonlinear Schrödinger equation, 7^{th} ***Chandigarh Science Congress***, Panjab University Chandigarh, Feb. 26-28, 2013.

Selected

Reprints/Preprints